People's Democratic Republic of Algeria
Ministry of Higher Education and Scientific Research
University of A. MIRA-BEJAIA

Faculty of Technology
Department of Electrical Engineering
Laboratory of Medical Informatics and Intelligent and Dynamic Environments (LIMED)

Thesis

FOR THE OBTAINING OF THE DOCTORATE DIPLOMA

Domain: Science and Technology Specialty: Telecommunication
Option: Networks and Telecommunications

Presented by:
Mr Yacine OUAZZIZ

Title

Contribution to the Optimization of Radio Resources Sharing in LTE/5G Networks

Defended on : **08/11/2025** Before the jury composed of:

Full name	Rank	University	
Mr Reda Kasmi	Professor	Univ. of Bejaia	Chair
Mr Mohamed Azni	Professor	Univ. of Bejaia	Supervisor
Mr Mohamed Tounsi	MCB	Univ. of Bejaia	Co-Supervisor
Mr Yassine Bensafia	Professor	Univ. of Bouira	Examinator
Mr Abdenour Mekhmoukh	MCA	Univ. of Bejaia	Examinator

Academic year: 2025/2026

République Algérienne Démocratique et Populaire
Ministère de l'Enseignement Supérieur et de la Recherche Scientifique
Université A.MIRA-BEJAIA

جامعة بجاية
Tasdawit n Bgayet
Université de Béjaïa

Faculté de Technologie
Département Génie Electrique
Laboratoire ou unité de recherche de rattachement : LIMED

THÈSE

EN VUE DE L'OBTENTION DU DIPLOME DE DOCTORAT

Domaine : Sciences et Technologies Filière : Télécommunication
Spécialité : Réseaux et télécommunications

Présentée par
M^r^ OUAZZIZ Yacine

Thème

Contribution à l'optimisation du partage des ressources radio dans les réseaux LTE/5G

Soutenue le : 08/11/2025 **Devant le Jury composé de :**

Nom et Prénom	Grade		
Mr KASMI REDA	Professeur	Univ. De Bejaia	Président
Mr AZNI Mohamed	Professeur	Univ. De Bejaia	Rapporteur
Mr TOUNSI Mohamed	MCB	Univ. De Bejaia	Co-Rapporteur
Mr BENSAFIA Yassine	Professeur	Univ. De Bouira	Examinateur
Mr MEKHMOUKH Abdenour	MCA	Univ. De Béjaia	Examinateur

Année Universitaire : **2025/2026**

Contents

ACKNOWLEDGMENTS

First and foremost, I extend my deepest gratitude to my advisor, **Professor AZNI M.**, whose support, expertise, and unwavering trust have been the cornerstone of this research journey. His guidance went far beyond academic supervision,it shaped my critical thinking, scientific rigor, and perseverance.

I also wish to sincerely thank my co-advisor, **Dr. TOUNSI M.**, for his constant availability, constructive feedback, and patient mentorship throughout the project. His insight played a crucial role in overcoming many of the challenges I faced.

A special expression of appreciation goes to **Professor BELAID S.**, whose intellectual generosity and advice proved invaluable, even though she was not formally involved in this work. Her perspective illuminated paths I would not have otherwise considered.

I am profoundly grateful to my **mother** and **sister**, her husband and her daughters whose love and encouragement have sustained me through the most difficult moments. Their belief in me was my anchor, my motivation, and my refuge.

To my **future wife**, I owe more than words can convey. She stood by me in moments of doubt, reminded me why I began, and pushed me forward when I was ready to give up. This thesis is as much hers as it is mine.

I am also thankful to my **friends**, who walked this path with me,through every frustration and every small victory,and to the **ASMB Judo Family**, whose spirit, discipline, and camaraderie reminded me daily of the strength that lies in commitment.

A warm acknowledgment goes to my friend **Mohan Gumatay**, a.k.a. **DJ MoTwister**, whose energy, wit, and unwavering support from afar brought unexpected joy and balance throughout this journey.

Finally, to **everyone who contributed, in ways big or small, seen or unseen**, to my becoming a doctor,thank you! This milestone is the result of many shoulders that carried me and hands that held me steady when I stumbled.

This thesis is dedicated to all of you.

List of Figures

List of Tables

List of Abbreviations

3GPP	3rd Generation Partnership Project
4G	Fourth Generation
5G	Fifth Generation
6G	Sixth Generation
ADC	Analog-to-Digital Converter
AI	Artificial Intelligence
AMC	Adaptive Modulation and Coding
AR	Augmented Reality
AWGN	Additive White Gaussian Noise
BER	Bit Error Rate
BWP	Bandwidth Part
CDMA	Code Division Multiple Access
CP	Cyclic Prefix
CSI	Channel State Information
CSI-RS	Channel State Information Reference Signal
D2D	Device-to-Device
DL	Downlink
DSP	Digital Signal Processor
eMBB	enhanced Mobile Broadband
E2E	End-to-End
EVM	Error Vector Magnitude
FBMC	Filter Bank MultiCarrier
FEC	Forward Error Correction

FDMA	Frequency Division Multiple Access
FDD	Frequency Division Duplexing
FFT	Fast Fourier Transform
FIR	Finite Impulse Response
FPGA	Field-Programmable Gate Array
GFDM	Generalized Frequency Division Multiplexing
GSC	Generalized Sidelobe Canceller
GSM	Global System for Mobile Communications
ICI	Inter-Carrier Interference
ICI-SINR	Inter-Carrier Interference Signal-to-Interference-plus-Noise Ratio
IFFT	Inverse Fast Fourier Transform
INI	Inter-Numerology Interference
IoT	Internet of Things
IIR	Infinite Impulse Response
ISI	Inter-Symbol Interference
LDPC	Low-Density Parity-Check
LMS	Least Mean Squares
LPWA	Low-Power Wide-Area
LTE	Long Term Evolution
M2M	Machine-to-Machine
mMTC	massive Machine-Type Communication
MIMO	Multiple-Input Multiple-Output
mmWave	Millimeter Wave
MPA	Message Passing Algorithm
MRI	Magnetic Resonance Imaging
MRF	Markov Random Field
NFV	Network Function Virtualization
NOMA	Non-Orthogonal Multiple Access
NR	New Radio

OFDMA Orthogonal Frequency Division Multiple Access

OFDM Orthogonal Frequency Division Multiplexing

OOB Out-of-Band

PAPR Peak-to-Average Power Ratio

PBCH Physical Broadcast Channel

PDCCH Physical Downlink Control Channel

PDSCH Physical Downlink Shared Channel

PSD Power Spectral Density

PSNR Peak Signal-to-Noise Ratio

PTRS Phase Tracking Reference Signal

QAM Quadrature Amplitude Modulation

QoS Quality of Service

RB Resource Block

RE Resource Element

RAN Radio Access Network

RFI Radio Frequency Interference

RLS Recursive Least Squares

RIS Reconfigurable Intelligent Surface

SC-FDMA Single Carrier Frequency Division Multiple Access

SCMA Sparse Code Multiple Access

SCS Subcarrier Spacing

SDN Software-Defined Networking

SE Spectral Efficiency

SIC Successive Interference Cancellation

SINR Signal-to-Interference-plus-Noise Ratio

SNR Signal-to-Noise Ratio

SBA Service-Based Architecture

TDD Time Division Duplexing

TDMA Time Division Multiple Access

UE User Equipment

UL Uplink

URLLC Ultra-Reliable Low-Latency Communication

VR Virtual Reality

Introduction

1 Context and Motivation

The advancement of wireless communication technologies has seen an unprecedented surge in recent years, driven by the exponential demand for higher data rates, greater connection density, and ultra-low-latency applications [1]. Fifth-generation (5G) networks lie at the core of this transformation, promising to meet these stringent requirements through architectural and physical layer innovations [2].

5G networks are fundamentally designed for flexibility and scalability, enabling support for a diverse set of service categories such as enhanced Mobile Broadband (eMBB), ultra-Reliable Low-Latency Communication (URLLC), and massive Machine-Type Communication (mMTC) [3–6]. These services impose varying constraints on throughput, reliability, and latency, requiring transmission schemes that adapt accordingly. Consequently, traditional fixed-numerology frameworks used in prior generations like LTE are no longer sufficient.

To accommodate this diversity, 5G introduces the concept of *multi-numerology*, where different waveform configurations, characterized by different subcarrier spacings, symbol durations, and cyclic prefix lengths, can coexist within the same carrier bandwidth [5]. While this flexibility enables optimized performance across different services and use cases, it disrupts the orthogonality between subcarriers, resulting in **inter-numerology interference (INI)**.

The rise of INI significantly impacts system performance, particularly in scenarios involving dense deployments, unsynchronized transmissions, and mixed-service environments [4, 6–8]. Furthermore, as future generations like 6G envision even more aggressive spectrum sharing, extreme network densification, and AI-native adaptation, interference mitigation becomes increasingly critical [2, 5, 9].

Effectively managing INI is, therefore, essential to unlock the full potential of 5G and lay the groundwork for the next generation of wireless technologies.

2 Problem Statement

The coexistence of multiple numerologies in 5G introduces a fundamental challenge: the loss of orthogonality among subcarriers of different numerologies. This results in spectral leakage and interference, collectively referred to as *inter-numerology interference (INI)* [4, 5, 10]. INI causes unwanted power leakage across adjacent numerology blocks, degrading signal quality and reducing both spectral efficiency and throughput.

The severity of INI is affected by factors such as numerology spacing ratios, relative transmit powers, frequency alignment, and guard band configuration [6, 11–14].

Moreover, INI is particularly pronounced at the numerology boundaries where subcarrier spacing mismatches result in overlapping sidelobes and spectral contamination.

These interference effects are exacerbated in dynamic and heterogeneous networks where users with different quality-of-service requirements may be scheduled simultaneously [5, 10, 15–17]. As a result, the accurate modeling, analysis, and mitigation of INI are essential for maintaining the reliability and efficiency of 5G NR deployments.

3 Research Objectives and Contributions

This thesis aims to address the INI challenge in 5G NR by implementing a dual-mitigation strategy based on:

1. **Time alignment**, which synchronizes OFDM symbols across BWPs to minimize temporal misalignment at symbol boundaries.
2. **High-order FIR filtering**, applied to the interfering waveform to suppress spectral leakage and limit out-of-band emissions.

The proposed approach improves overall system robustness while maintaining compatibility with 3GPP numerology configurations.

The key research objectives are:

- To model INI in dual-numerology OFDM systems and characterize its impact on key performance metrics.
- To investigate the effectiveness of time alignment in reducing interference without modifying the waveform structure.
- To design and apply FIR filters tailored for spectral suppression in the interfering BWP.
- To evaluate the combined performance of these methods using MATLAB simulations over a wide range of modulation schemes and SNR values.

The main contributions of this thesis are:

- A practical simulation framework for evaluating INI in dual-numerology OFDM with realistic 5G NR parameters.
- A combined time-domain and frequency-domain mitigation approach that does not rely on channel knowledge or adaptive feedback.
- Demonstrated improvements in BER, EVM, SINR, and Spectral Efficiency metrics across multiple modulation orders.
- Insights into the trade-offs of filtering, including processing overhead and its impact on spectral confinement.

4 Thesis Structure

This thesis is organized into five chapters, each addressing a key aspect of the study on inter-numerology interference (INI) mitigation in 5G New Radio (NR) systems:

- **Chapter 1** introduces the motivation behind this research, formulates the problem of inter-numerology interference, defines the objectives, and outlines the contributions made.
- **Chapter 2** reviews the foundational concepts of 5G NR, including the numerology framework, the rationale for multi-numerology coexistence, and the challenges it introduces at the physical layer.
- **Chapter 3** provides a mathematical and simulation-based characterization of INI, and presents a detailed survey of state-of-the-art mitigation techniques including filtering, time alignment, guard banding, windowing, and interference cancellation strategies.
- **Chapter 4** presents the proposed INI mitigation approach based on time alignment and frequency-domain FIR filtering. The chapter includes a full system model, simulation setup, and performance evaluation across various modulation schemes and SNR values, focusing on BER, EVM, SINR, and Spectral Efficiency metrics.
- **Chapter 5** concludes the thesis by summarizing the key findings, analyzing the trade-offs and limitations of the proposed method, and outlining potential directions for future work, including real-time implementation and hybrid approaches combining filtering with interference prediction or machine learning.

Chapter 1

Technical Foundations of 5G NR

Introduction

The evolution from fourth-generation (4G) Long-Term Evolution networks to fifth-generation (5G) systems represents a significant leap forward in wireless communication technology, propelled by the escalating demand for mobile data and the increasingly diverse requirements of modern applications [18]. Fourth-generation networks offered a robust platform for mobile broadband, fostering the growth of the app economy, but their foundational architecture was primarily designed around a "one-size-fits-most" approach, which, while sufficient for human-centric applications, falls short of meeting the dynamic and heterogeneous demands of contemporary digital ecosystems [19].

In contrast, Fifth-generation New Radio is engineered as a versatile, software-defined communication framework capable of accommodating a wide spectrum of services across various sectors, including autonomous vehicles, intelligent manufacturing, e-health, immersive media, and large-scale Internet of Things deployments [20]. Departing from the incremental upgrade model of previous generations, Fifth-generation introduces architectural and physical-layer innovations that enable scalability across three key dimensions: capacity, latency, and connection density [21].

The advent of modern mobile communication networks has been driven by the ever-increasing demand for faster download speeds and low latency, enabling seamless connectivity to work and social digital platforms [22]. These networks have become essential for supporting a wide range of applications, including video streaming, online gaming, and augmented reality, which require high data transfer rates and minimal delays [23]. The transition to fifth-generation networks facilitates enhanced mobile broadband, massive machine-type communications, and ultra-reliable low-latency communications [4]. The stringent performance objectives set by the International Telecommunication Union encompass data rates reaching up to 20 Gbps, latency levels below 1 ms, connection densities exceeding 1 million devices per square kilometer, and spectral efficiencies surpassing those of fourth-generation networks by several orders of magnitude [24]. Achieving these ambitious targets requires a comprehensive redesign of the radio access network, the core network, and the underlying physical-layer technologies.

This chapter outlines the limitations of 4G LTE in meeting modern communication demands and introduces the key performance goals and architectural requirements of 5G. It highlights the three core service categories defined by the ITU (eMBB, URLLC, and mMTC) that shape 5G NR's design.

The discussion then shifts to the 5G architecture, covering service-based core net-

works, RAN configurations, and key enabling technologies such as flexible numerology, massive MIMO, dynamic TDD, and NOMA, which together enable adaptable and efficient wireless services.

By establishing the motivations and foundational technologies of 5G NR, this chapter provides the necessary context for the thesis's focus on advanced interference management in multi-numerology OFDM systems and resource optimization.

1.1 Transition from 4G to 5G

1.1.1 Limtiations of 4G

The fourth generation (4G), while bringing a significant improvement over 3G, struggles to meet the demands of emerging applications and services [4]. The technology's main limitations are listed below :

- **Limited capacity:** 4G networks are reaching their capacity limits in densely populated areas, leading to congestion and reduced data rates, especially during peak hours. [25]
- **Inability to support massive connectivity:** 4G networks are not designed to handle the massive number of connected devices envisioned in the Internet of Things, leading to scalability issues. [23, 26]
- **High latency:** 4G networks have relatively high latency, making them unsuitable for applications that require real-time communication, such as augmented reality, virtual reality, and autonomous vehicles. [27, 28]
- **Lack of flexibility:** 4G networks are not flexible enough to support the diverse requirements of different applications and services, leading to inefficient resource utilization. [19, 29]
- **Limited spectrum:** 4G networks rely on licensed spectrum, which is expensive and limited, hindering the deployment of new services and applications. [30]

These limitations have driven the development of 5G, which is designed to address these challenges and enable a new era of wireless communication.

1.1.2 Challenges and New Requirements of 5G

Fifth generation networks are designed to overcome the limitations of 4G and meet the ever-increasing demands of wireless communication, introducing a new set of challenges and requirements [28, 31].

These challenges are multifaceted, spanning from technological hurdles to deployment complexities, requiring innovative solutions and approaches.

as shown in Table 1.1, 5G must support significantly higher data rates compared to 4G, with target peak data rates of up to 20 Gbps and user-experienced data rates of up to 100 Mbps. [25, 28]

One of the most critical requirements of 5G is ultra-low latency, with target end-to-end latency of 1 ms for mission-critical applications such as industrial automation and remote surgery [28, 32].

Table 1.1: Performance Comparison Between 4G LTE and 5G NR

Metric	**4G LTE**	**5G NR**
Peak Data Rate	Up to 1 Gbps (DL), 100 Mbps (UL)	Up to 20 Gbps (DL), 10 Gbps (UL)
User Experienced Data Rate	10–100 Mbps	100 Mbps–1 Gbps
Latency (Air Interface)	∼10 ms	∼1 ms (URLLC)
Mobility Support	Up to 350 km/h	Up to 500 km/h
Connection Density	$\sim 10^5$ devices/km^2	$\sim 10^6$ devices/km^2
Spectrum Efficiency	Baseline (1x)	∼3x improvement
Energy Efficiency	Moderate	Higher (up to 100x improvement)
Network Architecture	EPC (centralized)	SBA (cloud-native, virtualized)
Numerology	Fixed (15 kHz)	Scalable (15–240 kHz)
Deployment Band	Sub-6 GHz	Sub-6 GHz + mmWave (up to 100 GHz)

In addition, 5G must be able to support a massive number of connected devices, with a target of up to 1 million devices per square kilometer, enabling the widespread deployment of IoT devices and services [3, 19, 33]

To ensure seamless connectivity and coverage, 5G must provide high network availability and reliability, with target availability of 99.999 for critical applications. [4, 19, 34]

5G networks must be flexible enough to support a wide range of applications and services, each with its own specific requirements, enabling efficient resource utilization and customized service delivery. [10, 28, 33, 35]

The networks must be designed to be energy-efficient, minimizing power consumption and reducing the environmental impact of wireless communication.

meeting these goals introduces a series of new requirements :

- **Spectrum Efficiency and mmWave Integration:** Operating in mmWave bands opens access to vast unused spectrum but introduces challenges such as higher attenuation and limited range. 5G addresses this using beamforming, massive MIMO, and advanced propagation models to maintain link reliability and spectral efficiency [32, 33].

- **Device Scalability and Grant-Free Access:** Massive IoT deployments necessitate scalable access mechanisms. Techniques such as grant-free transmission and non-orthogonal multiple access (NOMA) help minimize control signaling and conserve energy in low-complexity devices [4, 36].

- **Network Slicing and Edge Computing:** The ability to create virtualized, independent network slices allows 5G to allocate resources dynamically based on

specific service requirements. This combined with Mobile Edge Computing, reduces latency by processing data closer to the source, crucial for applications like autonomous vehicles and real-time video analytics [3, 37, 38].

- **Energy-Aware Design:** The densification of 5G networks through small cells and mmWave access increases power demands. To remain sustainable, 5G systems must incorporate energy-efficient protocols and hardware, particularly for battery-operated IoT devices. [26, 39, 40]
- **Security and Privacy:** With an increased attack surface due to more connected devices and virtualization, 5G networks must provide robust security mechanisms. This includes enhanced authentication, encryption, and policies that protect user data and prevent unauthorized access to network resources [3, 41].
- **Backhaul Capacity:** 5G's enhanced capabilities and services add strain to backhaul networks, necessitating ultra-low latency and high capacity. [23, 28, 42]

In summary, 5G is not merely a faster version of LTE, it is an entirely new architectural and operational paradigm. While its potential is vast, delivering on its promises requires innovations across the protocol stack, hardware design, and network intelligence.

1.2 Fundamentals of 5G Communication Systems

1.2.1 5G Use Cases

With its modular design and expansive feature set, 5G is engineered to support a wide array of services that highly differ in their performance requirements. When considered as a block, these services seem impossible to implement, so in order to organize this diversity, the Iternational Tellecommunication Union identified three primary usage scenarios: enhanced Mobile Broadband (eMBB), Massive Machine Type Communications (mMTC), and Ultra-Reliable Low Latency Communications as depicted in Figure 1.1 [4, 32]

- **Enhanced Mobile Broadband (eMBB)** eMBB is the evolution of 4G LTE, aiming at improving spectral efficiency and throughput performance to support services with high data rates, such as virtual reality, augmented reality, and high-definition video streaming [4, 25, 44] .
- **Ultra-Reliable Low-Latency Communications (URLLC)** URLLC is tailored for applications that require extremely low latency and high reliability, such as autonomous driving, remote surgery, and industrial automation [32, 45, 46].
- **Massive Machine-Type Communications (mMTC)** mMTC is designed to support the interconnection of a massive number of low-cost, low-power devices for IoT applications, such as smart cities, smart agriculture, and smart metering. [3, 32].

These three categories represent a wide range of applications and services that 5G is designed to support [4]. The network can be customized and adapted to meet the

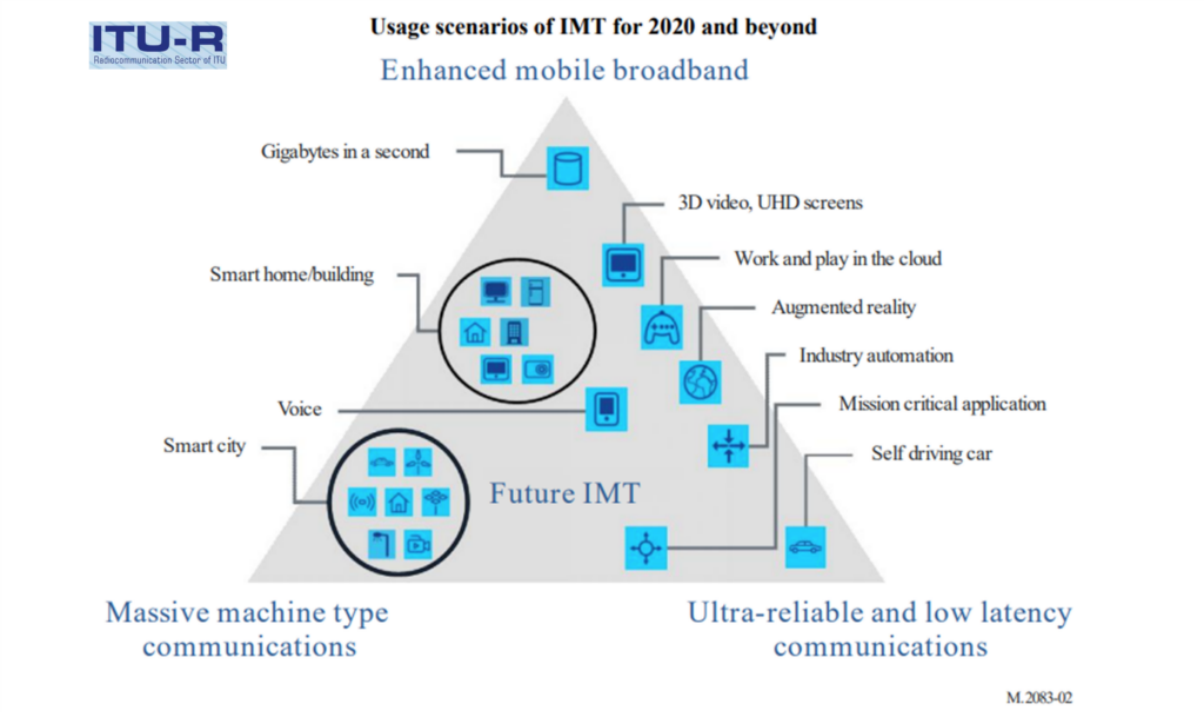

Figure 1.1: ITU-defined 5G use cases[43].

specific requirements of each use case [47]. 5G's general applications are wide, including healthcare, transportation, smart grids, and entertainment. [3, 48, 49]

To accomodate this diversity, 5G employs a combination of a software defined architecture, network slicing, and edge computing, allowing to dynamically allocate and manage resources based on the specific needs of each application. [3, 38, 50]

The introduction of 5G has opened up new avenues for industrial IoT, enabling applications such as remote monitoring, predictive maintenance, and real-time control [51]. It facilitates high-speed data transfer, ultra-low latency, and reliable connectivity, which are essential for efficient and effective communication in smart grid environments [3]. 5G networks offer enhanced capabilities for traffic management and reduced costs of spectrum utilization through network slicing, catering to the distinctive service differentiation needs demonstrated by various vertical industries [49]. The enhanced capabilities of 5G networks have spurred interest across diverse sectors, with industrial IoT standing out as a key area.

1.2.2 5G Network Architecture

The architecture of 5G networks represents a paradigm shift from previous generations, embracing virtualization, softwarization, and cloudification to achieve unprecedented flexibility, scalability, and efficiency. [3, 32, 52]

The 5G architecture is designed to support the wide range of use cases and deployment scenarios, from enhanced mobile broadband to massive machine-type communications and ultra-reliable low-latency communications [4, 11, 33]. Figure 1.2 provides an overview of a modern 5G network, highlighting its key components and structural layers.

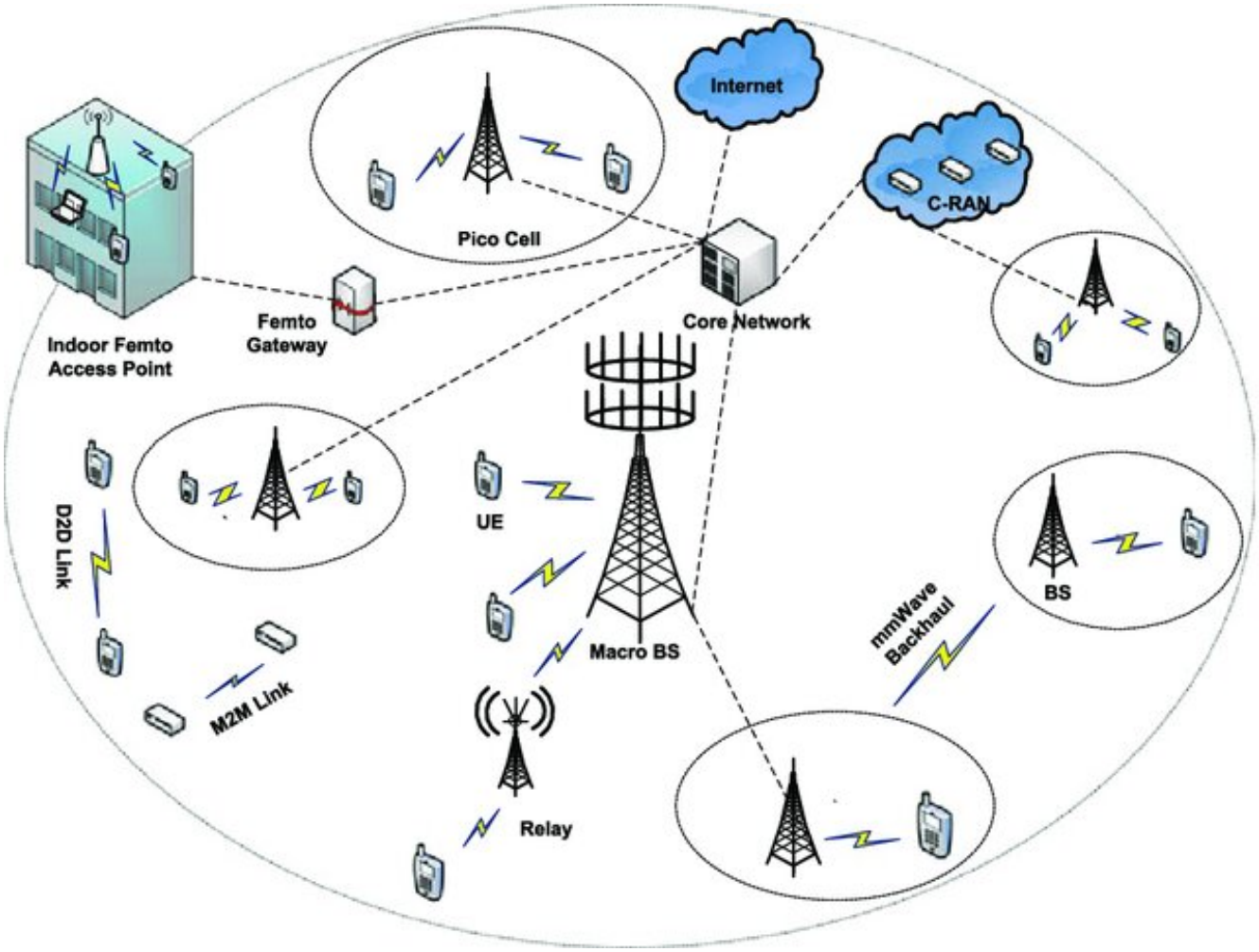

Figure 1.2: Overview of the 5G network architecture[53].

A. Core Network and Service-Based Architecture (SBA)

The 5GC is the heart of the 5G network, responsible for managing connectivity, mobility, and security.

Unlike previous generations, which relied on monolithic architectures, the 5GC adopts a service-based architecture, where network functions are implemented as modular software components that can be deployed and scaled independently [32, 54]

The SBA enables network operators to rapidly develop and deploy new services, customize network functions to meet specific requirements, and optimize resource utilization [46, 55, 56]

Key functions of the 5GC include: [3, 50, 56, 57]

- **Authentication and authorization:** Verifying the identity of users and devices and granting access to network resources.
- **Mobility management:** Tracking the location of users and devices and ensuring seamless handover between base stations.
- **Session management:** Establishing and maintaining communication sessions between users and applications.
- **Policy control:** Enforcing network policies and ensuring quality of service.

B. Radio Access Network (RAN) and C-RAN

The RAN is the part of the network that provides wireless connectivity to user devices[3, 22, 23, 33, 42].

It comprises base stations (gNodeBs or eNodeBs in the case of non-standalone deployments) that transmit and receive radio signals [3].

- **Macrobase stations (gNodeBs):** provide wide-area coverage and support high transmission power levels. They serve as mobility anchors and backhaul aggregation points in suburban and rural regions. [58, 59]
- **Small cells (picocells, femtocells):** provide coverage in dense urban areas and indoor environments. [4, 32, 60, 61]

To further enhance efficiency, many operators are adopting a centralized archi¬tecture, where the baseband processing units are centralized, and the remote radio heads are distributed at the cell sites. It is known as centralized RAN. It enables cooperat¬ive radio resource management, interference coordination, and load balancing. [48, 60, 62–64]

C. Millimeter-Wave Backhaul and Fronthaul

Backhaul solutions for 5G must address both capacity and latency constraints to support the high data rates and low latency requirements of 5G applications. Millimeter-wave (mmWave) technology offers a promising solution for 5G backhaul, providing high bandwidth and low latency connectivity [65]. However, mmWave signals are susceptible to atmospheric attenuation and blockage, which can limit the range and reliability of mmWave backhaul links.

The backhaul network represents a critical segment that facilitates interconnection and support for billions of devices originating from the core network [23]. It is expected

that the conventional cellular system architecture will struggle to handle Gigabit-level data traffic while maintaining cost-effectiveness and ecological sustainability, especially considering the increasing demand for wireless data traffic [66].

The introduction of 5G has placed additional demands on the backhaul network, including ultra-low latency requirements and support for ultra-dense networks [23]. 5G backhaul networks need to support high traffic volumes from the core network while adhering to strict latency constraints. Meeting the capacity and latency requirements of 5G backhaul networks necessitates the utilization of high-capacity, low-latency technologies such as fiber optics and millimeter-wave communication.

The fronthaul refers to the network connecting the remote radio unit to the baseband unit in a centralized RAN architecture [67]. The key requirements for fronthaul networks include high bandwidth, low latency, and synchronization [4].

5G NR introduces innovative approaches to radio resource sharing, enhancing spectral efficiency and network capacity [4].

D. Device-to-Device (D2D) and Machine-to-Machine (M2M) Communications

Device-to-device (D2D) communication allows devices to communicate directly with each other without traversing the base station [32]. This can improve the efficiency and latency of communication in certain scenarios. D2D communication holds substantial importance in 5G networks, primarily due to its ability to enhance network efficiency and reduce latency [68–70].

The integration of D2D communication into 5G networks has the potential to enable a wide range of new applications and services. By enabling direct communication between devices, D2D can improve the efficiency of communication, reduce latency, and extend battery life. M2M communication is a key enabler of the IoT, allowing devices to communicate and exchange data with minimal human intervention. [32, 71, 72]

The advent of 5G has spurred the development of applications like Mobile Edge Computing, Artificial Intelligence, Internet of Things, and Internet of Vehicles [73]. These applications have driven the evolution and advancement of wireless communication technology [19, 74].

E. User Equipment (UE)

The UE is the device that connects to the 5G network, such as smartphones, tablets, and IoT devices. 5G devices are equipped with advanced capabilities, including support for multiple frequency bands, wide bandwidth channels, and advanced antenna technologies. The transition from cell-centric to user-centric networking is a paradigm shift in 5G, bringing devices closer and emphasizing proximity discovery to trigger direct communication [32]. The network intelligently manages resource allocation, enabling seamless data exchange and control signaling, optimizing the use of resources for both D2D and D2N communications [32, 68, 69]

Table 1.2 outlines the primary roles and application contexts of key components in the 5G network architecture.

In 5G NR, several key features revolutionize wireless communication, addressing the diverse and demanding requirements of modern applications [4].

Table 1.2: Roles of Key Components in 5G Network Architecture[53].

Component	**Primary Function**	**Application Context**
Core Network (SBA)	Virtualized control and user plane functions	Slice orchestration, QoS enforcement, interconnectivity
Macro Base Station (gNodeB)	Long-range coverage and high-power connectivity	Rural, suburban, and macro-urban deployment
Small Cells (Pico/Femto)	Short-range, high-capacity local access	Dense urban zones, indoor environments
C-RAN	Centralized baseband processing for RAN virtualization	Latency-sensitive and resource-coordinated deployments
mmWave Backhaul	High-speed wireless link between RAN and core or edge cloud	Fiber alternative in urban densification
Device-to-Device (D2D)	Peer-to-peer communication without routing via RAN	V2X, emergency services, proximity sharing
Machine-to-Machine (M2M)	Efficient, scalable IoT communication	Smart grids, sensor networks, industrial telemetry
Relay Nodes	Intermediate nodes to extend coverage and fill coverage holes	Underground or remote areas
User Equipment (UE)	Access terminal for consuming or generating traffic	Smartphones, AR/VR headsets, sensors, vehicles

F. Key Architectural Principles

The 5G NR architecture is built upon several key principles, including flexibility, scalability, and efficiency. Flexibility is achieved through the use of software-defined networking and network functions virtualization, which allows network operators to rapidly deploy new services and customize network functions to meet specific requirements.

Scalability is achieved through the use of a distributed architecture, where network functions are deployed across multiple nodes.

Efficiency is achieved through the use of advanced technologies such as massive MIMO, beamforming, and network slicing, which enable network operators to optimize resource utilization and improve network performance [32].

The transition towards 5G represents a move from cell-centric to user-centric networking, enhancing user experiences by removing cell boundaries and enabling seamless mobility [32]. The architecture also employs SDN and NFV to enable network slicing, offering customized virtual networks tailored to diverse application needs [32]. With the deployment of 5G networks, improved mobile internet communication, broader functionalities, and greater service accessibility have become reality [75].

G.Software-defined networking and network function virtualization

Software-defined networking and network function virtualization are key enablers of the 5G NR architecture, providing the flexibility and agility needed to support the diverse requirements of 5G applications. SDN allows network operators to control the network

programmatically, while NFV allows network functions to be virtualized and deployed on commodity hardware.

SDN centralizes network control, enabling dynamic configuration and optimization. NFV virtualizes network functions, offering scalability and flexibility by running them on commodity hardware [32]. These technologies enable the creation of network slices, where virtualized network resources are partitioned to meet the specific needs of different applications and services [32]. 5G leverages software to manage and control the network, facilitating efficient resource allocation and management [32]. The softwarization of 5G enables the efficient utilization of its vast prospects and usability, ensuring reliable control in diverse scenarios. Decoupling the control plane from the user plane through SDN enables efficient and separate optimization of each plane [32]. SDN offers centralized network control through a programmable interface, while NFV virtualizes network functions on standard hardware, allowing flexible and scalable deployment of network services [46]. NFV and SDN stand out as essential components of the 5G architecture, enabling flexible network management and resource optimization [32].

In 5G NR, several key features revolutionize wireless communication, addressing the diverse and demanding requirements of modern applications.

1.3 5G NR Key Features

5G New Radio incorporates key technological advancements to meet its ambitious performance targets. 5G NR employs several key features to achieve its goals, including:

1.3.1 Flexible Numerology

5G NR introduces flexible numerology to accommodate diverse deployment scenarios and service requirements [4]. Unlike 4G LTE, which uses a fixed numerology, 5G NR supports multiple numerologies with varying subcarrier spacings and symbol durations [15]. Figure 1.3 illustrates the concept of scalable numerology in 5G NR, where different subcarrier spacings are used to support diverse service requirements.

This flexibility enables the network to adapt to different frequency bands, bandwidths, and latency requirements. 5G NR leverages a flexible numerology based on OFDM, allowing for the adjustment of subcarrier spacing to optimize performance in different scenarios. The selection of numerology depends on several factors, including the operating frequency band, channel conditions, and the desired trade-off between spectral efficiency and latency.

Smaller subcarrier spacing increases the symbol duration, improving robustness to delay spread in large coverage areas and mobility, but also increasing latency and reducing spectral efficiency. Conversely, larger subcarrier spacing reduces the symbol duration, decreasing latency and increasing spectral efficiency, but also making the system more susceptible to delay spread and phase noise. 5G NR's adoption of scalable subcarrier spacings, including 15, 30, 60, and 120 kHz, provides adaptability for various services and frequency bands [7]. The flexibility in choosing the numerology is crucial for supporting the diverse range of 5G use cases, including enhanced mobile broadband (eMBB), ultra-reliable low-latency communications, and massive machine-type communications. The adoption of OFDM in 5G NR ensures backward compatibility with 4G LTE systems [7]. The term numerology refers to the PHY waveform parametrization [77]. Subcarrier

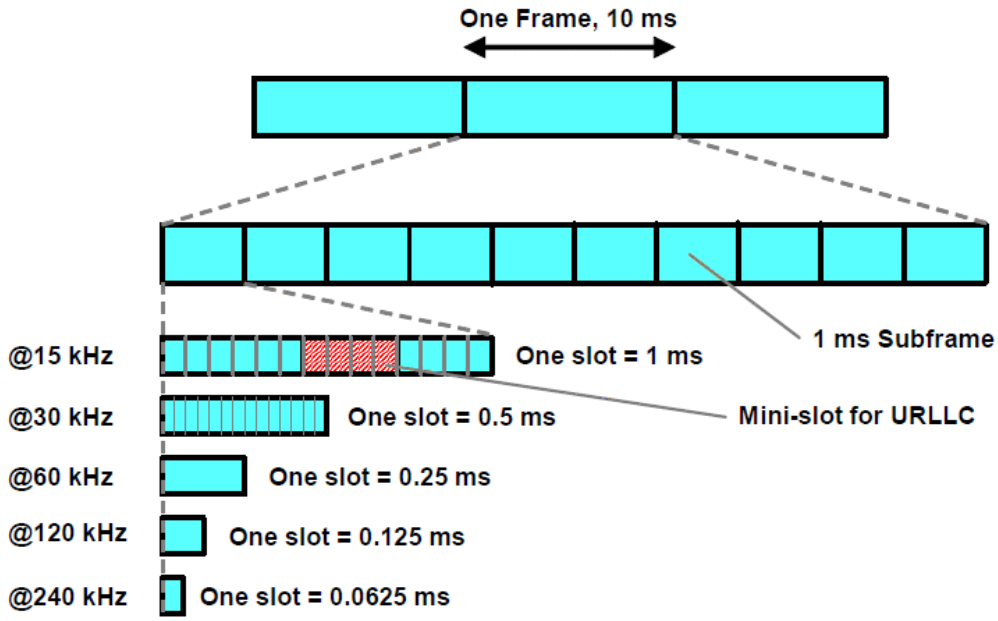

Figure 1.3: Scalable numerology in 5G NR[76].

spacing is the most important parameter when defining a numerology and impacts various parameters such as CP length, windowing, and filter characteristics [7].

The fundamental numerology of 5G NR is based on a subcarrier spacing of 15 kHz, which is the same as that used in 4G LTE. This numerology is suitable for many common use cases and provides a good balance between spectral efficiency and latency. 5G NR can also use smaller or larger subcarrier spacings to optimize performance for specific scenarios. For example, a smaller subcarrier spacing of 7.5 kHz can be used to improve coverage in rural areas, while a larger subcarrier spacing of 30 kHz can be used to reduce latency in ultra-reliable low-latency communications [7]. By dynamically adjusting the numerology based on the specific requirements of each service, 5G NR can achieve optimal performance across a wide range of applications.

1.3.2 Massive MIMO and advanced beamforming

Massive MIMO is a key enabler of 5G NR, allowing for significant improvements in network capacity, coverage, and energy efficiency. Massive MIMO is a technology that uses a large number of antennas at the base station to transmit and receive data simultaneously to multiple users.

By employing a large number of antennas, massive MIMO can focus the radio signal towards the intended user, improving signal strength, reducing interference, and enhancing network capacity. Massive MIMO leverages spatial multiplexing to transmit multiple data streams simultaneously over the same frequency band, increasing spectral efficiency and data throughput.

The principle behind massive MIMO is to exploit spatial diversity and multiplexing gains by using a large number of antennas at the base station. This enables the base station to transmit and receive data simultaneously to multiple users on the same frequency band, thereby increasing spectral efficiency and network capacity [78]. Massive MIMO improves energy efficiency by focusing the radio signal towards the intended user, reducing the amount of power wasted on unintended users or areas.

Massive MIMO can enhance spectrum and energy efficiency through beamforming and combining technology [4]. With the use of multiple antennas for transmission and reception, massive MIMO is considered to be one of the key technologies of 5G [4]. Beamforming is a technique that focuses the radio signal towards the intended user, improving signal strength and reducing interference [79]. Beamforming enables the targeted use of spectrum, which could result in uniform data speeds across the network [32]. The phased array also allows changing the phase of each element electronically, which can be used to steer the radio beam in a different direction to avoid interference coming from a specific direction [80]. Massive MIMO systems use advanced beamforming algorithms to optimize the direction and shape of the radio beams, further improving performance [4]. A comparison of different varieties of beamforming methodologies for determining the most efficient massive MIMO network is carried out in [81].

Massive MIMO networks are more resistant to interference and intentional jamming than current systems that only utilize a handful of antennas [32]. Therefore, it is more difficult to intercept massive MIMO communication, which is important for military applications. Figure 1.4 illustrates how Massive MIMO and beamforming techniques enable spatial multiplexing and improve signal quality in 5G systems, as described in [82]. Massive MIMO also enables spatial multiplexing, where multiple data streams are transmitted simultaneously over the same frequency band to different users.

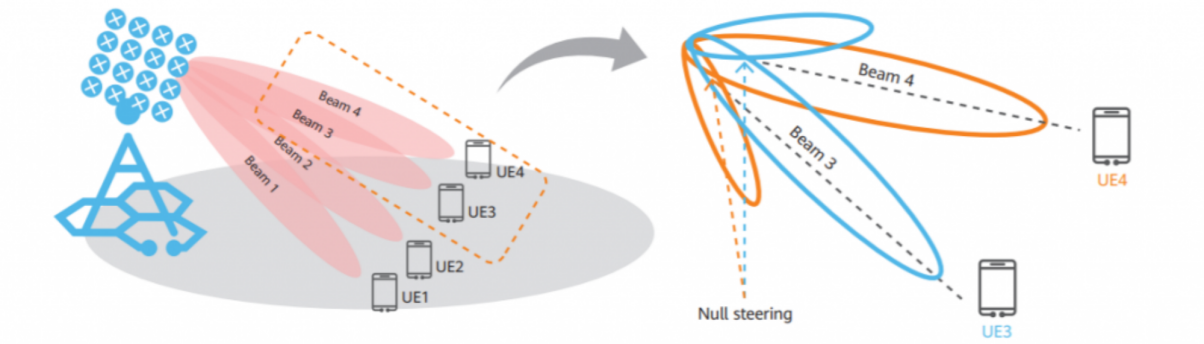

Figure 1.4: Massive MIMO and beamforming in 5G NR[32].

1.3.3 Mini-slot scheduling and preemption

Traditional LTE systems relied on fixed Transmission Time Intervals for scheduling and data transmission, which can introduce latency, especially for short packets. 5G NR introduces mini-slot scheduling to address this limitation by allowing for shorter and more flexible scheduling intervals. Mini-slot scheduling enables the transmission of data in shorter time intervals, reducing latency and improving responsiveness for delay-sensitive applications. Figure 1.5 illustrates the 5G NR mini-slot scheduling mechanism, where low-latency URLLC transmissions can preempt ongoing eMBB slots.

5G NR also supports preemption, which allows a high-priority transmission to interrupt a lower-priority transmission if needed. Preemption ensures that critical data is transmitted with minimal delay, even if other transmissions are already in progress.

These technologies have a lot of applications in future communication systems.

By combining mini-slot scheduling and preemption, 5G NR can provide ultra-reliable low-latency communication for critical applications such as industrial automation, remote surgery, and autonomous vehicles [3].

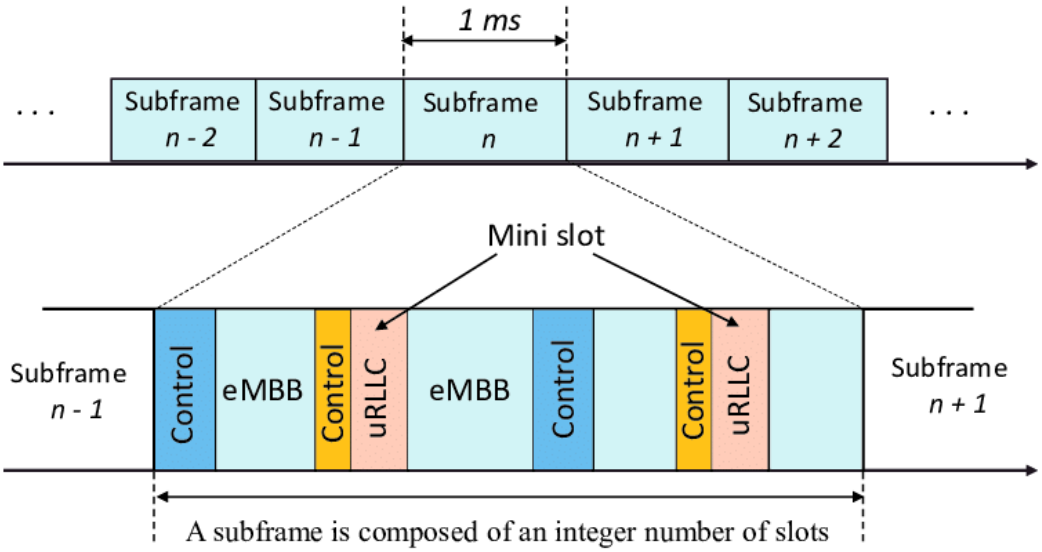

Figure 1.5: Illustration of 5G NR mini-slot scheduling and preemption [83].

5G NR also includes a variety of other features that improve performance and flexibility, such as carrier aggregation, dynamic spectrum sharing, and network slicing. By using these technologies, 5G NR can support a wide range of services and applications with different requirements.

The standardization of 5G wireless systems is still in its early stages, but it is already clear that this technology will have a major impact on the way we live and work [84].

1.3.4 Dynamic Time Division Duplexing (TDD)

5G NR adopts dynamic TDD to efficiently utilize radio resources by dynamically adjusting the allocation of uplink and downlink resources based on traffic demands [4]. Unlike traditional FDD and TDD systems with fixed uplink and downlink allocations, dynamic TDD enables flexible adaptation to changing traffic patterns and user demands [4]. Figure 1.5 illustrates the concept of 5G NR mini-slot scheduling and preemption, where short URLLC bursts can interrupt ongoing eMBB transmissions to meet latency constraints. This mechanism is standardized in 3GPP TS 38.300 [83]. Figure 1.6 depicts the principle of Dynamic TDD in 5G NR, which allows flexible switching between uplink and downlink slots based on traffic demand.

In 5G NR, dynamic TDD allows the network to allocate more resources to downlink when there is a higher demand for downlink traffic, such as video streaming or data downloads. Conversely, when there is a higher demand for uplink traffic, such as video conferencing or file uploads, the network can allocate more resources to uplink [4]. This adaptability ensures that network resources are utilized efficiently, improving overall system performance and user experience.

Compared to LTE, 5G NR shifts the UL and DL division based on OFDM symbols which makes it more efficient [4].

The use of TDD has become more widespread as the cost of FDD spectrum has increased.

In dynamic TDD, resource allocation between DL and UL can be dynamically adjusted which can provide significant performance improvements. The same frame structure will

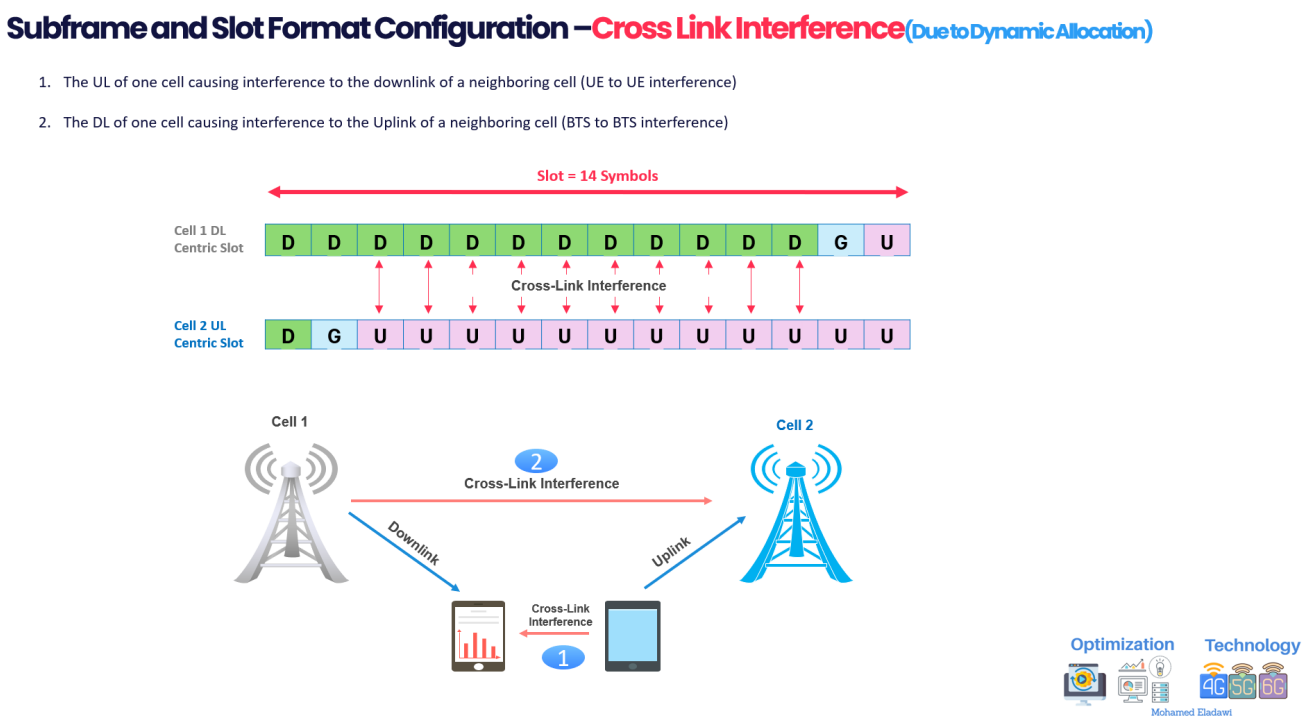

Figure 1.6: Dynamic TDD in 5G NR [85].

be used for both TDD and FDD in 5G NR networks, unlike LTE which employs two separate frames for TDD and FDD [4].

1.3.5 Carrier Aggregation

Carrier aggregation enables 5G NR to combine multiple component carriers to increase bandwidth and data rates [86]. By aggregating multiple carriers, 5G NR can provide wider bandwidths and higher data rates than would be possible with a single carrier [87].

The aggregated carriers can be either contiguous or non-contiguous in frequency, providing flexibility in spectrum allocation and utilization. Carrier aggregation also allows for the combination of carriers from different frequency bands, enabling the use of both low-band and high-band spectrum to improve coverage and capacity [4, 33, 88, 89].

This technology has been used in previous generations of wireless technology to increase the data rates and throughput of wireless networks.

By combining multiple component carriers, 5G NR can achieve higher data rates, improved spectral efficiency, and enhanced user experience, supporting a wide range of applications and services [3, 4, 23, 86]. Figure 1.7 illustrates the main types of carrier aggregation supported in 5G NR.

1.3.6 Network slicing

Network slicing is another key feature of 5G NR that allows for the creation of virtualized and isolated logical networks on a shared physical infrastructure. Network slicing enables operators to provide customized services and meet the specific requirements of different applications and use cases [32]. Figure 1.8 illustrates how 5G network slicing allows multiple logical networks to coexist over the same physical infrastructure, with each slice

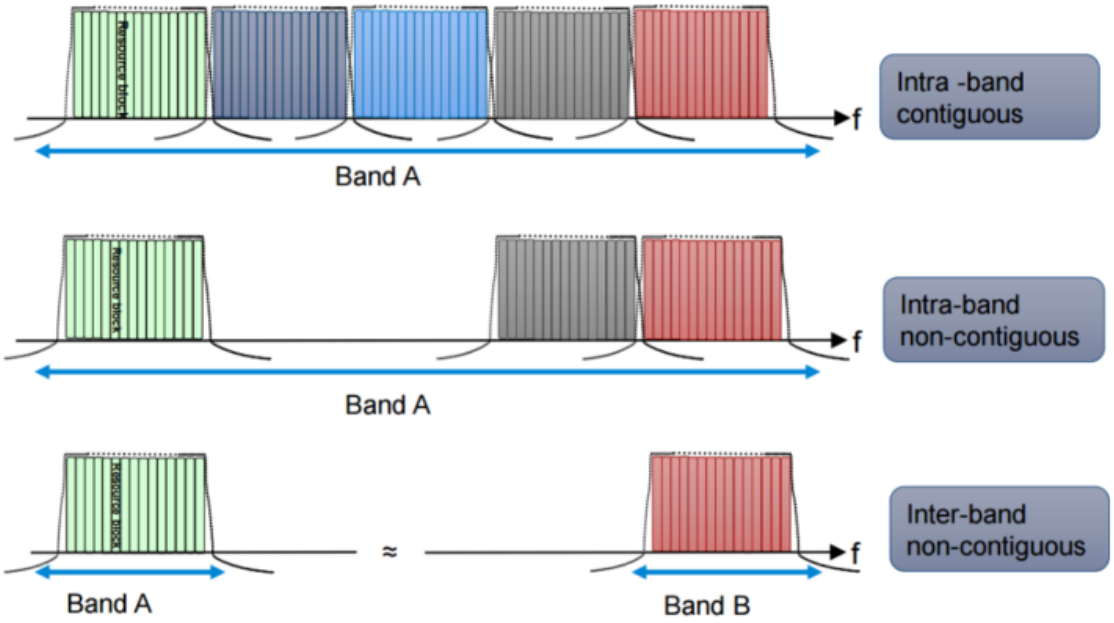

Figure 1.7: Types of carrier aggregation in 5G NR[90].

tailored to specific service requirements. The architecture and principles are standardized in 3GPP TS 23.501

Each network slice can be configured with its own dedicated resources, security policies, and quality of service parameters, providing isolation and independence between different services. For example, one network slice can be dedicated to enhanced mobile broadband (eMBB) services, providing high data rates and low latency for video streaming and online gaming. Another network slice can be dedicated to ultra-reliable low-latency communications for industrial automation and autonomous vehicles [92].

Network slicing enables operators to offer differentiated services, optimize network performance, and monetize their infrastructure by supporting a wide range of applications and use cases with varying requirements [32].

Network slicing is defined as a bundle of services, a logical network, a type of virtual networking architecture or a chain of network functions created on top of a cloud infrastructure [93].

The radio access network should enable the dynamic creation of network slices as well as the ability to combine network slices [92].

Technologies such as Software-Defined Networks and Network Function Virtualization are key enablers to the implementation of network slicing [32].

These features collectively contribute to the enhanced capabilities of 5G NR, enabling it to meet the diverse and demanding requirements of modern wireless communication systems [94].

1.3.7 Grant-free access and Low-Power Wide-Area Networks

5G NR incorporates grant-free access mechanisms to reduce latency and signaling overhead for IoT devices and other low-power devices. In traditional cellular networks, devices need to request a grant from the base station before transmitting data, which can add delay and consume significant energy.

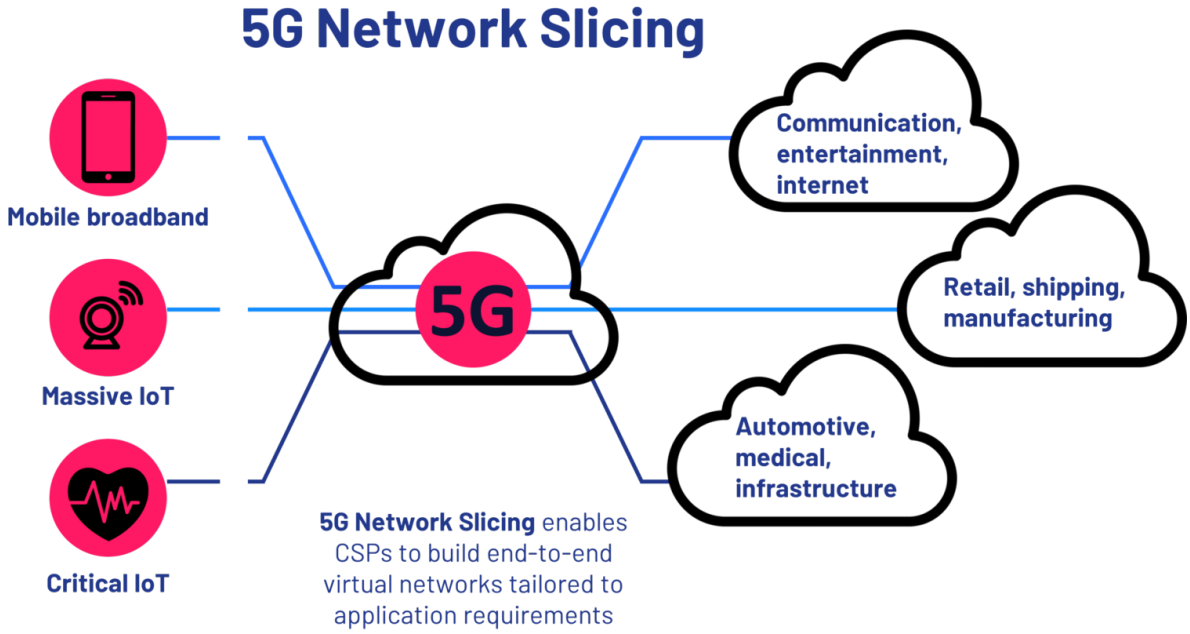

Figure 1.8: 5G network slicing[91].

Grant-free access allows devices to transmit data without explicitly requesting a grant, reducing latency and improving energy efficiency .

5G NR also supports Low-Power Wide-Area network technologies such as Narrowband IoT and enhanced Machine-Type Communication (eMTC) to enable connectivity for a massive number of IoT devices with low power consumption and wide-area coverage. These technologies are designed to support a wide range of IoT applications, such as smart metering, environmental monitoring, and asset tracking [3]. Figure 1.9 compares grant-based and grant-free uplink transmissions in 5G NR. Grant-based transmissions require scheduling requests and uplink grants, while grant-free transmissions allow pre-configured, low-latency access.

Table 1.3 summarizes how the major 5G NR features are mapped to the three ITU-defined use cases: enhanced Mobile Broadband (eMBB), Ultra-Reliable Low-Latency Communications (URLLC), and massive Machine-Type Communications (mMTC).

These features collectively provide the technical bedrock for 5G NR's ability to deliver targeted performance across vastly different service categories. Rather than serving a single traffic profile, 5G NR empowers the network to dynamically mold itself around real-time requirements, enabling seamless service convergence across verticals. To support this flexibility at the physical layer, 5G NR employs a range of multiple access techniques tailored to the specific demands of each use case. In the following section, we delve into these multiple access methods and explore how they contribute to the efficient utilization of radio resources in 5G networks.

1.4 Multiple Access Techniques in Cellular Networks

Multiple access techniques enable simultaneous communication by multiple users over a shared communication medium. Each mobile network generation introduced different multiple access strategies to meet growing demands for spectral efficiency, user capacity,

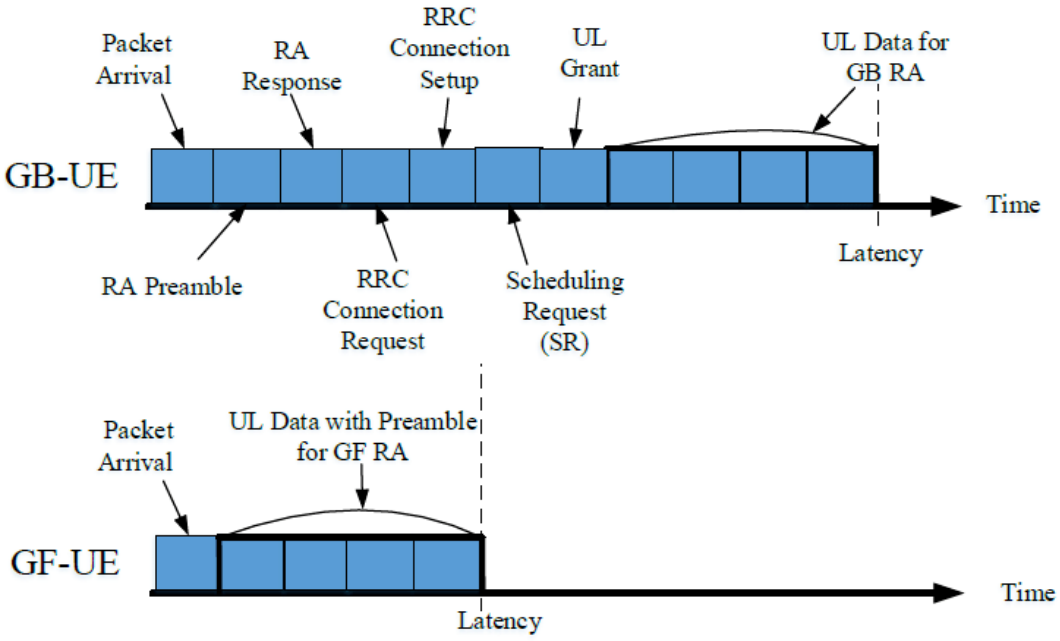

Figure 1.9: grant-based .vs. grant-free uplink transmissions in 5G NR[85].

Table 1.3: Mapping of Key 5G NR Features to Major Use Cases[83]

5G NR Feature	**eMBB**	**URLLC**	**mMTC**
Scalable Numerology	✓	✓	✓
Mini-Slot Scheduling		✓	
Massive MIMO and Beamforming	✓	✓	
Network Slicing	✓	✓	✓
Dynamic TDD	✓	✓	
Carrier Aggregation	✓		
Flexible Frame Design	✓	✓	✓
mmWave Support	✓	✓	
Grant-Free Access		✓	✓
Low-Power Wide-Area (LPWA) Support			✓

and service quality. The International Telecommunication Union establishes standards like FDMA, TDMA, CDMA and OFDMA for wireless communication [95]. The evolution from Frequency Division Multiple Access to Non-Orthogonal Multiple Access represents a significant paradigm shift in cellular network design, driven by the relentless pursuit of higher spectral efficiency and massive connectivity [96].

1.4.1 Legacy Techniques: From FDMA to CDMA

Early generations of cellular networks relied on orthogonal resource separation strategies to support multi-user access. These approaches are illustrated in Figure 1.10 , and each evolved to address the shortcomings of its predecessor.

- **FDMA (Frequency Division Multiple Access):** FDMA divides the available spectrum into distinct frequency bands, allocating each band to a different user, preventing interference by ensuring that users transmit on non-overlapping frequencies [95]. In FDMA, a carrier frequency is assigned to a single user, where the channel is occupied by the single user for the entire duration of the call [95]. Lower frequencies are used in mobile devices because propagation decay is logarithmic as a function of frequency [95]. It was deployed in first-generation (1G) cellular systems like AMPS, but its spectral efficiency is limited because of the rigid frequency allocation and the need for guard bands between channels [95]. .
- **TDMA (Time Division Multiple Access):** TDMA allows multiple users to share the same frequency channel by allocating different time slots to each user, where each user transmits in its assigned time slot, and the receiver extracts the data by listening only during the corresponding time slot. It was adopted in 2G systems like GSM, offered improved spectral efficiency compared to FDMA by allowing multiple users to share the same frequency channel, but it still suffers from limitations in terms of the number of users that can be supported simultaneously. [95, 97] . Moreover, as user demand grows and services like messaging and data begin to dominate, TDMA's rigid structure becomes a bottleneck. These limitations necessitated a solution where all users could access the spectrum simultaneously and more flexibly, a challenge addressed by CDMA.
- **CDMA (Code Division Multiple Access):** The key technology behind 3G networks such as WCDMA. enables multiple users to transmit simultaneously over the same frequency band by assigning a unique orthogonal code to each user [95]. The signals from different users are separated at the receiver using these orthogonal codes [95]. CDMA, employed in 3G systems like IS-95, further enhanced spectral efficiency and offered better resilience to interference, becoming a cornerstone of 3G technology by allowing multiple users to transmit simultaneously over the same frequency band.

While these orthogonal multiple access schemes provided a solid foundation for early cellular networks, their spectral efficiency is fundamentally limited by the orthogonal nature of the resource allocation, which prevents full utilization of the available spectrum when user activity is bursty or channel conditions vary significantly.

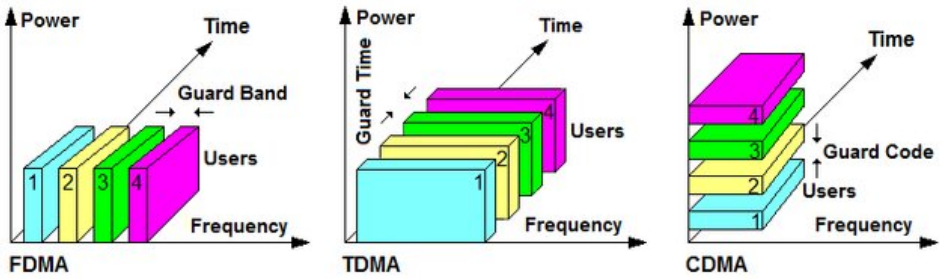

Figure 1.10: FDMA,TDMA and CDMA[98]

1.4.2 OFDMA and SC-FDMA in 4G

To address the limitations of CDMA, particularly its poor scalability and sensitivity to power imbalance, 4G LTE introduced more advanced multiple access techniques: OFDMA for the downlink and SC-FDMA for the uplink. Figure 1.11 compares OFDMA and SC-FDMA as employed in the LTE downlink and uplink, respectively. SC-FDMA was specifically chosen for the uplink to reduce the Peak-to-Average Power Ratio (PAPR), making it more power-efficient for mobile devices.

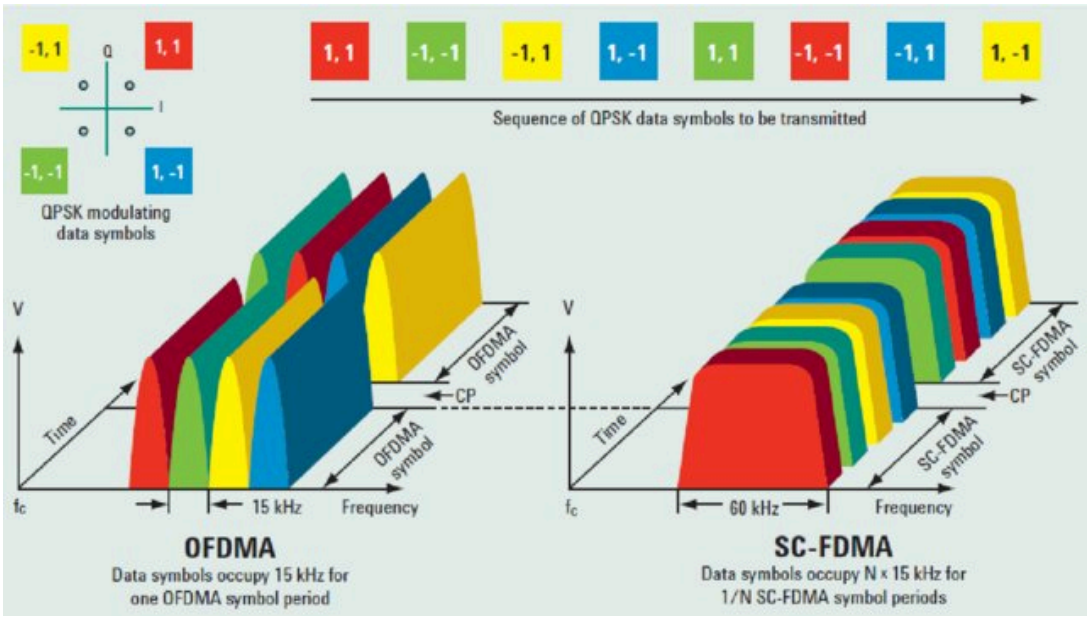

Figure 1.11: Comparison of OFDMA and SC-FDMA used in 4G LTE [99]

- **OFDMA (Orthogonal Frequency Division Multiple Access):** OFDMA is a multi-carrier transmission scheme where the available bandwidth is divided into multiple orthogonal subcarriers, and each subcarrier is allocated to a different user. OFDMA is an extension of FDMA, where each frequency band is placed at the null of the adjacent frequency band [95].

  OFDMA was adopted in 4G LTE systems, offering significant improvements in spectral efficiency and flexibility compared to its predecessors [100]. It allows for dynamic allocation of subcarriers to users based on their channel conditions and traffic demands, enabling efficient use of the available spectrum and support for a

large number of users [101]. WiMAX and LTE protocols use the OFDMA multiple access technique [95].

- **SC-FDMA (Single Carrier Frequency Division Multiple Access):** To overcome the PAPR drawback in the uplink, LTE uses SC-FDMA for transmissions from user equipment (UE). As shown on the right side of the figure, SC-FDMA applies a DFT precoding stage that spreads each symbol over the assigned subcarriers. This results in a time-domain signal with a single-carrier structure, reducing PAPR. Although SC-FDMA slightly limits scheduling granularity compared to OFDMA, it is better suited for power-constrained devices and provides efficient uplink operation with good spectral efficiency[101].

While OFDMA provides orthogonal access through subcarrier partitioning, SC-FDMA uses DFT-spreading to reduce PAPR for uplink transmission. To boost spectral efficiency, advanced approaches like multiple-input multiple-output and beamforming have been integrated with orthogonal multiple access schemes. Single-carrier FDMA is a variation of OFDMA used in the uplink of LTE systems, where it offers advantages in terms of power efficiency compared to OFDMA. Despite their widespread adoption, OFDMA and SC-FDMA still have limitations in terms of spectral efficiency, particularly in scenarios with high user density and diverse channel conditions.

1.4.3 Modern Techniques in 5G Networks

Building upon the success of OFDMA in 4G, 5G New Radio (NR) extends and adapts orthogonal access methods while introducing non-orthogonal schemes to address the demands of emerging use cases. These techniques aim to support enhanced mobile broadband (eMBB), ultra-reliable low-latency communications (URLLC), and massive machine-type communications (mMTC)[4].

- **OFDMA with Flexible Numerology:** In 5G NR, OFDMA remains the primary access scheme for both downlink and uplink, but with enhanced flexibility. The subcarrier spacing Δf is scalable according to $\Delta f = 15 \times 2^k$ kHz, with $k \in \{0, 1, 2, 3, 4\}$, allowing the frame structure to adapt to different latency and bandwidth requirements. For instance, low-latency applications can use wider spacing (e.g., 60 kHz), while narrowband IoT traffic may use 15 kHz. Additionally, the concept of Bandwidth Parts (BWPs) enables users to operate on tailored frequency segments within a wider carrier bandwidth, reducing UE complexity and energy consumption. Despite its flexibility, orthogonal resource allocation remains inherently limited in spectral efficiency, particularly under massive connectivity[4].

- **NOMA (Non-Orthogonal Multiple Access):** To overcome the spectral limitations of orthogonal schemes like OFDMA, 5G introduces Non-Orthogonal Multiple Access (NOMA) as an optional multi-user access strategy. Unlike traditional methods that strictly allocate orthogonal resources to each user, NOMA allows multiple users to share the same time-frequency resources by differentiating them either in power or code domains. This enables increased spectral efficiency, better user fairness, and support for massive connectivity[48, 102].

  - **Power-Domain NOMA:** In power-domain NOMA, the base station superimposes signals for different users on the same subcarrier by assigning them

different power levels. Typically, users with poor channel conditions (e.g., cell-edge users) are allocated more power, while those with better channels receive less. At the receiver side, users equipped with Successive Interference Cancellation (SIC) can decode the stronger signal first, subtract it, and then decode the weaker one

Figure 1.12 illustrates the concept of power-domain NOMA, where users are multiplexed in the power domain and distinguished at the receiver using successive interference cancellation (SIC). This access technique has been proposed as a key enabler of massive connectivity in 5G and beyond. UE-2 receives a strong signal and decodes its own data directly. UE-1, however, first performs SIC to remove UE-2's signal before decoding its own. This layered decoding approach allows users to coexist non-orthogonally within the same resource block.

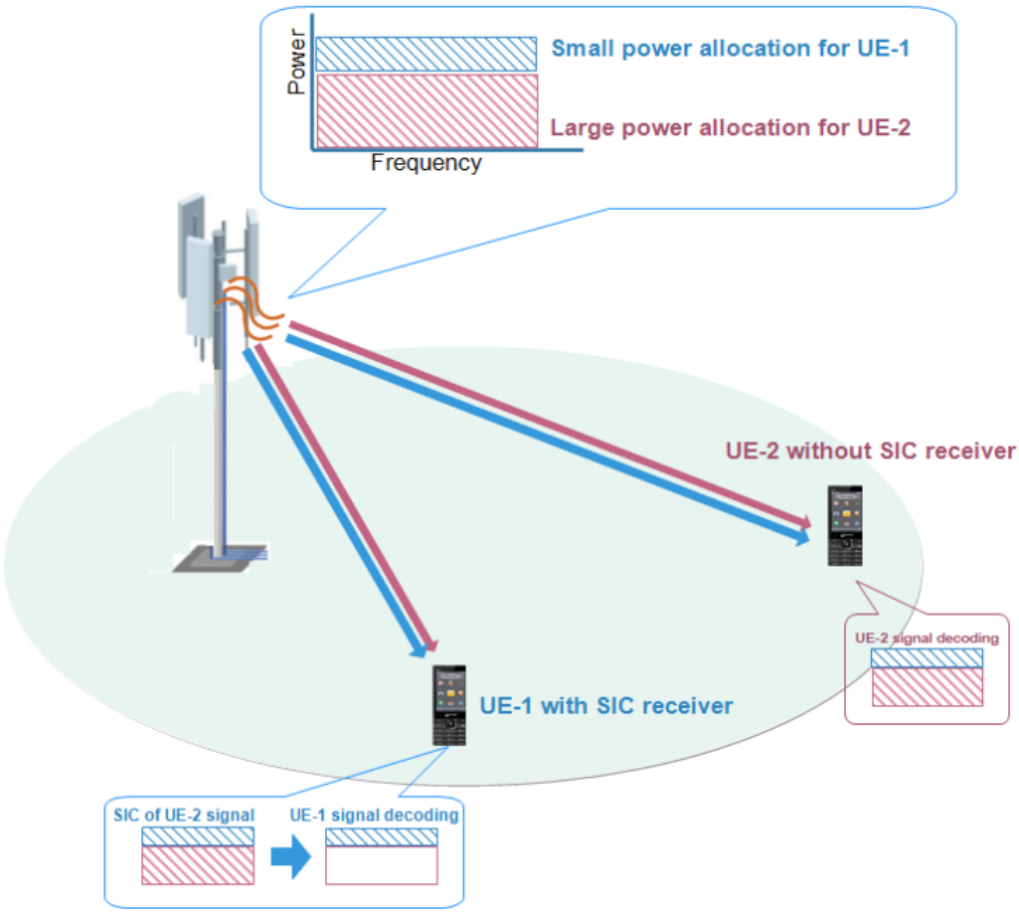

Figure 1.12: Power-domain NOMA[103].

– **Code-Domain NOMA (e.g., Sparse Code Multiple Access (SCMA)):** In contrast to power-domain NOMA, code-domain NOMA distinguishes users by assigning them unique sparse codebooks. A prominent example is Sparse Code Multiple Access (SCMA), where each user's bitstream is first encoded and then mapped onto a sparse multi-dimensional codeword from a predefined codebook[104].

  Figure 1.13 shows the principle of code-domain NOMA using Sparse Code Multiple Access (SCMA), where users are separated via distinct sparse codebooks

over shared resource elements. SCMA enables efficient multi-user detection with low-complexity receivers using the message passing algorithm. Multiple users' symbols are transmitted over the same subcarriers and OFDM symbols but are differentiated by sparse spreading patterns. The receiver performs multi-user detection using the Message Passing Algorithm (MPA), which efficiently decodes overlapping signals by leveraging codeword sparsity.

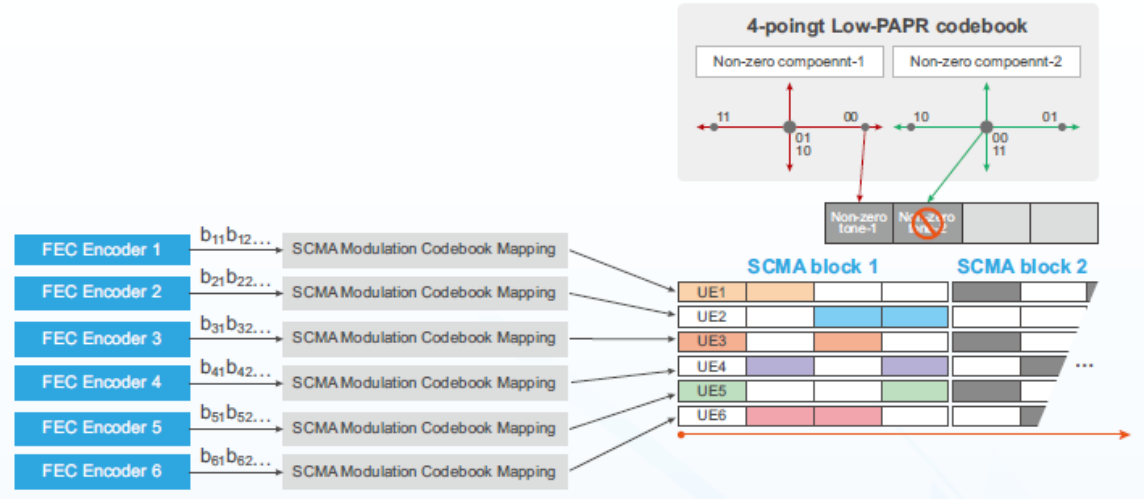

Figure 1.13: Code Domain NOMA: SCMA [105]

Advantages of NOMA:

* Increased spectral efficiency and system throughput.
* Improved performance for cell-edge users.
* Enhanced support for massive access in mMTC scenarios.

Challenges of NOMA:

* Receiver complexity increases due to SIC and joint detection.
* Performance is sensitive to power allocation and channel estimation errors.
* Optimal pairing of users with disparate channel conditions is essential but non-trivial.

While NOMA presents theoretical benefits, its practical deployment is currently more suitable for specific contexts, such as IoT, ultra-dense networks, or environments where user devices have significantly different link qualities.

1.5 OFDMA and Modulation Schemes in 5G NR

Orthogonal Frequency Division Multiple Access (OFDMA) forms the backbone of both downlink and uplink transmissions in 5G New Radio (NR). Combined with advanced modulation techniques, OFDMA enables high spectral efficiency, robust

multi-user access, and adaptability to diverse service requirements such as enhanced Mobile Broadband (eMBB), Ultra-Reliable Low-Latency Communications (URLLC), and massive Machine-Type Communications (mMTC)[3, 77, 102].

Figure 1.14 illustrates the complete end-to-end transmission and reception chain for Orthogonal Frequency Division Multiple Access (OFDMA) in 5G New Radio (NR). On the left, the transmitter processing stages map raw data bits onto OFDM waveforms using a sequence of coding, modulation, and transformation blocks. On the right, the receiver reverses this process to recover the original bitstream. In between, the signal undergoes channel effects such as fading and noise.

In the following subsections, we provide a step-by-step breakdown of each block in this diagram, from bitstream generation and modulation to IFFT processing and cyclic prefix insertion at the transmitter, and from cyclic prefix removal to decoding at the receiver. This detailed exposition highlights how 5G NR leverages OFDMA's structure and flexibility to meet diverse service requirements across a wide range of channel conditions.

1.5.1 Input Bitstream

The transmission process begins with the generation of the **input bitstream**, which represents the raw data to be transmitted over the air. This bitstream can originate from various sources such as user data (e.g., application-layer packets), control signaling (e.g., scheduling requests), or reference signals required for channel estimation and synchronization[4, 106, 107].

In 5G NR, the bitstream is structured into **transport blocks** (TBs), each of which is processed independently through the physical layer. The size of a transport block depends on several factors, including modulation and coding scheme (MCS), the allocated bandwidth part (BWP), and the number of assigned resource blocks[7, 108, 109].

At this stage, no physical-layer transformation has yet occurred, the bits are a sequential stream of information, agnostic to modulation or transmission format. These bits will soon undergo channel coding and modulation tailored to link conditions and quality-of-service (QoS) requirements[33, 110, 111].

The bitstream is also the point at which logical channels (e.g., for data or signaling) are multiplexed and passed to the physical layer, where prioritization, segmentation, and scheduling begin to take effect[110, 112, 113].

1.5.2 Channel Coding (LDPC / Polar)

Once the input bitstream is prepared, the next stage is **channel coding**, which introduces controlled redundancy to protect the information against errors caused by noise, fading, and interference during transmission[19, 114].

In 5G NR, two types of forward error correction (FEC) codes are employed:

- **Low-Density Parity-Check (LDPC) Codes**: Used for data channels (i.e., PDSCH for downlink and PUSCH for uplink). LDPC codes are block-based

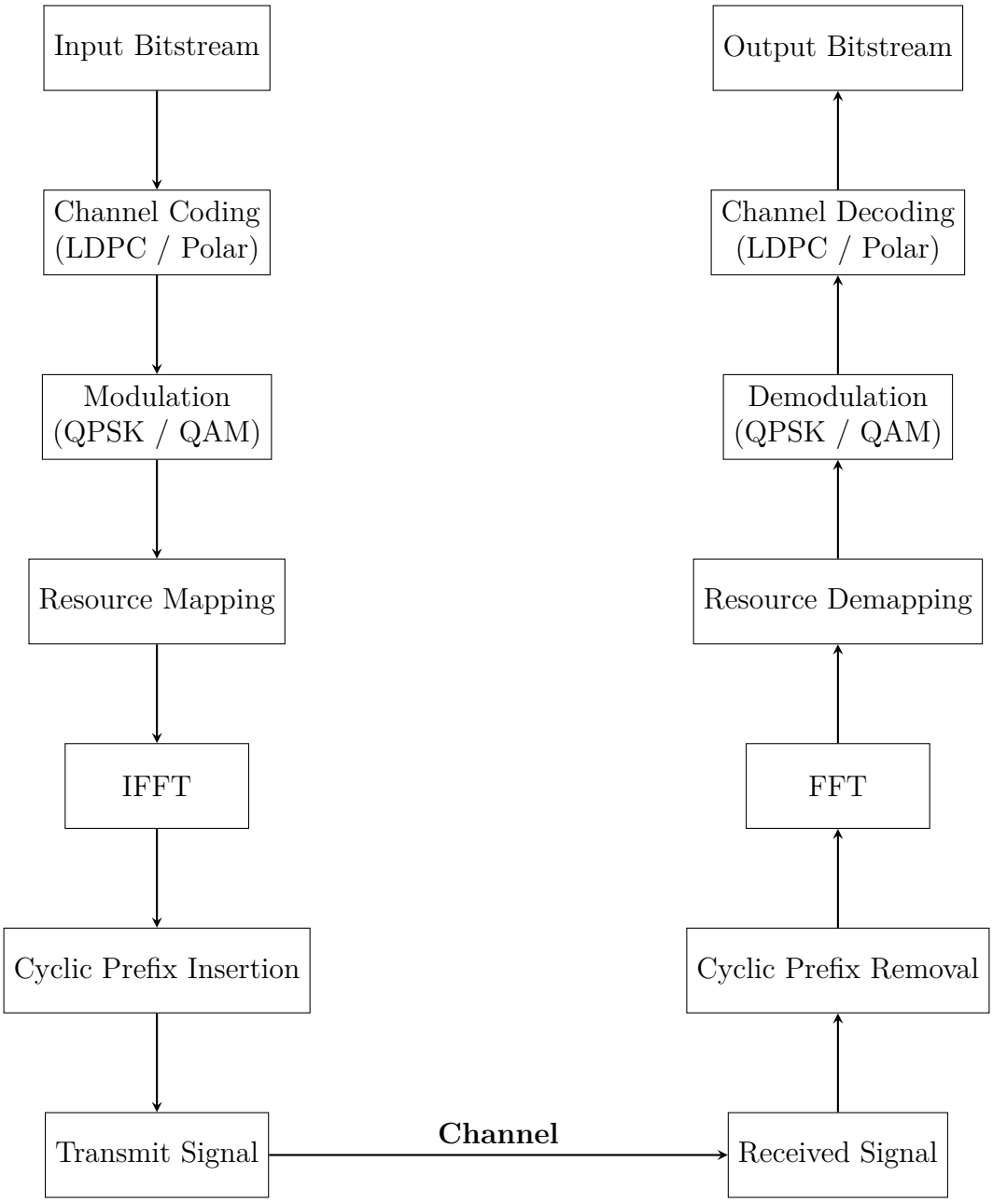

Figure 1.14: OFDMA Trasceiver Chain in 5G NR.

linear error correcting codes characterized by sparse parity-check matrices. They provide excellent performance near the Shannon limit and support parallelizable decoding algorithms, making them highly suitable for high-throughput data transmission[19, 48, 115].

– **Polar Codes**: Applied to control channels (e.g., PDCCH and PUCCH). Polar codes are capacity-achieving block codes that exploit the phenomenon of channel polarization. They are particularly well-suited for short block lengths and low latency applications. Successive cancellation list decoding enhances their error correction performance[116, 117].

The channel coding process typically includes:

1. **Segmentation**: Large transport blocks may be split into smaller code blocks to facilitate parallel processing and decoding.
2. **CRC Insertion**: A cyclic redundancy check is appended to detect errors during decoding.
3. **Encoding**: Each block is passed through either an LDPC or Polar encoder.
4. **Rate Matching**: The output is adjusted to fit the number of available resource elements (e.g., through puncturing or repetition).

This stage ensures robust protection of data, balancing redundancy and spectral efficiency depending on channel conditions and service requirements.

1.5.3 Modulation Schemes in 5G NR

Modulation plays a critical role in determining how digital bitstreams are mapped onto complex symbols for transmission. In 5G NR, the modulation scheme is dynamically selected based on channel quality indicators (CQI) reported by the receiver, enabling adaptive modulation and coding (AMC) to maximize throughput while ensuring link reliability[118, 119].

Figure 1.15 illustrates the typical spatial deployment of modulation schemes in a 5G NR cell. As users move farther from the base station and signal quality degrades, the modulation scheme becomes progressively more robust to maintain link reliability.

A.Supported Modulation Formats

5G NR supports the following modulation schemes[48]:

– **QPSK (Quadrature Phase Shift Keying):** Encodes 2 bits per symbol by modulating the carrier phase across four discrete values. Due to its robustness against noise and low SNR tolerance, QPSK is widely used for control channels and in ultra-reliable low-latency communication (URLLC).

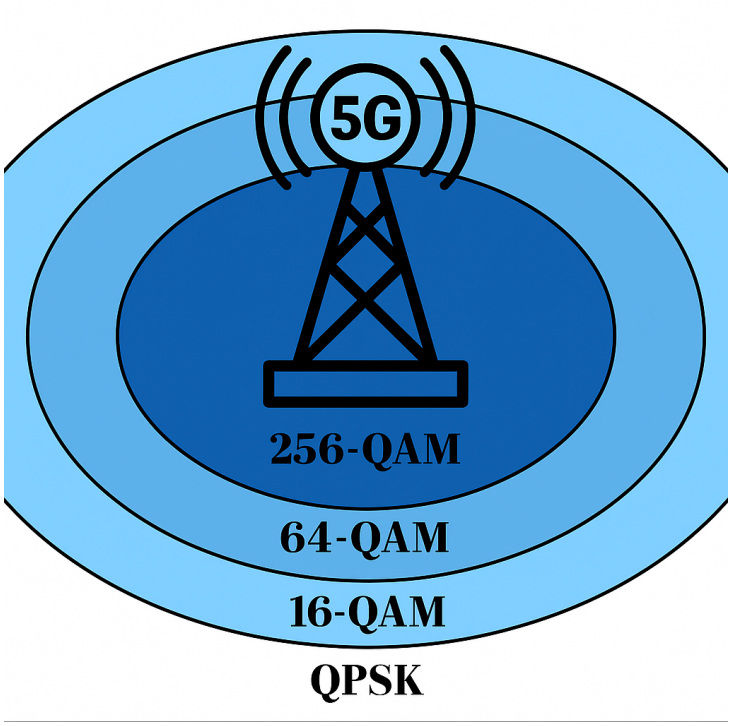

Figure 1.15: Modulation schemes in 5G NR.

- **16-QAM (Quadrature Amplitude Modulation):** Maps 4 bits per symbol using a grid of 16 points in the I/Q plane. It offers a good trade-off between spectral efficiency and robustness, making it suitable for moderate channel conditions.
- **64-QAM:** Encodes 6 bits per symbol over 64 constellation points. It is effective for enhanced Mobile Broadband (eMBB) scenarios under favorable SNR conditions.
- **256-QAM:** Maps 8 bits per symbol onto a dense 16×16 constellation. This scheme achieves high spectral efficiency but requires excellent link quality and is mostly used in the downlink.

B.Mathematical Representations

- **QPSK:**

$$s_k = A \cdot e^{j\phi_k}, \quad \phi_k \in \left\{0, \frac{\pi}{2}, \pi, \frac{3\pi}{2}\right\}$$

  where each phase corresponds to a unique 2-bit pair.

- **M-QAM:**

$$s_k = a_k + jb_k, \quad a_k, b_k \in \left\{\pm 1, \pm 3, \ldots, \pm(\sqrt{M} - 1)\right\}$$

  Each M-QAM symbol is selected from a square constellation of M points and normalized to ensure uniform average symbol energy.

C.Impact on Performance

The choice of modulation affects key performance indicators such as[118]:

- **Spectral Efficiency:** Higher-order QAM formats (e.g., 256-QAM) allow more bits per symbol, thus increasing throughput.
- **SNR Requirements:** As modulation order increases, minimum required SNR for reliable decoding also increases.
- **Error Resilience:** Lower-order schemes (e.g., QPSK) are more resilient to noise and multipath fading, making them preferable in poor channel conditions.
- **Power Amplifier Efficiency:** Higher-order QAM leads to a higher Peak-to-Average Power Ratio (PAPR), complicating RF chain design, especially for uplink transmissions.

D. Constellation Diagrams

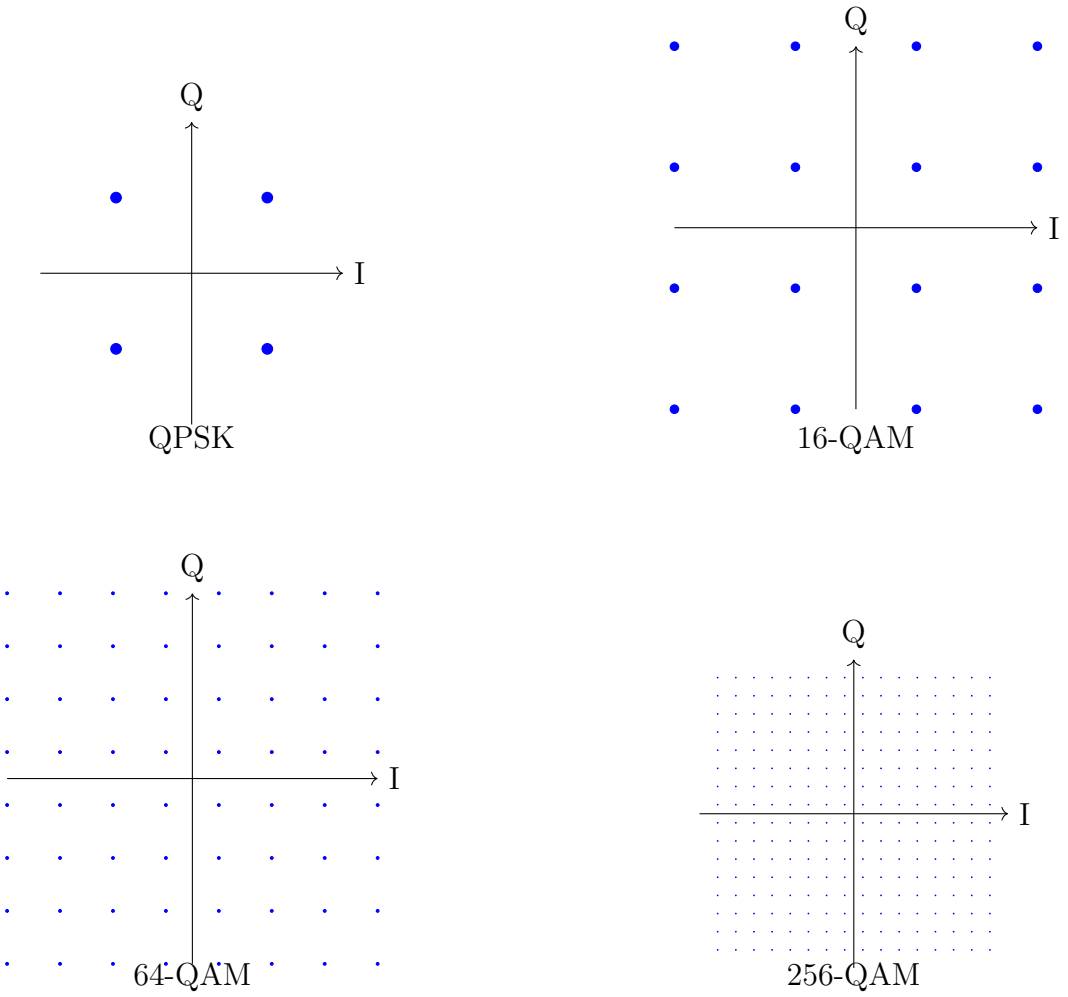

Figure 1.16: Constellation diagrams.

These constellations illustrate the increasing symbol density associated with higher-order modulation schemes. As the number of bits per symbol increases, from 2 in QPSK to 8 in 256-QAM, spectral efficiency improves, enabling higher data rates. However, this also reduces the Euclidean distance between constellation points, making the signal more sensitive to noise, distortion, and fading effects, particularly at the cell edge.

1.5.4 Resource Mapping in 5G NR

In 5G New Radio (NR), the time-frequency structure is organized as a **resource grid**, where each unit of transmission occupies one **Resource Element (RE)**, the smallest physical resource, defined by the intersection of a single subcarrier (frequency domain) and one OFDM symbol (time domain). A group of 12 consecutive subcarriers over one slot (typically 14 OFDM symbols) forms a **Resource Block (RB)**, the basic scheduling unit in both downlink and uplink. A higher-level structure called the **Bandwidth Part (BWP)** is composed of multiple contiguous RBs and allows the network to operate multiple numerologies within the same carrier bandwidth, enabling flexible and power-efficient allocation[46].

Figure 1.17 illustrates the 5G NR resource grid, showing the mapping of key physical channels and signals across two slots in a 10 ms frame. This resource allocation structure is defined in 3GPP TS 38.211 .

Each 1 ms subframe consists of one or more slots (typically 14 OFDM symbols per slot), depending on the subcarrier spacing defined by the selected numerology. The figure provides a slot-level view of how various physical channels and reference signals are mapped in both time and frequency[109, 120]:

- **PSS/SSS (Primary and Secondary Synchronization Signals):** Indicated in purple and green, these are transmitted once per frame and assist the UE in achieving synchronization with the base station.
- **PBCH (Physical Broadcast Channel):** Shown in dark blue, PBCH carries the Master Information Block (MIB) and is transmitted along with the PSS/SSS during the synchronization signal block (SSB).
- **PBCH DMRS (Demodulation Reference signals):** These Demodulation Reference Signals are associated with PBCH and assist in channel estimation for decoding the MIB.
- **PDCCH (Physical Downlink Control Channel):** This channel occupies the beginning OFDM symbols in each slot and carries scheduling assignments and control information.
- **PDCCH DMRS :** Embedded within PDCCH regions, they support coherent demodulation of the control channel.
- **PDSCH (Physical Downlink Shared Channel):** PDSCH carries user data. It is dynamically scheduled across the available frequency-time resources.

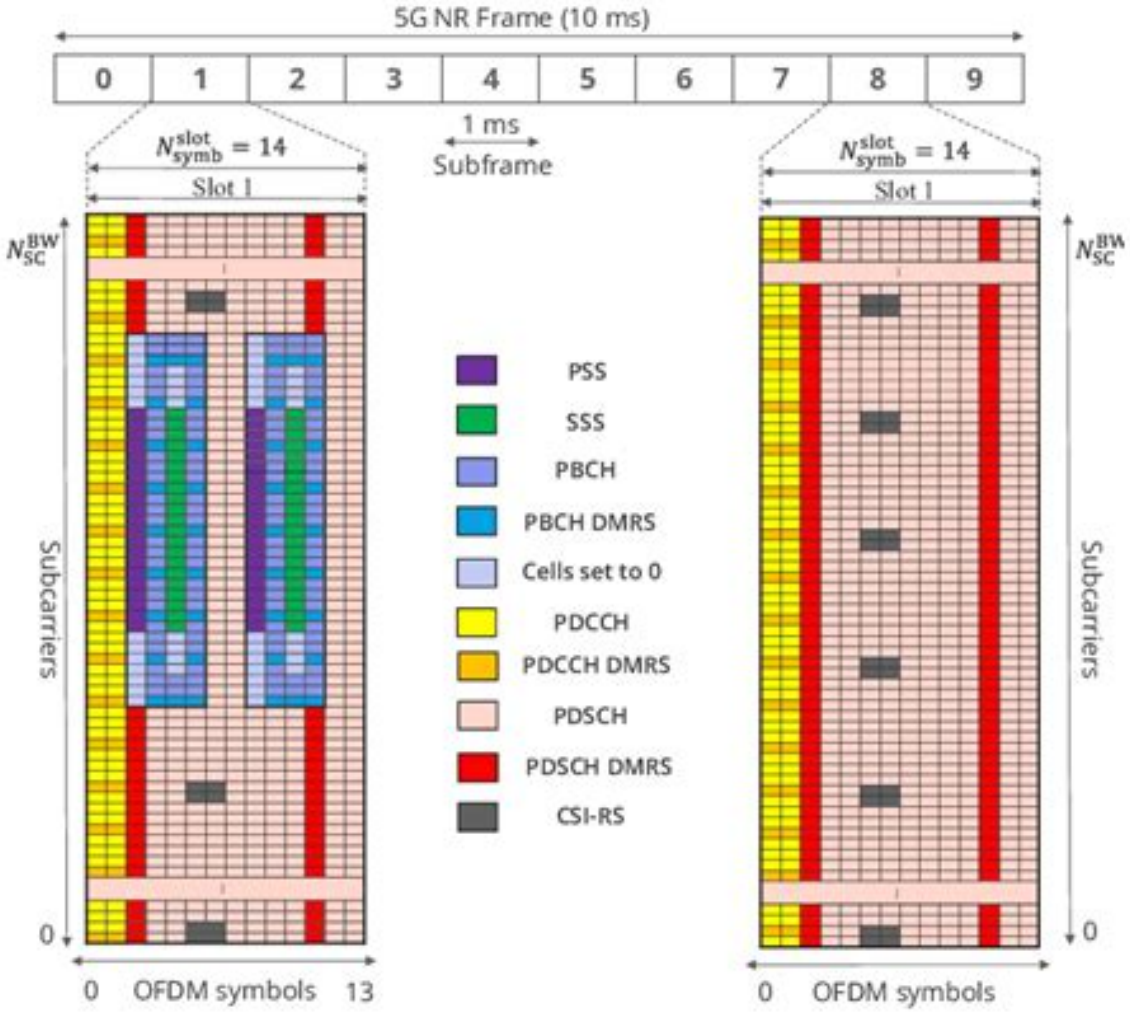

Figure 1.17: 5G NR resource grid [76]

- **PDSCH DMRS (Dark Red):** Used for channel estimation when decoding the PDSCH data.
- **CSI-RS (Channel State Information Reference Signals):** Shown in gray, these provide the UE with information to estimate channel quality for link adaptation and beam management.

This mapping strategy provides high flexibility in resource scheduling, allowing the network to dynamically allocate control, data, and reference signals based on traffic demand, QoS requirements, and channel conditions. Additionally, such mapping ensures backward compatibility, numerology coexistence, and efficient use of spectrum within a unified OFDMA-based frame structure.

A.Mapping Procedure and Scheduling

The 5G NR scheduler dynamically assigns Resource Blocks (RBs) to users based on multiple criteria [121, 122] :

- Quality-of-Service (QoS) requirements such as eMBB, URLLC, or mMTC,
- Channel conditions via Channel Quality Indicator (CQI) feedback,
- Transmission Time Interval (TTI) granularity, e.g., full slot or mini-slot-based scheduling,
- Interference constraints, especially in multi-numerology environments.

Control channels like the Physical Downlink Control Channel (PDCCH) are always prioritized and mapped at the beginning of the slot, as they carry scheduling grants and HARQ feedback. Once control regions are allocated, the remaining RBs are used for data channels (PDSCH) and uplink transmissions (PUSCH). Demodulation reference signals (DMRS), phase tracking reference signals (PTRS), and channel state information reference signals (CSI-RS) are inserted according to standard-defined patterns and help maintain robust channel estimation and tracking [114, 123].

Each Bandwidth Part (BWP) defines a contiguous block of RBs within a carrier and enables numerology-specific scheduling. The number of RBs in a BWP depends on:

- The total bandwidth (e.g., 20 MHz, 100 MHz),
- The subcarrier spacing (e.g., 15 kHz, 30 kHz, 60 kHz).

For example:

- A 20 MHz bandwidth with 15 kHz subcarrier spacing supports up to **106 RBs**,
- A 100 MHz bandwidth with 30 kHz spacing allows up to **273 RBs**,

– Wider bandwidths with higher subcarrier spacing (e.g., 120 kHz) are used in FR2 (mmWave) and allow BWPs of over **300 RBs**.

Resource mapping bridges modulation and waveform generation by assigning complex QAM symbols to resource elements (REs) in a two-dimensional grid, while ensuring orthogonality, spectral efficiency, and timing alignment. This flexible design enables 5G NR to serve highly diverse traffic profiles, from massive IoT to ultra-reliable low-latency and gigabit broadband, all within the same unified OFDMA-based air interface[77, 124]. Table 1.4 presents the maximum number of resource blocks (RBs) supported per bandwidth part (BWP) under various subcarrier spacing configurations in 5G NR.

Table 1.4: Maximum Number of Resource Blocks (RBs) per Bandwidth Part in 5G NR[125]

Bandwidth (MHz)	**Subcarrier Spacing (kHz)**	**FFT Size**	**Max RBs**
5	15	512	25
10	15	1024	52
15	15	1024	79
20	15	2048	106
40	30	2048	133
50	30	4096	162
100	30	4096	273
100	60	4096	136
200	60	8192	273
400	120	8192	264

1.5.5 IFFT and Time-Domain Conversion

After mapping complex modulation symbols onto subcarriers in the frequency domain, 5G NR uses an Inverse Fast Fourier Transform (IFFT) to convert them into a composite time-domain signal. This step is essential for creating the OFDM waveform, where each subcarrier contributes a sinusoidal component and maintains orthogonality with the others [4, 8].

Let $X[k]$ denote the complex symbol on subcarrier k, and N the FFT size. The time-domain output $x[n]$ is given by:

$$x[n] = \frac{1}{N} \sum_{k=0}^{N-1} X[k] e^{j2\pi kn/N}, \quad n = 0, 1, \ldots, N-1$$

Each resulting OFDM symbol consists of N time-domain samples. However, to mitigate inter-symbol interference (ISI) caused by multipath propagation, a **Cyclic Prefix (CP)** is appended to each symbol. This CP is a repetition of the last N_{CP} samples from the IFFT output and is inserted at the beginning of the symbol.

Figure 1.18 illustrates the process of cyclic prefix (CP) insertion in 5G NR, where a portion of the end of each OFDM symbol is copied and prepended to the symbol. This results in a total symbol duration of $N + N_{\text{CP}}$ samples. The CP serves

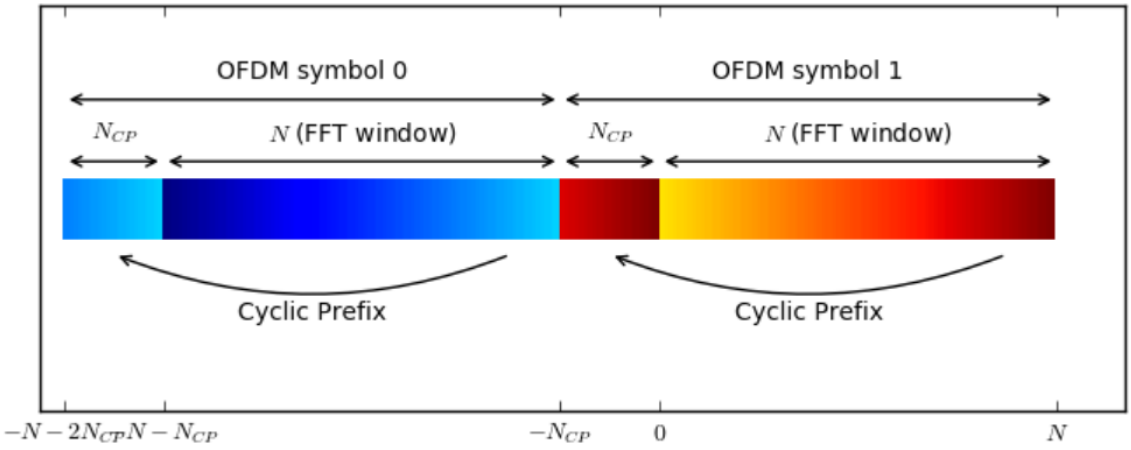

Figure 1.18: Cyclic Prefix insertion in 5G NR.[76]

as a guard interval that mitigates inter-symbol interference and allows the linear convolution of the channel to be treated as circular. This property preserves the orthogonality of subcarriers, even in frequency-selective fading environments.

This time-domain waveform, composed of a sequence of CP-extended OFDM symbols, is then transmitted over the radio interface. The process ensures efficient channel utilization, robustness to multipath fading, and low-complexity receiver design.

1.5.6 Receiver Side Summary

At the receiver, the incoming OFDM waveform first undergoes CP removal to isolate each OFDM symbol. The remaining signal is converted back into the frequency domain via FFT. After this, the receiver performs resource demapping to extract the allocated REs.

Demodulation is then applied to recover the symbol sequence, followed by channel decoding (LDPC or Polar) to reconstruct the original bitstream. Synchronization, channel estimation, and equalization are integrated throughout the process, aided by embedded reference signals such as DMRS and CSI-RS.

Together, this processing chain enables reliable, high-throughput communication in a dynamic and interference-prone wireless environment.

Conclusion

This chapter has provided a comprehensive overview of the motivations, architecture, and enabling technologies of 5G New Radio (NR), highlighting its evolution from 4G LTE and its readiness to support a vast spectrum of next-generation services. Unlike its predecessor, which primarily focused on mobile broadband, 5G is designed as a flexible and extensible framework that integrates high-throughput applications, ultra-reliable services, and massive-scale IoT within a single platform.

We began by articulating the performance bottlenecks and structural constraints inherent in 4G networks, which catalyzed the development of 5G. The chapter

then detailed the stringent requirements introduced by emerging use cases, ranging from sub-millisecond latency and gigabit throughput to energy-efficient massive connectivity, and how 5G addresses these through a modular architecture.

Fundamental enhancements in 5G NR include scalable subcarrier spacing via flexible numerology, the use of advanced physical-layer technologies such as massive MIMO and mini-slot scheduling, and the adoption of network softwarization principles via SDN and NFV. Together, these features provide the agility and efficiency required to dynamically adapt to traffic demands, user profiles, and service-level agreements across highly variable network conditions.

In addition, the chapter examined the evolution of multiple access techniques,from orthogonal schemes such as OFDMA and SC-FDMA to modern non-orthogonal solutions like power-domain NOMA and code-domain SCMA. These approaches are instrumental in supporting the massive concurrency and spectrum reuse required for 5G's envisioned scale.

However, with increased flexibility and multiplexing capabilities comes new complexity. One of the critical challenges in 5G NR is managing the interference introduced by multi-numerology operation, where different services may use varying symbol durations, subcarrier spacings, and guard configurations. Such configurations, while beneficial in isolation, often introduce inter-numerology interference (INI) when coexisting in the same spectrum.

The next chapter transitions from this architectural foundation toward a focused study of INI and its mitigation. We will formally define the problem, review existing approaches, and identify the gaps that motivate our proposed solutions, thereby linking the theoretical underpinnings of 5G with our specific research contributions.

Chapter 2

Problem Statement and State of the Art

Introduction

The advent of 5G New Radio (NR) introduces a transformative physical layer design through the adoption of multi-numerology, a feature enabling the coexistence of different subcarrier spacings, symbol durations, and cyclic prefix lengths within the same carrier bandwidth [6, 10, 77]. This innovation is essential for fulfilling the diverse requirements of enhanced Mobile Broadband (eMBB), ultra-Reliable Low-Latency Communications(uRLLC) , and massive Machine-Type Communications (mMTC). However, this flexibility breaks the orthogonality inherent in traditional OFDM systems, giving rise to inter-numerology interference (INI), a major impediment to system performance and standard compliance. [6, 12, 126]

Unlike LTE, which operates under a single numerology, 5G NR supports scalable numerologies defined by Delta f = 15 cdot 2mu kHz, where mu in 0,1,2,3,4. When these numerologies are multiplexed, spectral misalignment causes significant side lobe leakage, especially at numerology boundaries, leading to power leakage and degradation in signal fidelity. INI becomes particularly detrimental in scenarios with dense user deployments, unsynchronized transmissions, or tight spectral packing common in modern 5G use cases. [4, 9, 127]

Numerous studies have addressed the manifestation of INI in both time and frequency domains, revealing that its severity increases with higher numerology ratios and denser subcarrier packing. [6, 7, 13]Moreover, sidelobe interference and symbol misalignment are exacerbated by multipath fading, power imbalance, and dynamic scheduling, rendering INI a multidimensional problem that cannot be treated through simple static guard band insertion. [7, 128]

This chapter presents a comprehensive study of inter-numerology interference in 5G NR systems, beginning with the definition and structural implications of multi-numerology. We then develop analytical models in both continuous and discrete time to characterize INI through subcarrier correlation and spectral overlap. These derivations are supported by visual illustrations and simulation-backed insights that reveal the underlying interference structure. We further provide a detailed state-of-the-art review of mitigation strategies, including filtering, windowing, scheduling,

interference cancellation, and AI-driven methods, with a special emphasis on trade-offs between performance, complexity, and spectral efficiency.

Finally, we identify key gaps in the current literature, such as limited mathematical models of INI in discrete time, insufficient experimental validation under dual numerology, and underutilization of sidelobe structure for interference suppression. This motivates the approach in the next chapter, where we present a novel adaptive interference suppression strategy, building upon our previously published work on filtering-based mitigation of INI.

2.1 Multi-Numerology in 5G NR

In the context of 5G NR, numerology refers to the set of parameters that define the physical layer transmission characteristics, primarily the subcarrier spacing (Δf), symbol duration (T_s), and cyclic prefix duration (T_{CP}). Unlike LTE, which employs a fixed subcarrier spacing of 15 kHz, 5G NR supports multiple numerologies, each suited for specific deployment scenarios and service requirements. The subcarrier spacing (Δf) in 5G NR is defined as

$$\Delta f = 15 \times 2^{\mu}\,\text{kHz}$$

Where μ is an integer ranging from 0 to 4 [12].

2.1.1 Supported Numerologies

5G NR defines numerologies with subcarrier spacings that are integer multiples of 15 kHz, as shown in Table 2.1. [8, 12] This scaling allows for the flexible allocation of resources and the coexistence of multiple services within the same network [8].

Table 2.1: 5G NR Numerologies

μ	Δf	T_s	T_{CP}	**Slot Duration**
0	15 kHz	66.67 μs	4.69 μs	1 ms
1	30 kHz	33.33 μs	2.34 μs	0.5 ms
2	60 kHz	16.67 μs	1.17 μs	0.25 ms
3	120 kHz	8.33 μs	0.57 μs	0.125 ms
4	240 kHz	4.17 μs	0.29 μs	0.0625 ms

The choice of numerology depends on several factors, including the target service, channel conditions, and deployment scenario. Smaller subcarrier spacings (e.g., 15 kHz) are suitable for wide-area coverage and delay-tolerant applications, while larger subcarrier spacings (e.g., 60 kHz or 120 kHz) are preferred for low-latency and high-throughput applications [7, 127].

The incorporation of multiple numerologies into the 5G NR framework represents a strategic response to the multifaceted demands of contemporary wireless communication ecosystems, facilitating the tailored optimization of physical layer parameters to meet the distinct performance benchmarks of diverse applications and deployment contexts [5]. This architectural flexibility not only enhances resource

utilization and spectral efficiency but also empowers network operators to dynamically adapt to evolving user demands and service requirements, thereby augmenting the overall robustness and versatility of 5G networks [22, 129].

2.1.2 Comparison with LTE Frame Structure

LTE employs a fixed numerology with a subcarrier spacing of 15 kHz, leading to a uniform frame structure across the network. In contrast, 5G NR's flexible numerology allows for variable subcarrier spacings, enabling the network to adapt to different service requirements and deployment scenarios [77, 130].

As illustrated in Figure2.1, the frame duration in LTE is fixed at 10 ms, divided into 10 subframes of 1 ms each. Each subframe consists of two slots, each with a duration of 0.5 ms. In 5G NR, the frame duration is also 10 ms, but the number of slots per subframe varies depending on the numerology [4]. For example, with a subcarrier spacing of 15 kHz, there are 10 slots per subframe, while with a subcarrier spacing of 30 kHz, there are 20 slots per subframe. This variability enables the dynamic allocation of resources and the efficient support of diverse services [15].

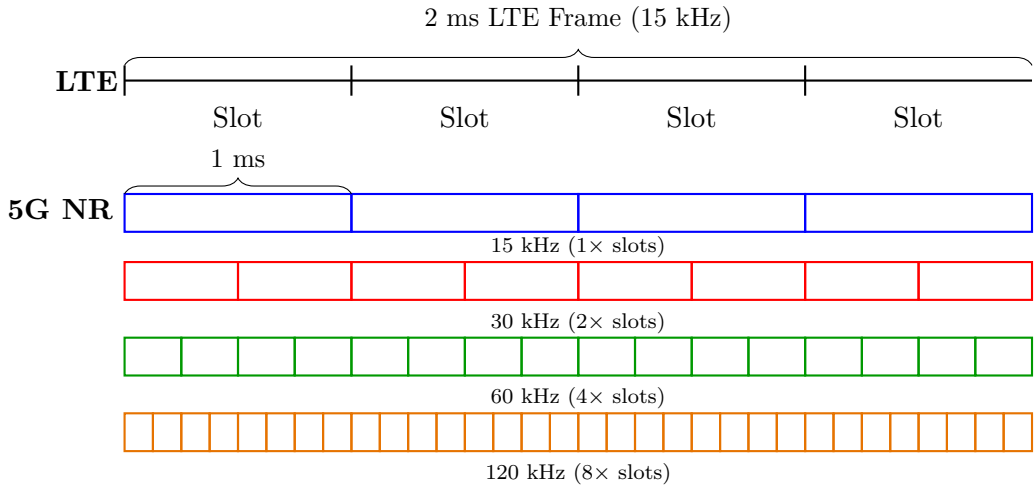

Figure 2.1: Comparison of LTE and 5G NR frame structures.

2.1.3 Implications of Multi-Numerology

The introduction of multiple numerologies in 5G NR enhances the network's flexibility but also introduces challenges:

- **Inter-Numerology Interference (INI)**:The coexistence of different numerologies can lead to interference between subcarriers, especially at the boundaries of numerology domains, or BandWidth Parts(BWP), leading to performance degradation for both types of users [35].
- **Complex Resource Allocation**: Managing resources across multiple numerologies requires sophisticated scheduling algorithms to ensure efficient utilization, QoS provisioning and fairness [131].

– **Increased Receiver Complexity**: Receivers must be capable of handling signals with varying numerologies, necessitating more complex signal processing techniques, such as symbol allignement and clock synchronization [14].

In the subsequent sections of this chapter, we undertake a comprehensive investigation of inter-numerology interference (INI), a critical challenge in multi-numerology systems such as 5G NR. We begin by analyzing the fundamental mechanisms underlying INI, followed by the development of rigorous mathematical models that capture its behavior across multiple domains. Specifically, we formulate these models in both continuous and discrete time, providing insights into temporal interference characteristics. Furthermore, we extend our analysis to the frequency domain to better understand spectral interactions between coexisting numerologies. This multi-domain modeling approach lays the foundation for the interference mitigation strategies proposed in later sections.

2.2 Inter-Numerology Interference in Continuous Time

In 5G New Radio (NR), multiple numerologies may coexist within the same frequency band to support diverse service requirements. This flexibility, however, comes at the cost of losing the strict orthogonality guaranteed in conventional OFDM systems, leading to *inter-numerology interference* (INI).

Figure 2.2 illustrates a conceptual transceiver architecture for a two-numerology OFDM system. Each numerology operates with its own subcarrier spacing, denoted $\Delta f^{(1)}$ and $\Delta f^{(2)}$, and corresponding symbol durations $T^{(1)} = 1/\Delta f^{(1)}$ and $T^{(2)} = 1/\Delta f^{(2)}$. To comply with 3GPP's scalable numerology structure, we define:

$$\Delta f^{(2)} = v \cdot \Delta f^{(1)}, \quad T^{(2)} = \frac{T^{(1)}}{v}, \quad v \in \mathbb{N}. \tag{2.1}$$

Each symbol $s_m^{(i)}$ from numerology $i \in \{1, 2\}$ is modulated using a subcarrier-specific basis function $\phi_m^{(i)}(t)$:

$$\phi_m^{(i)}(t) = \frac{1}{\sqrt{T^{(i)}}} e^{j2\pi m \Delta f^{(i)} t} \cdot \Pi_{T^{(i)}}(t), \tag{2.2}$$

where $\Pi_T(t)$ denotes a rectangular window of duration T.

The aggregate transmitted signal is:

$$x(t) = \sum_m s_m^{(1)} \phi_m^{(1)}(t) + \sum_n s_n^{(2)} \phi_n^{(2)}(t), \tag{2.3}$$

and the received signal under AWGN becomes:

$$r(t) = x(t) + w(t), \tag{2.4}$$

where $w(t)$ is additive white Gaussian noise.

At the receiver, matched filters based on the transmit basis functions are used for demodulation. The estimated symbol is recovered as:

$$\hat{s}_m^{(i)} = \int r(t)\, \phi_m^{(i)*}(t)\, dt. \tag{2.5}$$

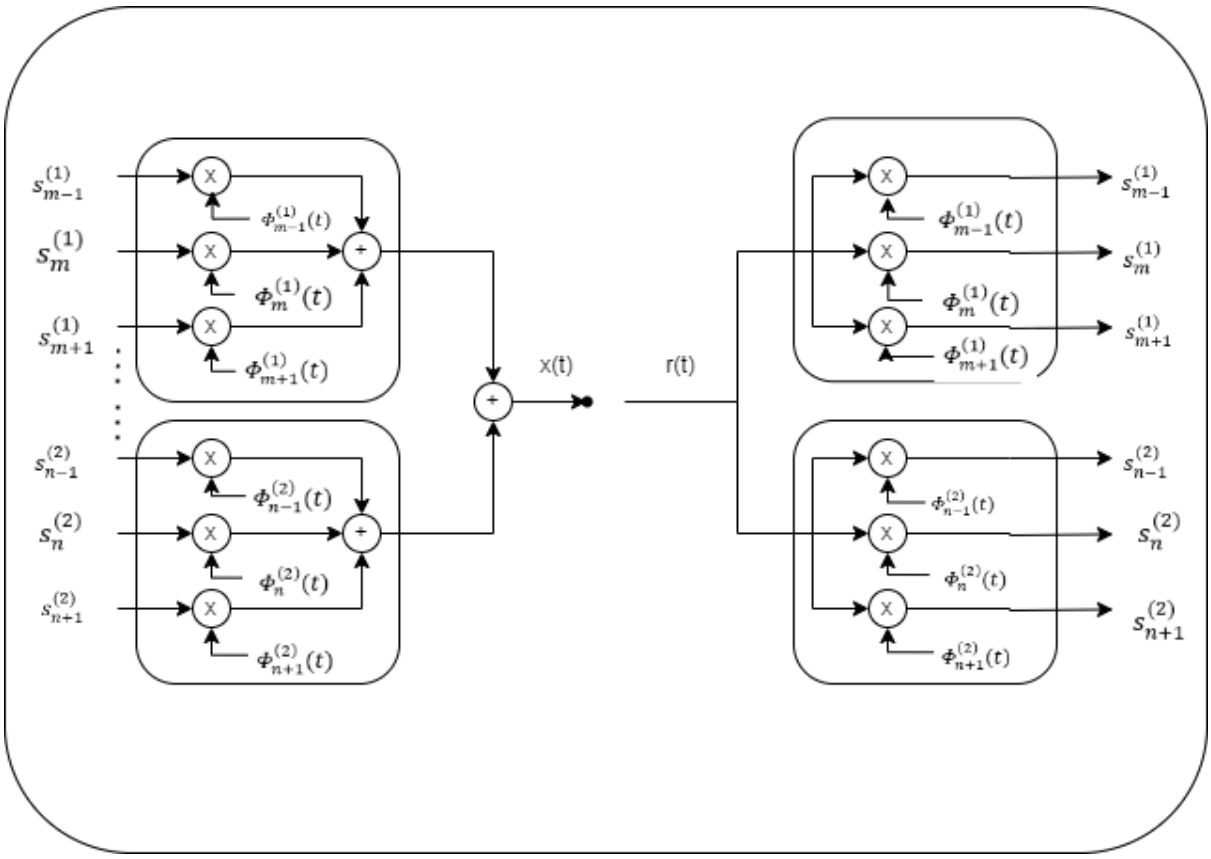

Figure 2.2: Transceiver architecture for a multi-numerology OFDM system with two numerologies.

A.Inter-Numerology Interference (INI)

In the presence of multiple numerologies, orthogonality is not preserved due to mismatches in subcarrier spacing and symbol duration. This results in cross-interference between subcarriers of different numerologies. The demodulated symbols become:

$$\hat{s}_m^{(1)} = s_m^{(1)} + \sum_n s_n^{(2)} \langle \phi_n^{(2)}(t), \phi_m^{(1)}(t) \rangle, \tag{2.6}$$

$$\hat{s}_n^{(2)} = s_n^{(2)} + \sum_m s_m^{(1)} \langle \phi_m^{(1)}(t), \phi_n^{(2)}(t) \rangle, \tag{2.7}$$

where the inner product $\langle \phi_a(t), \phi_b(t) \rangle = \int \phi_a(t) \phi_b^*(t)\, dt$ quantifies the interference leakage.

When $\Delta f^{(1)} \neq \Delta f^{(2)}$, these cross terms no longer vanish, in contrast to single-numerology OFDM systems where orthogonality ensures no inter-subcarrier interference.

2.2.1 Symbol Duration Overlap and Temporal Aliasing

The INI becomes particularly pronounced when symbol durations overlap in time. For example, if $v = 2$, each symbol from Numerology 2 spans the duration of two symbols from Numerology 1, as shown in Figure 2.3. This temporal misalignment introduces spectral leakage and disrupts orthogonality across numerologies.

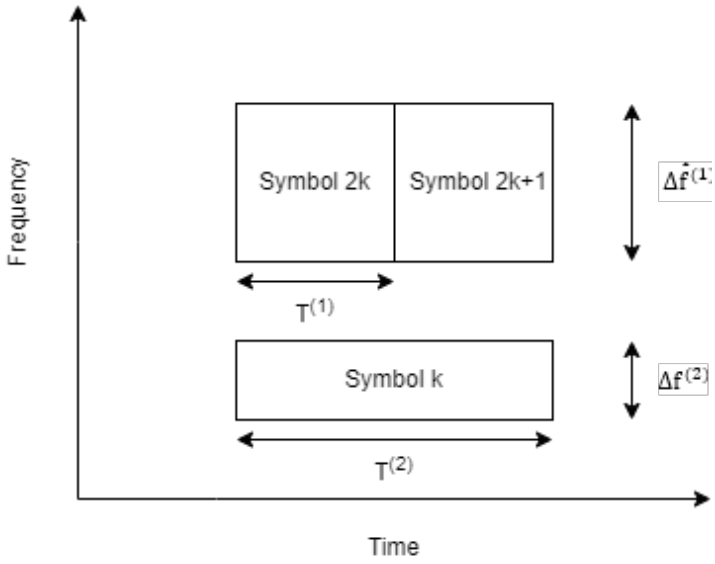

Figure 2.3: Overlap of symbol durations for $v = 2$

2.2.2 Full Transmission Model

Extending the model to multiple OFDM symbols over time, the continuous-time baseband signal for numerology i becomes:

$$x^{(i)}(t) = \sum_{k=-\infty}^{+\infty} \sum_{m=0}^{N^{(i)}-1} s_{k,m}^{(i)} \, \phi_m^{(i)}(t - kT^{(i)}), \tag{2.8}$$

where $s_{k,m}^{(i)}$ is the k-th OFDM symbol on the m-th subcarrier. The total signal is:

$$x(t) = x^{(1)}(t) + x^{(2)}(t), \tag{2.9}$$

capturing both numerologies in a shared spectrum, leading to time-domain and frequency-domain interference.

2.3 Subcarrier Correlation and Inter-Numerology Interference

In OFDM systems, subcarrier waveforms are orthogonal within a given numerology due to uniform subcarrier spacing and symbol durations. However, this orthogonality breaks down when multiple numerologies coexist, resulting in inter-numerology interference (INI). The degree of interference can be quantified through the inner product between subcarrier waveforms from different numerologies.

2.3.1 Subcarrier Inner Product

Let $\phi_m^{(i)}(t)$ denote the baseband waveform of the m-th subcarrier in numerology i, defined as:

$$\phi_m^{(i)}(t) = \frac{1}{\sqrt{T_i}} e^{j2\pi m \Delta f^{(i)} t} \cdot \Pi_{T_i}(t), \tag{2.10}$$

where $\Delta f^{(i)} = 1/T_i$ is the subcarrier spacing and $\Pi_{T_i}(t)$ is a rectangular window of duration T_i.

The inner product between subcarriers from numerologies 1 and 2 is:

$$\rho_{m,n}^{1\leftarrow 2} = \int_0^T \phi_m^{(1)}(t) \cdot \left[\phi_n^{(2)}(t)\right]^* dt, \tag{2.11}$$

where T is a common integration window (e.g., least common multiple of T_1 and T_2).

Substituting the waveforms:

$$\rho_{m,n}^{1\leftarrow 2} = \frac{1}{\sqrt{T_1 T_2}} \int_0^T e^{j2\pi(m\Delta f_1 - n\Delta f_2)t} dt. \tag{2.12}$$

For $\Delta f_2 = v \cdot \Delta f_1$, the expression becomes:

$$\rho_{m,n}^{1\leftarrow 2} = \frac{1}{\sqrt{T_1 T_2}} \cdot \frac{e^{j2\pi(m-nv)\Delta f_1 T} - 1}{j2\pi(m-nv)\Delta f_1}. \tag{2.13}$$

This shows that orthogonality is preserved only when $m = nv$. Otherwise, the inner product is nonzero, leading to INI.

Figure 2.4 shows the simulated magnitude of $\rho_{m,n}^{1\leftarrow 2}$ for numerology ratios $v = 2, 4, 8$. As v increases, more subcarriers from numerology 2 interfere with each subcarrier in numerology 1. The horizontal axis represents the subcarrier index offset $d = m - nv$, which measures how far an interfering numerology-2 subcarrier is from the desired numerology-1 subcarrier. Interference is strongest at $d = 0$ and decays as the offset increases.

2.4 Discrete-Time Modeling of Inter-Numerology Interference

In practical OFDM systems, signals are processed in discrete time via IFFT/FFT. Here, we analyze how interference manifests in the discrete domain.

2.4.1 System Setup

Consider two numerologies:

- Numerology 1: $\Delta f_1 = 15$ kHz, FFT size N_1

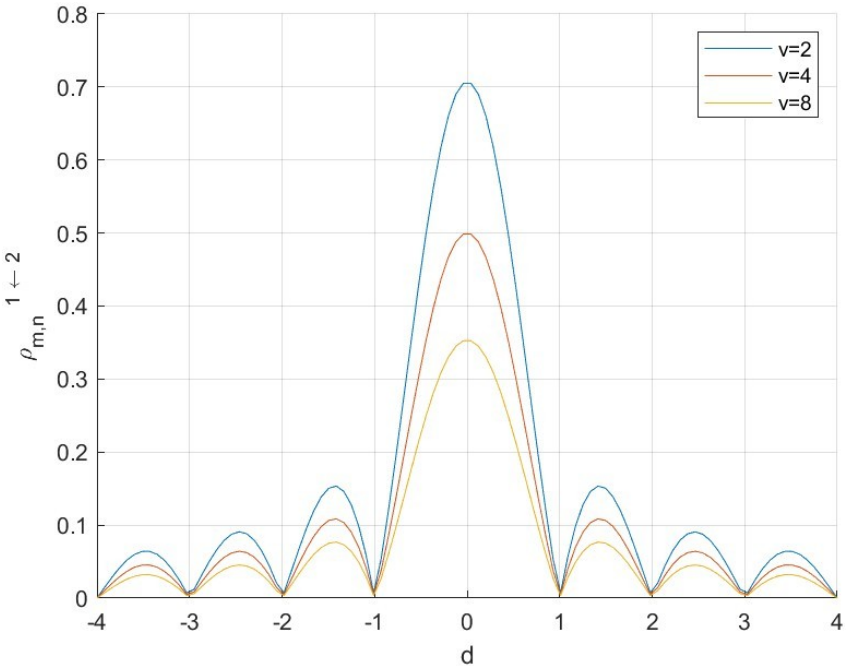

Figure 2.4: subcarrier correlation.

– Numerology 2: $\Delta f_2 = v \cdot \Delta f_1$, FFT size $N_2 = \frac{N_1}{v}$

Each OFDM symbol is:

$$x_i[n] = \frac{1}{\sqrt{N_i}} \sum_{k=0}^{N_i-1} X_k^{(i)} e^{j2\pi \frac{kn}{N_i}}, \quad n = 0, 1, \ldots, N_i - 1. \tag{2.14}$$

Assuming both are transmitted simultaneously:

$$r[n] = x_1[n] + x_2[n].$$

Numerology 1 demodulates via an N_1-point FFT:

$$Y_m^{(1)} = \frac{1}{\sqrt{N_1}} \sum_{n=0}^{N_1-1} r[n] \cdot e^{-j2\pi \frac{mn}{N_1}}. \tag{2.15}$$

This yields:

$$Y_m^{(1)} = \text{desired signal} + \text{INI}, \tag{2.16}$$

$$\text{INI}_m = \frac{1}{\sqrt{N_1 N_2}} \sum_{k=0}^{N_2-1} X_k^{(2)} \sum_{n=0}^{N_1-1} e^{j2\pi n \left(\frac{k}{N_2} - \frac{m}{N_1}\right)}. \tag{2.17}$$

Let $\delta_{k,m} = \frac{kv-m}{N_1}$. Then:

$$\sum_{n=0}^{N_1-1} e^{j2\pi n \delta_{k,m}} = \frac{\sin(\pi N_1 \delta_{k,m})}{\sin(\pi \delta_{k,m})} \cdot e^{j\pi(N_1-1)\delta_{k,m}},$$

So the interference term becomes:

$$\mathrm{INI}_m = \frac{1}{\sqrt{N_1 N_2}} \sum_{k=0}^{N_2-1} X_k^{(2)} \cdot \frac{\sin(\pi N_1 \delta_{k,m})}{\sin(\pi \delta_{k,m})} \cdot e^{j\pi(N_1-1)\delta_{k,m}}. \tag{2.18}$$

This quantifies the leakage from numerology 2 into each subcarrier of numerology 1.

2.5 Spectral Interpretation and Orthogonality Breakdown

In the frequency domain, each OFDM subcarrier exhibits a sinc-shaped spectrum as a result of the rectangular windowing applied in the time domain. The sinc function has its maximum at the carrier's central frequency and decays symmetrically with zero crossings at integer multiples of the inverse symbol duration. This spectral property is critical for maintaining orthogonality between subcarriers.

In a single numerology system, where all subcarriers share the same subcarrier spacing (Δf), each subcarrier transmits when its corresponding sinc function reaches its maximum. Crucially, at that frequency, all other subcarriers have zeros due to their spectral alignment. This ensures that the demodulator observes no interference from adjacent subcarriers, as shown in Figure 2.5. The sidelobes of each subcarrier intersect exactly at the nulls of all others, preserving mutual orthogonality.

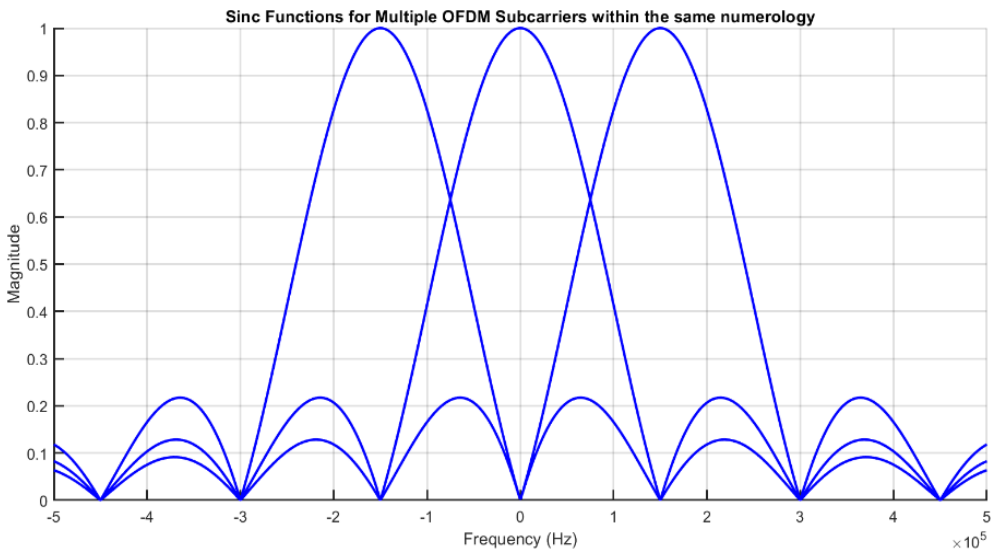

Figure 2.5: Spectrum of multiple OFDM subcarriers under the same numerology.

However, in a multi-numerology system, such as those adopted in 5G NR to simultaneously support diverse service requirements, different subcarrier spacings lead to sinc functions with mismatched zero-crossing intervals. As a result, when a subcarrier from one numerology transmits at its spectral peak, the sinc sidelobes of subcarriers from another numerology generally do not intersect at that frequency's

null. This misalignment breaks orthogonality and introduces inter-numerology interference (INI), even in ideal transmission conditions.

Figure 2.6 illustrates this phenomenon. Two numerologies, separated by a guard band, are shown. Despite the spacing, the sidelobes of one numerology intrude into the main lobe of the other, violating the zero-crossing property and resulting in cross-numerology leakage.

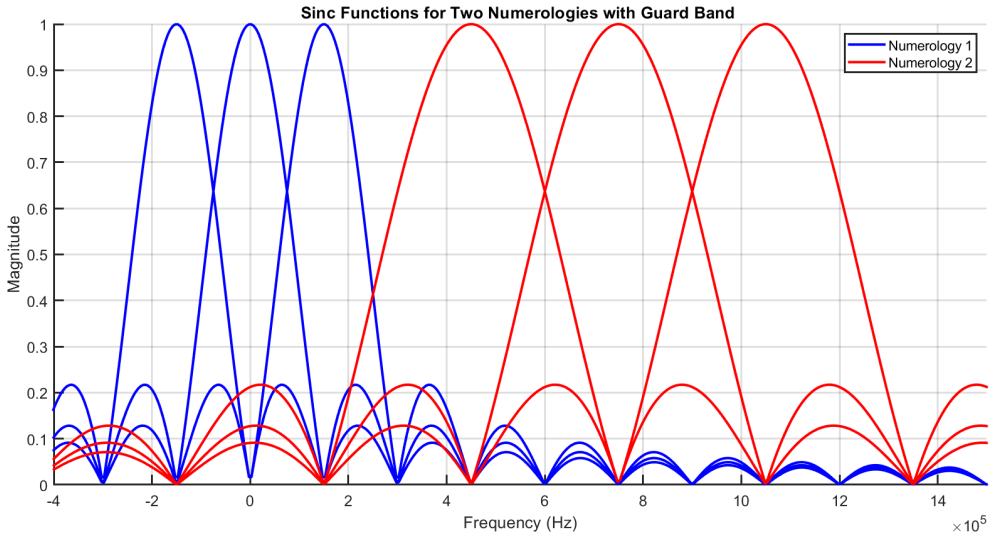

Figure 2.6: Spectral overlap between two numerologies.

This loss of orthogonality is a fundamental challenge in multi-numerology systems and motivates the development of various INI mitigation strategies, including frequency-domain filtering, time-domain windowing, and interference-aware resource allocation.

2.6 State of the Art in INI Mitigation Techniques

The flexibility introduced by multi-numerology in 5G NR is key to enabling diverse service categories such as eMBB, URLLC, and mMTC. However, it also introduces a major challenge: inter-numerology interference (INI). INI occurs when different numerologies, characterized by varying subcarrier spacings, cyclic prefix lengths, and symbol durations, coexist within the same bandwidth, thereby disrupting OFDM subcarrier orthogonality and degrading performance.

To address this issue, the literature has proposed a wide array of INI mitigation techniques, which can be categorized into six main classes: filtering and spectrum shaping, guard band and windowing, numerology-aware resource scheduling, interference cancellation, AI-based solutions, and hybrid techniques.

2.6.1 Filtering and Spectrum Shaping Techniques

Filtering and pulse-shaping approaches aim to confine the spectral footprint of each numerology:

- **Filtered-OFDM (f-OFDM)** : Applies bandpass filters to subbands, improving out-of-band emission control at the cost of potential inter-symbol interference.
- **Universal Filtered OFDM (UF-OFDM)**: Offers steeper spectral decay than f-OFDM, albeit with increased filter length and latency.
- **Windowed Overlap-and-Add (WOLA)**: Smooths transitions between OFDM symbols to reduce side lobes with minimal change to system structure.
- **Pulse-Shaped OFDM**: Uses non-rectangular pulses (e.g., raised cosine) to suppress leakage, potentially breaking orthogonality but improving spectral confinement.

These methods improve spectral localization but increase computational complexity and may affect latency.

2.6.2 Guard Band Allocation and Windowing

Simple yet effective, this class focuses on mitigating interference at the spectrum edges:

- **Guard Bands**: Reserve frequency gaps between numerologies to minimize spectral overlap. Effective in reducing adjacent-channel INI but decreases spectral efficiency.
- **Windowing**: Applies smoothing functions (e.g., Hanning, Kaiser) to reduce spectral leakage. Asymmetric windowing can be used to tailor signal edges for specific adjacent numerologies.

Though easy to implement, these techniques require a trade-off between spectral efficiency and interference suppression.

2.6.3 Numerology-Aware Resource Scheduling

This approach focuses on user allocation and scheduling to mitigate INI:

- **Static Grouping**: Assigns similar QoS-class users to the same numerology group.
- **Dynamic Scheduling**: Adapts numerology assignment in real-time based on traffic and channel conditions, often leveraging machine learning.
- **Edge-Aware Mapping**: Places users at the center of numerology blocks to avoid high interference at the numerology boundaries.
- **Non-Contiguous Mapping**: Allocates disjoint resource blocks to reduce direct overlap.

These techniques are scalable but rely on accurate interference modeling and responsive scheduling frameworks.

2.6.4 Interference Cancellation and Equalization

These signal processing methods cancel or suppress INI at the receiver:

- **Successive Interference Cancellation (SIC)** : Iteratively decodes and removes strong interference, requiring accurate CSI.
- **ICI Suppression Filters**: Design equalizers that nullify inter-carrier interference caused by numerology mismatch.
- **Generalized Sidelobe Canceller (GSC)**: Projects signals onto interference-free subspaces via adaptive filtering.
- **Time-Frequency Interference Cancellation**: Uses iterative algorithms to jointly suppress interference across domains.

While powerful, these methods often entail high complexity and may not suit latency-sensitive applications.

2.6.5 Machine Learning and AI-Based Techniques

AI brings adaptability to INI mitigation in dynamic networks:

- **Deep Learning**: Learns interference patterns and suggests real-time filtering or scheduling policies.
- **Reinforcement Learning (RL)** : Enables agents to optimize numerology selection and user scheduling via trial-and-error interaction.
- **Graph Neural Networks (GNNs)**: Models user interference graphs for distributed coordination.
- **Autoencoder Receivers**: Learns encoding/decoding strategies that inherently suppress INI.

Though promising, AI techniques require extensive data and careful real-time deployment strategies.

2.6.6 Hybrid Techniques and Cross-Layer Approaches

To achieve optimal trade-offs, multiple techniques are often combined:

- **Filter + Scheduler Co-Design**: Jointly optimize waveform shaping and user allocation.
- **AI-Driven Interference Cancellation**: Combines ML-based prediction with adaptive interference mitigation.

– **Real-Time Adaptive Control**: Modulates subcarrier spacing, guard band width, and transmit power on-the-fly.

These methods offer high performance but involve complex cross-layer integration and signaling overhead. in Table2.2, we draw a consolidated taxonomy of INI MItigation approaches

Table 2.2: Consolidated Taxonomy of INI Mitigation Approaches (2020–2023)

Category	**Technique and Representative Works**
Analytical Modeling	Closed-form INI models, reduced-form expressions. *Key papers:* [6], [7] ,[2],[10].
Waveform Processing	Filtering (f-OFDM, W-OFDM), windowing, common CP insertion. *Key papers:* [127] , [11, 132, 133].
Adaptive Guarding	Joint time-frequency guard optimization, multi-window approaches. *Key papers:* [133, 134]
Resource Scheduling	INI-aware scheduling (heuristic, ML-based), power allocation. *Key papers:* [9, 77, 135, 136]
MIMO-Aware Solutions	Spatial-domain interference analysis, precoding in massive MIMO. *Key papers:* [2].
Cross-Layer Integration	MAC + PHY scheduling, QoS-based adaptive allocation. *Key papers:* [9, 134].
Learning-Based	Deep RL (e.g., DQN, branching dueling Q-networks) for INI-aware allocation. *Key papers:* [136]
Transmitter Pre-Processing	Matrix-based INI pre-equalization eliminating INI before transmission. *Key paper:* [12].

2.6.7 Performance Comparison

Table 2.3 provides a comparative overview of major techniques proposed for mitigating inter-numerology interference (INI), evaluating each method in terms of interference reduction capability, computational complexity, and impact on spectral efficiency.

2.6.8 Summary

A wide range of solutions exist to suppress or avoid INI in multi-numerology systems. Each class of methods has strengths and limitations depending on implementation complexity, latency constraints, and spectrum availability. In practice,

Table 2.3: Comparison of Major INI Mitigation Techniques

Technique	**Interference Reduction**	**Complexity**	**Spectral Efficiency**
Filtering (f-OFDM, UF-OFDM)	High	Moderate to High	Moderate
Guard Bands and Windowing	Moderate	Low	Low
Numerology Grouping	Moderate to High	Moderate	High
Interference Cancellation	High	High	High
AI-Based Methods	Adaptive (Potentially High)	High	High
Hybrid Approaches	Very High	Very High	High

a hybrid approach combining waveform design, intelligent scheduling, and receiver-side mitigation often yields the best performance. Nonetheless, challenges remain in scaling these techniques to dense, heterogeneous networks.

In the following subsection, we outline the research gaps and identify promising future directions to further enhance INI mitigation in realistic 5G and beyond deployments.

2.7 Research Gap and Motivation

While 5G New Radio (NR) introduces flexible support for diverse service classes through its multi-numerology framework, this very flexibility creates a significant challenge in the form of *inter-numerology interference* (INI). INI arises due to the loss of orthogonality between coexisting numerologies with different subcarrier spacings and symbol durations, and it represents a major bottleneck for achieving reliable and efficient communication, particularly in dense, heterogeneous deployments.

Numerous mitigation strategies have been proposed in the literature, such as guard band insertion, time-domain windowing, frequency-domain filtering (e.g., UF-OFDM, f-OFDM), and interference-aware scheduling. While these approaches provide partial relief, they often incur non-trivial trade-offs in terms of spectral efficiency, hardware complexity, latency, or adaptability. Moreover, they frequently rely on idealized assumptions that rarely hold in real-world deployments, such as perfect channel state information (CSI), fixed numerology allocations, or homogeneous traffic distributions. These limitations are particularly acute in mixed-service environments, where low-latency URLLC transmissions may coexist with high-throughput eMBB users, or in Internet-of-Things (IoT) scenarios with tight power and complexity constraints.

A. Identified Research Gaps

A review of current approaches reveals several key limitations that motivate this work:

- **Lack of Unified INI Models:** Existing analytical models often oversimplify the nature of INI, neglecting important practical factors such as asynchronous transmissions, power disparities, or time-frequency misalignment. Many models only consider idealized, narrowband scenarios or assume fully synchronized operation. A more comprehensive mathematical model is needed, particularly in the discrete-time domain, to accurately capture the structure and behavior of INI in realistic systems.
- **Limited Analysis in Dual-Numerology Configurations:** Dual-numerology operation represents a practical baseline for many 5G use cases, yet it remains underexplored in both theoretical analysis and empirical evaluation. Specifically, the phenomenon of subcarrier correlation across numerologies, an inherent source of interference, has not been sufficiently examined in the context of discrete-time OFDM processing.
- **Trade-offs Between Complexity and Performance:** Many advanced interference suppression techniques achieve strong performance but are unsuitable for latency, or power, constrained systems due to their high computational or implementation complexity. This includes methods that rely on large FFT sizes, iterative cancellation, or fine-grained scheduling. There is a clear need for lightweight, effective solutions that balance interference suppression with implementation simplicity.
- **Lack of Adaptability to Dynamic Conditions:** Interference patterns in 5G systems can vary rapidly due to user mobility, bursty traffic, or changes in numerology configuration. Many current solutions assume static traffic and fixed user allocations, making them ill-suited for dynamic or uncoordinated deployments. Emerging AI-based methods promise adaptability but are still in early stages and lack robustness and interpretability.
- **Underutilization of Sidelobe Structure:** One of the most persistent sources of INI is sidelobe leakage between non-orthogonal subcarriers. However, most mitigation strategies treat sidelobes as noise to be suppressed rather than structured signals to be exploited. There exists an opportunity to develop smarter techniques that leverage predictable sidelobe patterns for more efficient cancellation or suppression.

B. Motivation for This Work

This work is motivated by the need to address the challenges posed by inter-numerology interference (INI) through a methodology that is both analytically robust and practically deployable. While many existing approaches treat INI as an unstructured spectral artifact, we demonstrate that it possesses a tractable mathematical and structural profile, one that can be exploited for effective suppression. Our proposed technique combines precise time-domain alignment and frequency-domain FIR filtering, informed by a detailed understanding of OFDM signal structure under multi-numerology configurations.

Specifically, this work contributes:

- **A refined discrete-time system model** that characterizes the temporal and spectral interplay between coexisting numerologies, capturing key non-idealities such as symbol misalignment and power disparity across bandwidth parts;
- **A formal framework for analyzing cross-numerology subcarrier interference**, leveraging discrete-time correlation structures to expose the precise mechanisms by which orthogonality breaks down;
- **Spectral visualizations and leakage profiling** that localize interference in the frequency domain and expose the subcarrier-specific impact of numerology mismatch, enabling informed filter design;
- **A targeted, computationally efficient FIR filtering solution**, which suppresses INI by shaping the spectral edges of the interfering numerology after carefully realigning the time-domain symbols for maximum effectiveness;
- **A performance evaluation framework grounded in 3GPP numerology standards**, simulating dual-numerology operation under realistic assumptions of synchronization offsets, power imbalances, and minimal guard bands.

Unlike traditional suppression strategies that rely on brute-force cancellation, wide guard bands, or full CSI availability, our approach operates under realistic constraints and is guided by a structural understanding of the INI problem. Through a principled combination of time alignment and filter shaping, we show that it is possible to achieve meaningful INI suppression while keeping good computational efficiency, bridging the gap between theoretical insight and practical applicability.

Conclusion

Conclusion

This chapter has presented a comprehensive and technically rigorous exploration of inter-numerology interference (INI) in 5G New Radio systems, highlighting its origin, structural behavior, and consequences on system performance. Beginning with the motivation behind multi-numerology design in 5G, namely, the need to accommodate heterogeneous service requirements, we demonstrated that this architectural flexibility introduces non-trivial spectral and temporal interference challenges, especially in dual-numerology deployments.

To lay a solid analytical foundation, we developed continuous-time and discrete-time models that capture the essence of INI. In particular, we showed how symbol duration mismatch and subcarrier spacing disparities lead to the loss of orthogonality, both in time and frequency. Our subcarrier correlation analysis revealed that interference is not a random artifact, but a predictable and structured phenomenon arising from sinc misalignment and sidelobe leakage. These findings were

Table 2.4: Mapping of Key Research Gaps to Contributions Proposed in This Work

Identified Research Gap	**Targeted Contribution in This Work**
Absence of discrete-time INI models that capture time-frequency dynamics under dual numerology	Formulation of a rigorous discrete-time model that accounts for inter-symbol and inter-carrier interference caused by numerology co-existence, symbol offset, and spectral misalignment.
Lack of analytical tools to characterize cross-numerology subcarrier interaction	Derivation and analysis of subcarrier correlation expressions across numerologies, highlighting the structured breakdown of orthogonality in the presence of spacing and timing mismatch.
Overreliance on static or unstructured filtering techniques	Design of a filter-aware mitigation scheme that leverages sidelobe localization and numerology-specific leakage patterns, rather than assuming uniform interference behavior.
Neglect of temporal misalignment in INI suppression strategies	Integration of time-domain alignment prior to frequency-domain filtering, enabling coherent interference mitigation and improved subcarrier orthogonality.
Limited validation under realistic 5G numerology conditions	Implementation of a simulation platform that adheres to 3GPP-defined numerologies, assessing performance under dual-numerology operation with realistic synchronization and power conditions.
Unaddressed trade-offs between suppression effectiveness and real-time complexity	Proposal of a computationally efficient FIR filtering solution that achieves measurable INI reduction while remaining suitable for deployment in constrained processing environments.

substantiated with simulation-backed visualizations, offering intuitive insights into the interference regions and leakage patterns.

Through this analysis, we established that existing mitigation strategies, while abundant, often fail to address the fundamental structure of INI. Many are overly reliant on static guard bands, wide-spectrum filtering, or idealized assumptions, making them either inefficient or impractical for real-world systems. This disconnect underscores a critical research gap: the need for mitigation techniques that are both structure-aware and implementation-feasible.

To bridge this gap, we identified a set of guiding principles that motivate the methodology presented in the next chapter. Rather than suppressing INI blindly or treating it as unstructured noise, we exploit its spectral and temporal regularities. Specifically, our approach combines time-domain alignment with a computationally efficient FIR filtering strategy, targeting the interference where it is most pronounced, at the spectral boundaries and sidelobe-dominant regions.

By grounding our method in realistic 3GPP numerology configurations and accounting for synchronization offsets and power imbalances, we ensure that the proposed solution is not only theoretically sound but also ready for deployment in practical 5G systems. The next chapter builds directly on the insights and tools developed here, presenting a novel INI mitigation framework that achieves high suppression performance without compromising computational efficiency or spectral flexibility.

Chapter 3

INI Mitigation via Time Alignment and Filtering in Multi-Numerology OFDM

Introduction

The increasing flexibility of 5G New Radio (NR) systems has been largely enabled by the introduction of multi-numerology structures, where different subcarrier spacings (SCS) coexist in the same frequency band to support diverse service requirements. While this flexibility enhances spectrum utilization and accommodates heterogeneous traffic,such as enhanced mobile broadband (eMBB) and ultra-reliable low-latency communications (URLLC),it also introduces a significant technical challenge: inter-numerology interference (INI).

Unlike legacy OFDM systems that rely on strict subcarrier orthogonality, multi-numerology OFDM breaks this orthogonality at the edges of numerology boundaries due to mismatches in symbol durations and cyclic prefixes. The resulting spectral leakage can cause substantial degradation in link quality, particularly for low-SCS users who are more vulnerable to the wider spectral footprint of higher-SCS numerologies.

This chapter presents a rigorous MATLAB-based simulation study to investigate the effects of INI in a downlink 5G OFDM system with two coexisting numerologies: a low-SCS Numerology1 (15,kHz) treated as the desired user and a high-SCS Numerology2 (30,kHz) acting as the interferer. The analysis begins by characterizing the system performance in the absence of mitigation, revealing the full extent of interference through various metrics including bit error rate (BER), error vector magnitude (EVM), signal-to-interference-plus-noise ratio (SINR), and spectral efficiency (SE).

Subsequently, the chapter introduces two complementary mitigation techniques: (1) time-domain symbol alignment via sample rate matching, and (2) frequency-domain filtering using a high-order FIR filter. By analyzing performance across different modulation schemes and signal-to-noise ratio (SNR) levels, we aim to answer a critical design question: When is time alignment alone sufficient, and when must additional filtering be applied to preserve communication quality?

Through detailed visualizations and quantitative metrics, this chapter builds a comprehensive understanding of the trade-offs between complexity, interference mitigation, and spectral efficiency in multi-numerology OFDM systems, laying the groundwork for more advanced scheduling and waveform engineering strategies in future chapters.

3.1 Performance Without Time Alignment and Filtering

To evaluate the severity of inter-numerology interference (INI), we first simulate the system without applying time alignment or filtering. In this scenario, the interfering and desired numerologies are generated independently and superposed in the time domain without any synchronization or mitigation, exposing the system to maximum INI.

3.1.1 System Model

This study considers a downlink multi-numerology OFDM system composed of two Bandwidth Parts (BWPs) configured with distinct Subcarrier Spacings (SCS). **Numerology 1**, operating at 15 kHz SCS, is treated as the desired signal, while **Numerology 2**, operating at 30 kHz SCS, acts as an interferer. Both numerologies are generated independently and multiplexed into the same spectrum without guard bands or time alignment, which results in inter-numerology interference (INI).

Each numerology employs 16-QAM modulation with a modulation order $M = 16$. The number of OFDM symbols per slot is fixed at 14 for both numerologies. Numerology 1 occupies 100 resource blocks (RBs), equivalent to 1200 subcarriers, while Numerology 2 uses 50 RBs (600 subcarriers), shifted in frequency via its `NStartGrid` parameter. (Figure 3.7)

- **Bit Generation and Modulation:** Random binary bits are mapped to 16-QAM symbols.
- **Resource Grid Mapping:** Modulated symbols are reshaped and mapped onto the respective OFDM grid for each numerology.
- **OFDM Modulation:** IFFT-based OFDM modulation with cyclic prefix insertion is applied using a fixed FFT size of 2048, and a common sample rate of $fs_1 = 30.76MHz$ for **NUM1** and $fs_2 = 2 \cdot fs_1$ for **NUM1**
- **Signal Superposition:** The two modulated waveforms are summed to simulate concurrent transmission.
- **AWGN Channel:** The composite waveform is passed through an additive white Gaussian noise channel.
- **Receiver Processing:** Only Numerology 1 is demodulated and evaluated at the receiver using OFDM demodulation.

Performance is assessed over a wide SNR range using the following metrics:

- **Bit Error Rate (BER):** The BER quantifies the ratio of incorrectly received bits to the total number of transmitted bits for Numerology 1. Let $\mathbf{b}_{\text{tx}}$ and $\mathbf{b}_{\text{rx}}$ be the vectors of transmitted and received bits, respectively. Then the BER is given by:

$$\text{BER} = \frac{1}{N_b} \sum_{i=1}^{N_b} \mathbb{1}_{\{b_{\text{tx},i} \neq b_{\text{rx},i}\}},$$

  where N_b is the total number of transmitted bits and $\mathbb{1}_{\{\cdot\}}$ is the indicator function that equals 1 if its argument is true and 0 otherwise. A lower BER indicates better demodulation performance under interference and noise.

- **Error Vector Magnitude (EVM):** EVM is a measure of the deviation of the received complex symbols from their ideal (reference) positions in the constellation diagram. It reflects the quality of the modulation and is sensitive to interference, distortion, and noise. It is calculated as:

$$\text{EVM (\%)} = 100 \times \sqrt{\frac{\sum_{k=1}^{N_s} |r_k - s_k|^2}{\sum_{k=1}^{N_s} |s_k|^2}},$$

  where s_k and r_k are the k-th transmitted and received symbols, respectively, and N_s is the total number of transmitted symbols. Lower EVM percentages indicate cleaner constellations and less distortion.

- **Signal-to-Interference-plus-Noise Ratio (SINR):** SINR measures the power of the desired signal relative to the combined power of interference and noise. It is computed per OFDM symbol for Numerology 1 as:

$$\text{SINR (dB)} = 10 \log_{10} \left(\frac{\mathbb{E}[|s_k|^2]}{\mathbb{E}[|r_k - s_k|^2]} \right),$$

  where s_k and r_k denote the transmitted and received symbols, respectively. Higher SINR values indicate stronger signal dominance over distortion and INI.

- **Spectral Efficiency (SE):** SE evaluates how efficiently the system transmits data over the available bandwidth. It is expressed in bits per second per Hertz (bps/Hz), and for Numerology 1 is computed as:

$$\text{SE} = \frac{R_b}{B \cdot T_{\text{sym}}} = \frac{N_c \cdot \log_2 M \cdot (1 - \text{BER})}{B \cdot T_{\text{sym}}},$$

  where R_b is the net bit rate, N_c is the number of correctly decoded symbols, M is the modulation order (e.g., 16 for 16-QAM), B is the occupied bandwidth, and T_{sym} is the OFDM symbol duration. SE reflects the trade-off between reliability (through BER) and capacity.

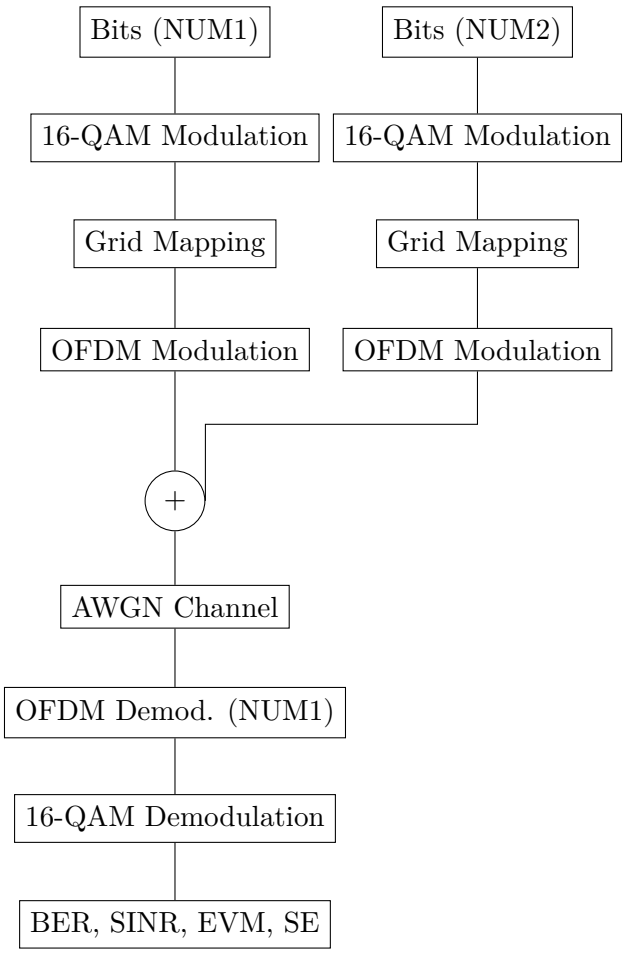

Figure 3.1: system model for downlink multi-numerology OFDM simulation.

3.1.2 Constellation at 20 dB SNR

Figure 3.2 shows the transmitted and received 16-QAM constellation diagrams for Numerology1 at an SNR of 20,dB without time alignment. The transmitted symbols form a clean grid with well-separated constellation points, while the received symbols appear heavily dispersed and clustered irregularly due to severe inter-numerology interference (INI) from Numerology2. This distortion is a result of spectral leakage caused by the lack of synchronization between the numerologies, which leads to significant degradation in demodulation quality, elevated error rates, and increased EVM, highlighting the necessity of mitigation strategies such as time-domain alignment or filtering.

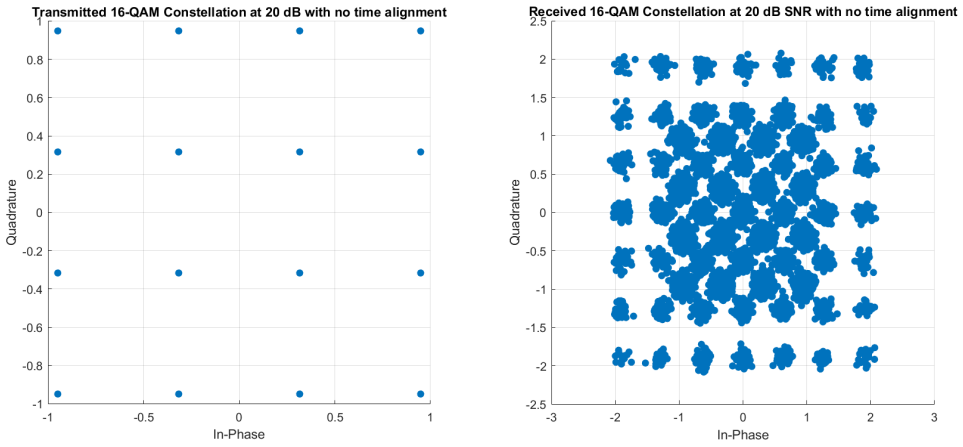

Figure 3.2: 16-QAM constellations with no time alignment or filtering

3.1.3 Error Vector Magnitude (EVM)

Figure 3.3 illustrates the Error Vector Magnitude (EVM) performance of the desired numerology in the absence of time alignment. The EVM remains extremely high across all SNR values, exceeding 100% at low SNRs and plateauing at elevated levels even beyond 20,dB. These values indicate a significant deviation of the received symbols from their ideal constellation points, confirming the severe distortion observed in the received constellation diagram (Figure 3.2). This persistent impairment is primarily caused by inter-numerology interference (INI) from the adjacent numerology operating without temporal synchronization, and underscores the inability of the system to preserve symbol integrity under such conditions.

3.1.4 Bit Error Rate (BER)

Figure 3.4 presents the BER curve for the desired numerology under the current configuration without time alignment. The curve exhibits a pronounced BER floor, with error rates remaining significantly high even at elevated SNR values. This plateau suggests that the receiver is unable to distinguish the transmitted bits from

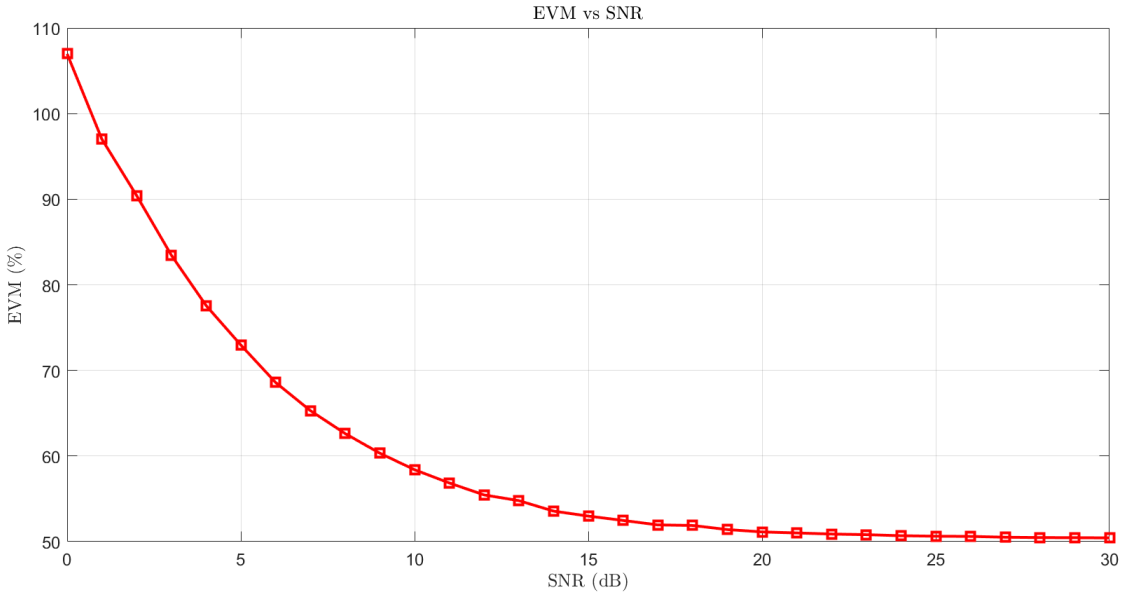

Figure 3.3: EVM with no time alignment or filtering

the received signal with sufficient reliability due to overwhelming inter-numerology interference. In such conditions, the demodulator performance approaches that of a random guess, indicating that the signal is effectively unrecoverable and the system's capacity is severely compromised.

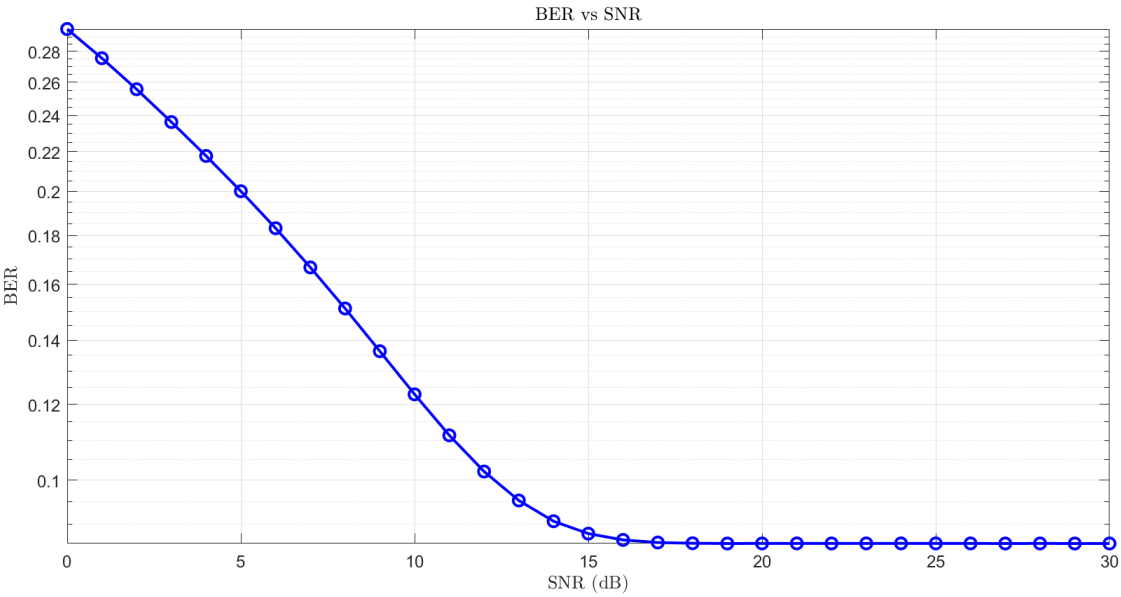

Figure 3.4: BER vs SNR with no time alignment or filtering (16-QAM)

3.1.5 Signal to Interference Noise Ratio (SINR)

Figure 3.5 depicts the Signal-to-Interference-plus-Noise Ratio (SINR) as a function of the SNR for the desired numerology when no time alignment is applied. While

SINR increases with SNR in the low range, it quickly saturates around 6,dB, forming a performance ceiling. This saturation indicates that beyond a certain point, increasing transmit power no longer improves signal quality due to persistent interference from the adjacent numerology. The plateau confirms that inter-numerology interference (INI), rather than thermal noise, becomes the dominant factor limiting system performance, aligning with the severe distortions observed in the constellation and the high BER and EVM levels previously discussed.

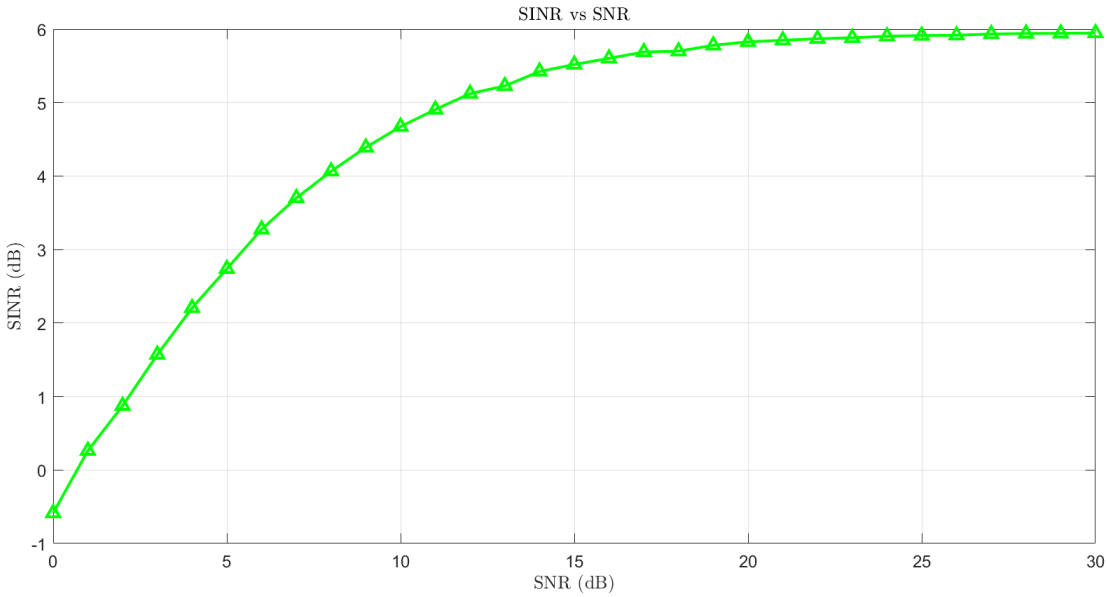

Figure 3.5: SINR vs SNR with no time alignment or filtering

3.1.6 Spectral efficiency

Figure 3.6 shows the spectral efficiency of the desired numerology as a function of SNR in the absence of time alignment. The curve increases with SNR and saturates near the theoretical maximum, despite the presence of strong inter-numerology interference (INI) observed in other metrics.

The theoretical maximum spectral efficiency for a 16-QAM system is computed as follows. Each subcarrier carries $\log_2(16) = 4$ bits per OFDM symbol. For the desired BWP:

- Number of subcarriers: $100 \times 12 = 1200$
- Subcarrier spacing: $15\,\text{kHz}$
- Total bandwidth: $B = 1200 \times 15 \times 10^3 = 18\,\text{MHz}$
- OFDM symbol duration (with CP):

$$T_{\text{sym}} = \frac{2048 + 144}{30.72 \times 10^6} \approx 7.13\,\mu\text{s}$$

– Symbols per second per subcarrier:

$$R = \frac{1}{T_{\text{sym}}} \approx 140270\,\text{symbols/s}$$

Thus, the theoretical spectral efficiency over the BWP is:

$$\text{SE}_{\text{max}} = \frac{1200 \times 4\,\text{bits/symbol}}{18 \times 10^6\,\text{Hz}} \times 140270\,\text{symbols/s} \approx 11.68\ \text{bps/Hz}$$

This matches the saturation level observed in the figure. However, unlike SINR, BER, or EVM, which clearly reflect the distortion caused by INI, spectral efficiency remains largely unaffected. This is because the SE metric considers only the ratio of correctly received bits to bandwidth and time, and does not penalize signal degradation unless the bit error rate is extremely high. In this case, although distortion is severe, the demodulator still recovers

$$90\%$$

of the bits, resulting in an SE value close to the ideal.

Nevertheless, most practical INI mitigation techniques, such as introducing guard bands, inherently reduce the usable bandwidth and may therefore degrade spectral efficiency. Our objective, therefore, is to develop mitigation strategies that reduce INI without sacrificing SE, by avoiding excessive spectral overhead or loss of transmission capacity.

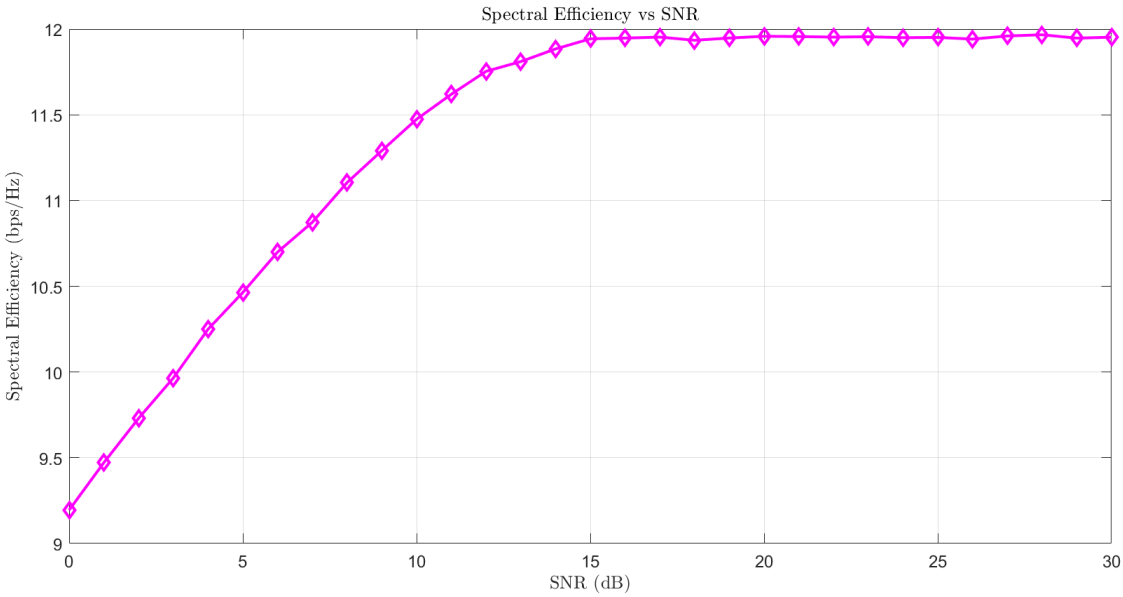

Figure 3.6: Spectral Efficiency vs SNR with no time alignment or filtering

3.2 Mitigation Strategies: Time Alignment and FIR-Based Filtering

To address the issue of inter-numerology interference (INI) in a dual-numerology OFDM downlink system, two complementary signal processing strategies are em-

ployed: (1) time-domain alignment, and (2) frequency-domain suppression via high-pass filtering. These are designed to align OFDM symbol boundaries across numerologies and reduce spectral leakage without introducing guard bands or reducing usable bandwidth.(Figure3.7)

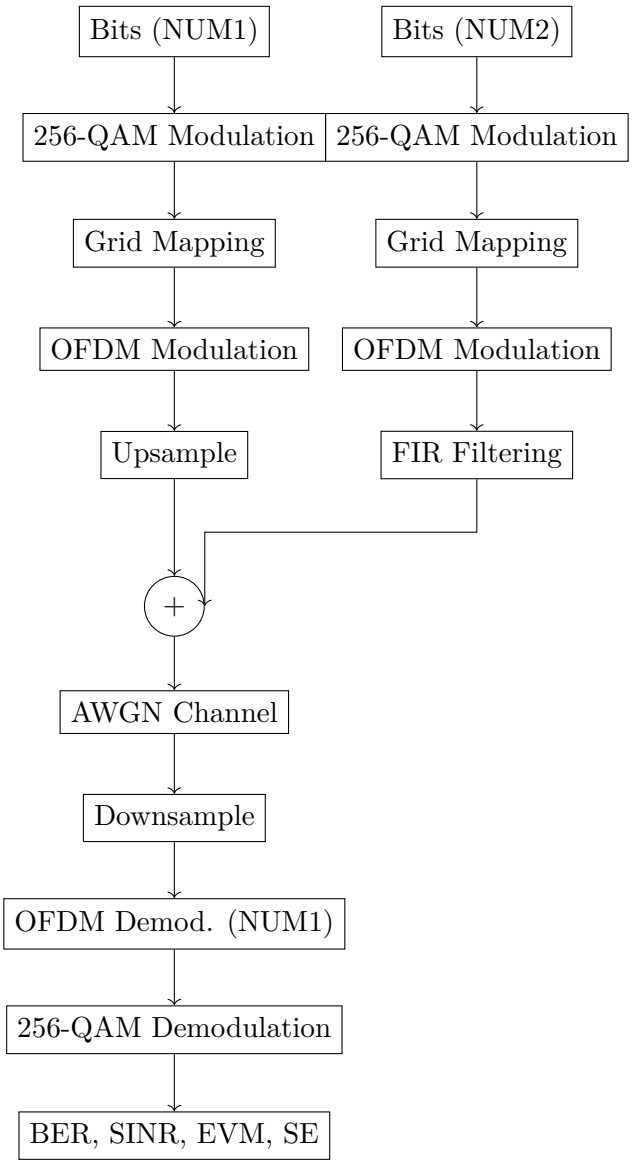

Figure 3.7: system model for downlink multi-numerology OFDM simulation with time alignment FIR filtering.

3.2.1 Time-Domain Symbol Alignment via Resampling

In multi-numerology systems, numerologies with different subcarrier spacings (SCS) have inherently different OFDM symbol durations. Specifically, a numerology with subcarrier spacing Δf has an OFDM symbol duration (excluding CP) of:

$$T = \frac{1}{\Delta f \cdot N},$$

where N is the number of subcarriers used in the IFFT. In our configuration, Numerology 1 has $\Delta f_1 = 15\,\text{kHz}$, and Numerology 2 has $\Delta f_2 = 30\,\text{kHz}$, resulting in:

$$T_2 = \frac{T_1}{2}.$$

To ensure symbol boundary alignment across both numerologies, we construct both waveforms such that their sampling grids match in time. Let f_{s1} be the sampling rate of Numerology 1. We set:

$$f_{s2} = 2f_{s1},$$

so that each OFDM symbol of Numerology 1 spans exactly two symbols of Numerology 2 in time. The transmitted waveform of Numerology 1 is then resampled (interpolated) by a factor of 2:

$$x_1^{(\uparrow)}[n] = \sum_{k=-\infty}^{\infty} x_1[k] \cdot h[n - 2k],$$

where $h[n]$ is an ideal interpolation filter. This operation increases the sample rate and aligns the waveform with the higher numerology's timing grid.

At the receiver, after combining both signals and adding noise, the received waveform is downsampled by a factor of 2 before demodulating Numerology 1. This downsampling is defined as:

$$x^{(\downarrow)}[n] = x[2n],$$

recovering the original sampling rate and ensuring proper demodulation timing.

3.2.2 Spectral Suppression via High-Pass FIR Filtering

Even with time-domain alignment, inter-numerology interference (INI) can persist due to the inherent spectral leakage of OFDM waveforms. In particular, the higher-subcarrier-spacing Numerology 2 (30 kHz SCS) produces significant out-of-band emissions that can leak into the spectral region of Numerology 1 (15 kHz SCS). To mitigate this spectral overlap, we employ a dedicated high-order FIR filter that attenuates the low-frequency components of the Numerology 2 signal prior to multiplexing.

Let $x_2[n]$ denote the discrete-time baseband signal for Numerology 2. The filtered signal is obtained via linear convolution:

$$x_2^{(\text{filt})}[n] = \sum_{k=0}^{N} h[k] \cdot x_2[n - k],$$

where $h[k]$ are the FIR filter coefficients and the filter order is set to $N = 32$, which we found sufficient to achieve the required selectivity in our setup. The filter is designed as a high-pass FIR filter using the window method:

- **Stopband edge frequency:** $f_{\text{stop}} = 9.15\,\text{MHz}$,
- **Passband start frequency:** $f_{\text{cutoff}} = 30\,\text{MHz}$,

– **Sampling frequency:** $f_s = 61.44\,\text{MHz}$.

In normalized digital frequency, the transition band is defined as:

$$\Omega = \left[\frac{2f_{\text{stop}}}{f_s}, \frac{2f_{\text{cutoff}}}{f_s} \right].$$

To achieve sharp frequency separation and preserve temporal fidelity, the filter is:

– **Linear-phase**, ensured by designing a symmetric impulse response:

$$h[n] = h[N - n], \quad \forall n \in [0, N],$$

– **Zero-phase**, implemented via forward-backward filtering using `filtfilt()`, thereby eliminating group delay,

– **Windowed using a Chebyshev window**, providing strong sidelobe attenuation and sharp spectral transition.

This filtering step significantly suppresses spectral leakage from Numerology 2 into the frequency band of Numerology 1, reducing INI without requiring additional guard bands or affecting the integrity of the transmitted data symbols.

Figure 3.8 illustrates the characteristics of the filter. The impulse response confirms symmetry, while the magnitude response shows over 100 dB attenuation below the stopband and a rapid transition to full transmission above 30 MHz.

3.2.3 Power Spectral Density Analysis

Figure 3.9 compares the power spectral density (PSD) of the composite signal before and after applying the mitigation techniques. The left plot shows the PSD without time alignment or filtering, where strong spectral leakage from BWP2 (30 kHz numerology) spills into the band allocated to BWP1 (15 kHz numerology). The right plot demonstrates the effect of applying both time-domain alignment and high-pass FIR filtering to BWP2.

The filtering operation significantly attenuates the out-of-band (OOB) emissions of BWP2, particularly in the lower frequency range where BWP1 resides. The result is a cleaner spectral separation between the two numerologies, confirming the effectiveness of the combined mitigation strategy in reducing inter-numerology interference (INI).

3.3 Performance Analysis

To assess the effectiveness of the proposed inter-numerology interference (INI) mitigation techniques, we evaluate the system under two configurations:

1. **Time alignment only**, in which the OFDM symbol boundaries of Numerology 1 and Numerology 2 are synchronized in the time domain through sample rate matching, but no additional filtering is applied.

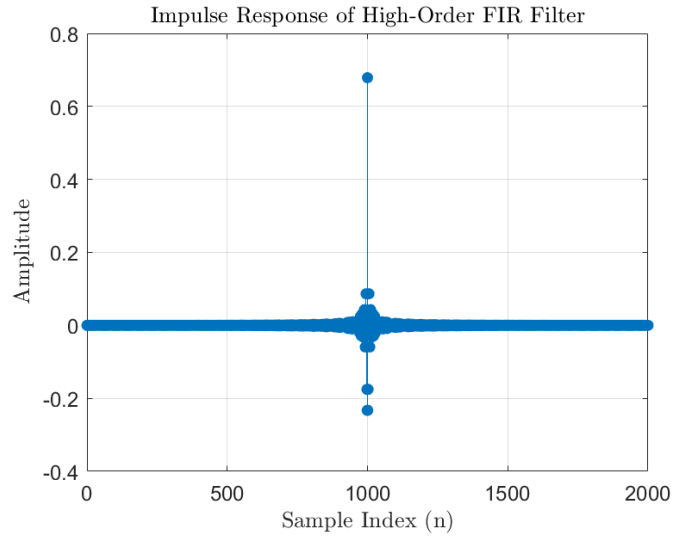

(a) Impulse response.

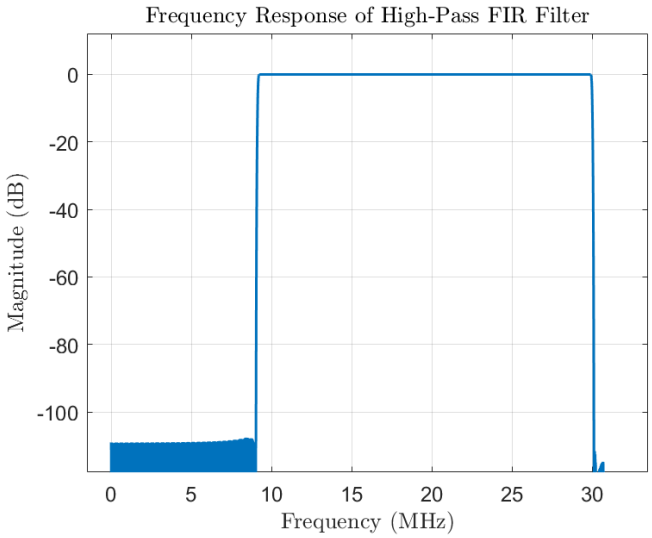

(b) Frequency response (magnitude in dB).

Figure 3.8: Impulse and frequency response of the high-pass FIR filter used to suppress out-of-band emissions from Numerology 2.

2. **Time alignment with FIR filtering**, in which a high-order high-pass filter is applied to the waveform of Numerology 2 to suppress its low-frequency sidelobes before signal superposition.

In both scenarios, Numerology 1 (15 kHz subcarrier spacing) is treated as the desired signal, while Numerology 2 (30 kHz subcarrier spacing) acts as the interferer. The objective is to determine under which conditions time alignment alone suffices to mitigate INI, and when additional spectral filtering becomes necessary to preserve the demodulation performance of Numerology 1.

The following subsections present constellation diagrams and bit error rate (BER) performance for various modulation orders, including QPSK, 16-QAM, 64-QAM, 128-QAM, and 256-QAM. Since the modulation order does not significantly affect metrics such as error vector magnitude (EVM), signal-to-interference-plus-noise

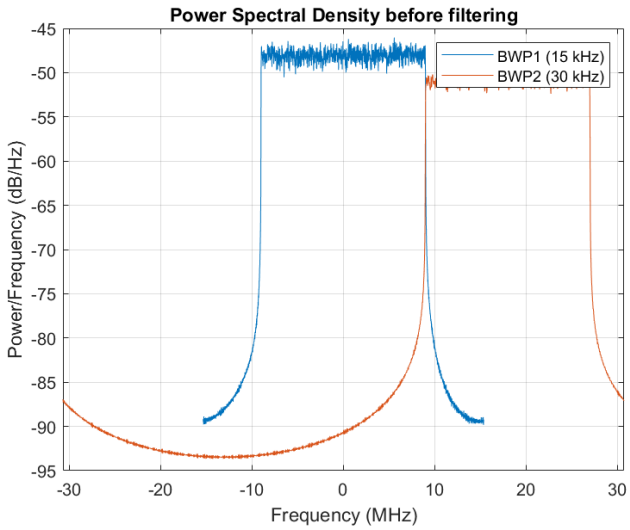

(a) PSD before filtering(alignment only).

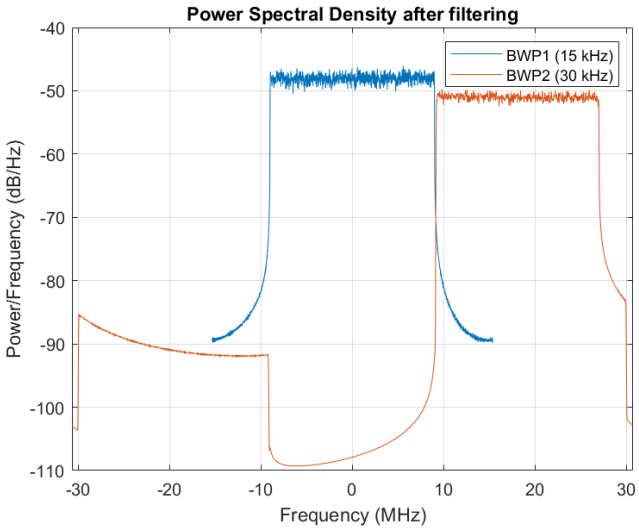

(b) PSD after filtering.

Figure 3.9: Power Spectral Density comparison.

ratio (SINR), and spectral efficiency (SE), these metrics are reported only for the 16-QAM case. All performance indicators are evaluated over a range of signal-to-noise ratio (SNR) values to analyze system behavior under varying channel conditions.

3.3.1 Constellation Diagrams

This subsection presents the transmitted and received constellations at 20 dB for various modulation orders under two configurations: (a) with time alignment only, and (b) with both time alignment and FIR filtering. The visual comparison highlights the distortion introduced by inter-numerology interference (INI) and the improvement achieved through filtering.

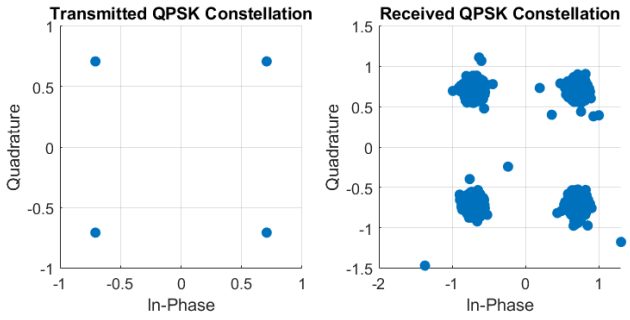

(a) Without filtering

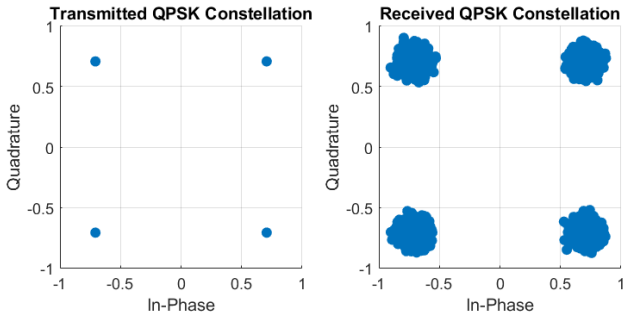

(b) With FIR filtering

Figure 3.10: QPSK constellation.

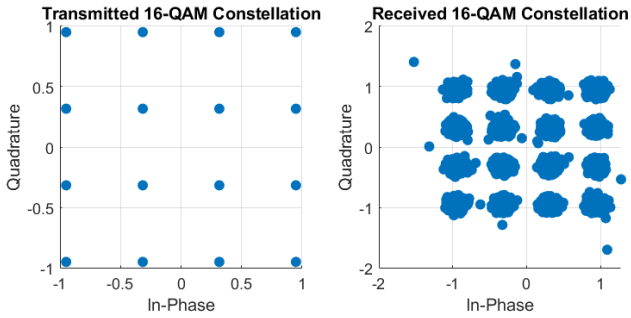

(a) Without filtering

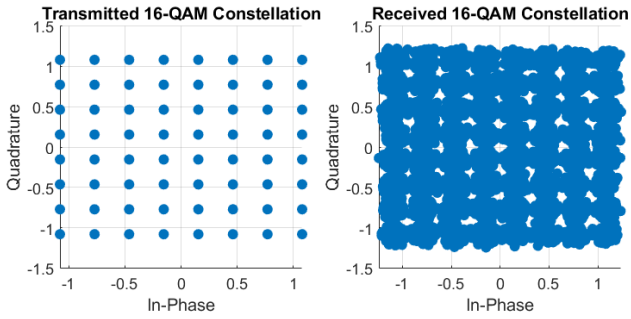

(b) With FIR filtering

Figure 3.11: 16-QAM constellation.

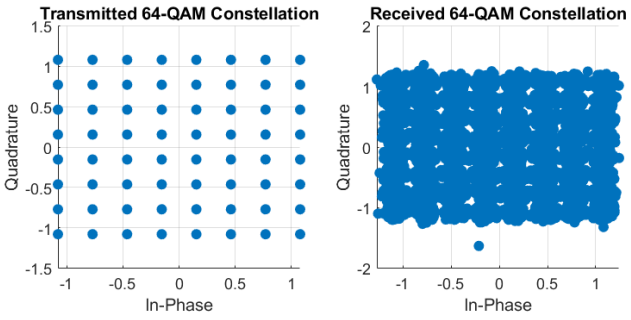

(a) Without filtering

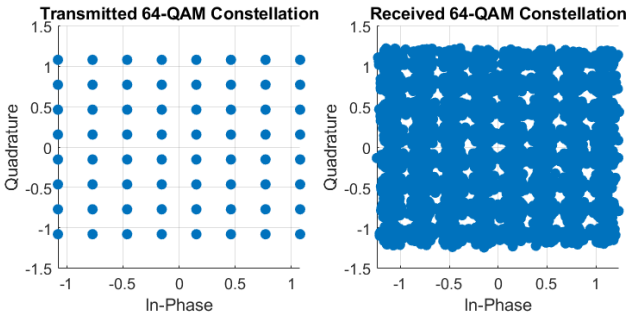

(b) With FIR filtering

Figure 3.12: 64-QAM.

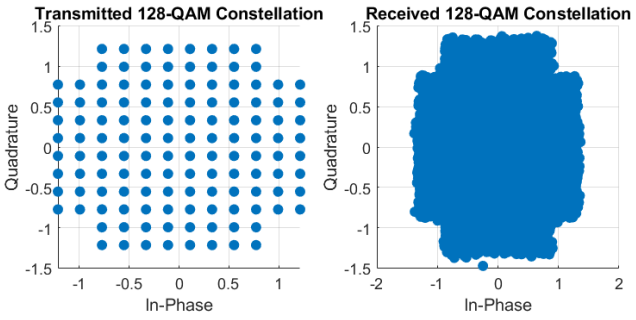

(a) Without filtering

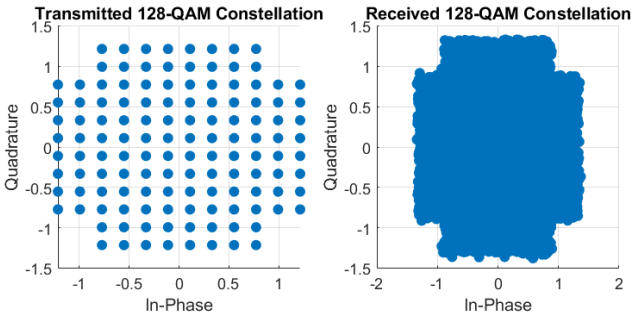

(b) With FIR filtering

Figure 3.13: 128-QAM.

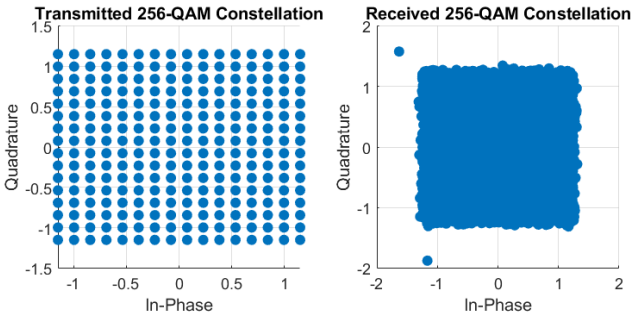

(a) Without filtering

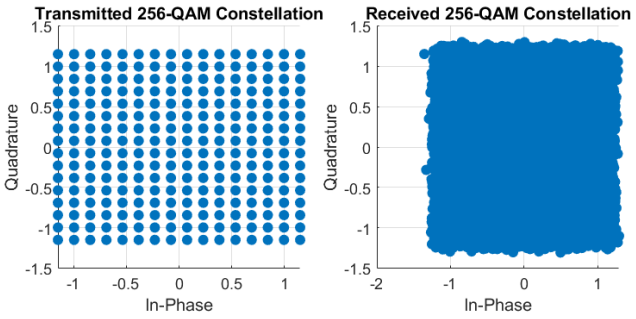

(b) With FIR filtering

Figure 3.14: 256-QAM.

Discussion

The results clearly indicate that INI causes significant symbol scattering in the received constellations, with severity increasing alongside modulation order due to tighter decision boundaries.As shown in Figures 3.10–3.14, when only time alignment is applied, high-order modulations such as 128-QAM and 256-QAM suffer from considerable distortion, leading to symbol overlap and degraded demodulation performance.

By contrast, applying FIR filtering to suppress low-frequency sidelobes of Numerology 2 results in noticeably cleaner constellations for all modulation orders. The received symbol clusters become tighter and better aligned with their transmitted reference points, validating the effectiveness of frequency-domain suppression. Filtering is therefore essential when using higher-order modulation schemes in the presence of inter-numerology interference.

3.3.2 BER Performance

This subsection presents the bit error rate (BER) performance of the system under two configurations, time alignment only and time alignment with FIR filtering, across a range of modulation schemes: QPSK, 16-QAM, 64-QAM, 128-QAM, and 256-QAM. The results illustrate the impact of inter-numerology interference (INI) on BER, and the improvement achieved by spectral filtering.

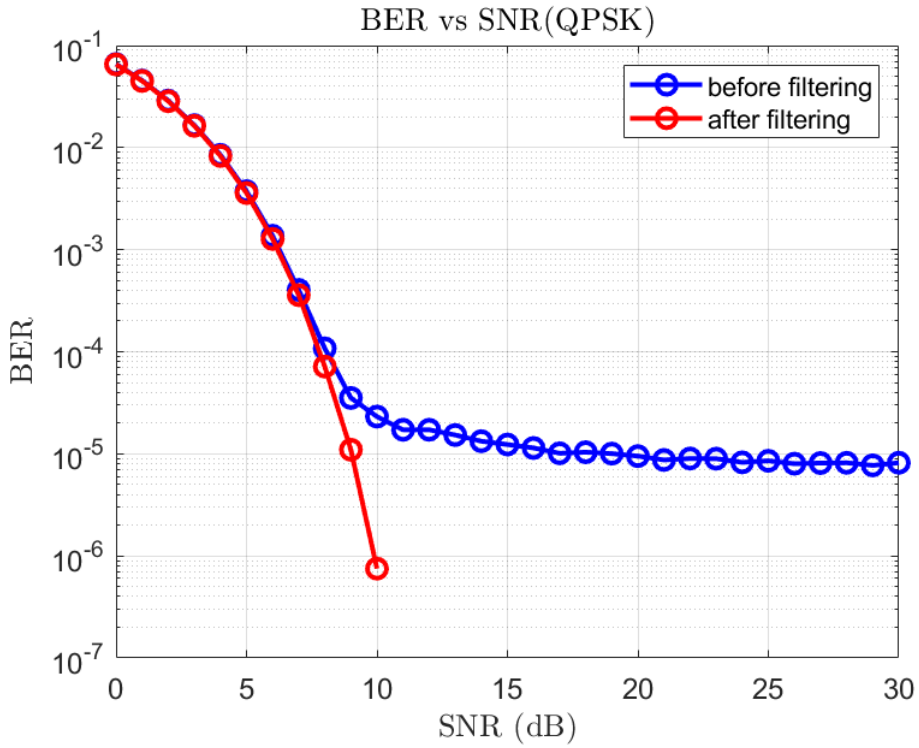

Figure 3.15: BER vs. SNR for QPSK with and without FIR filtering.

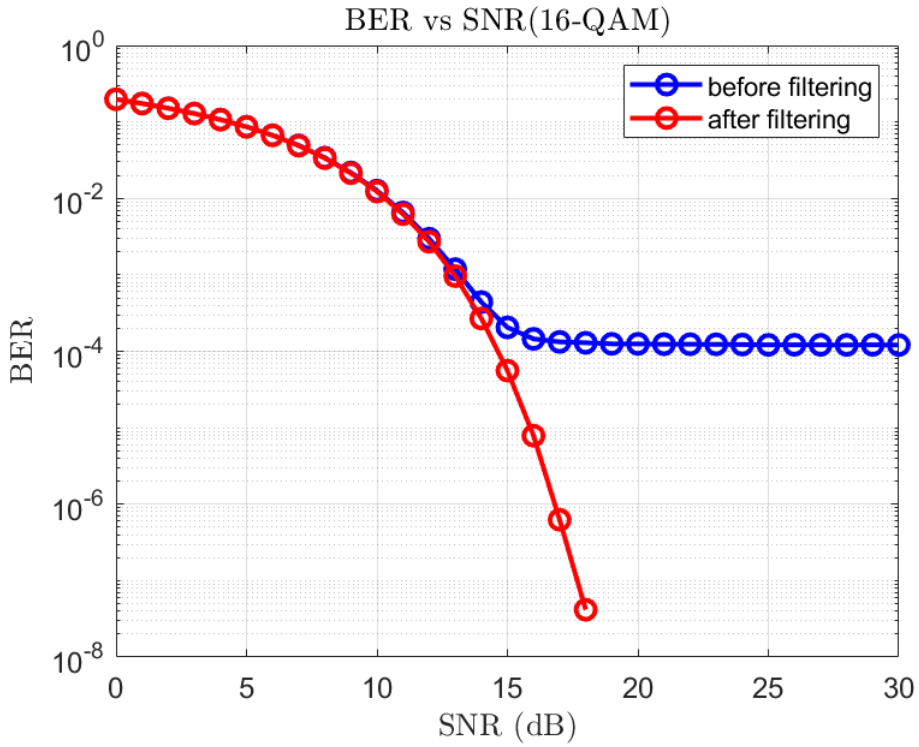

Figure 3.16: BER vs. SNR for 16-QAM with and without FIR filtering.

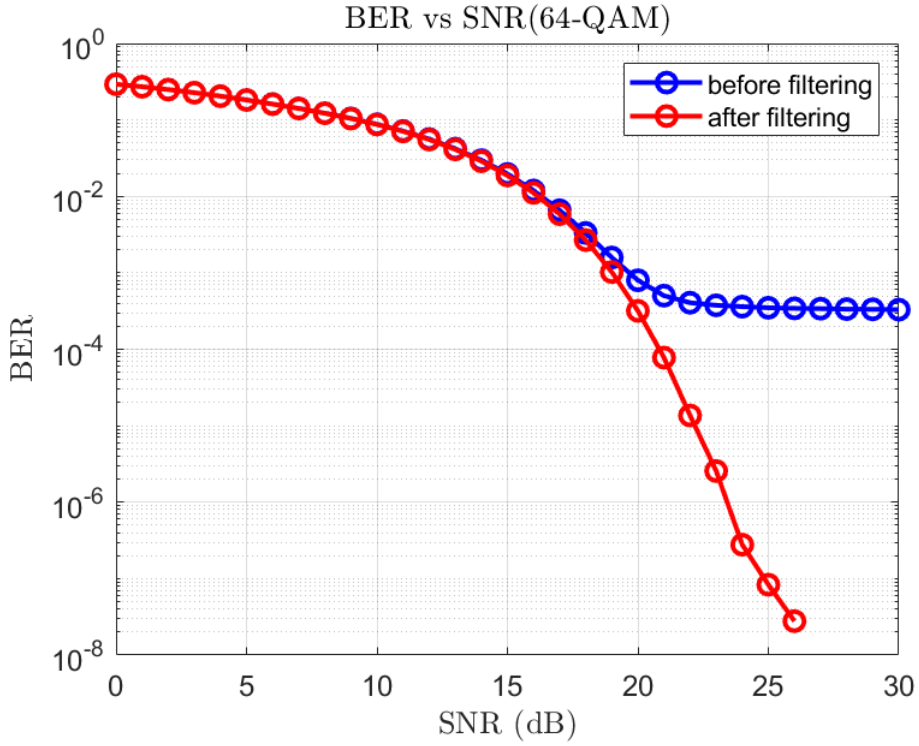

Figure 3.17: BER vs. SNR for 64-QAM with and without FIR filtering.

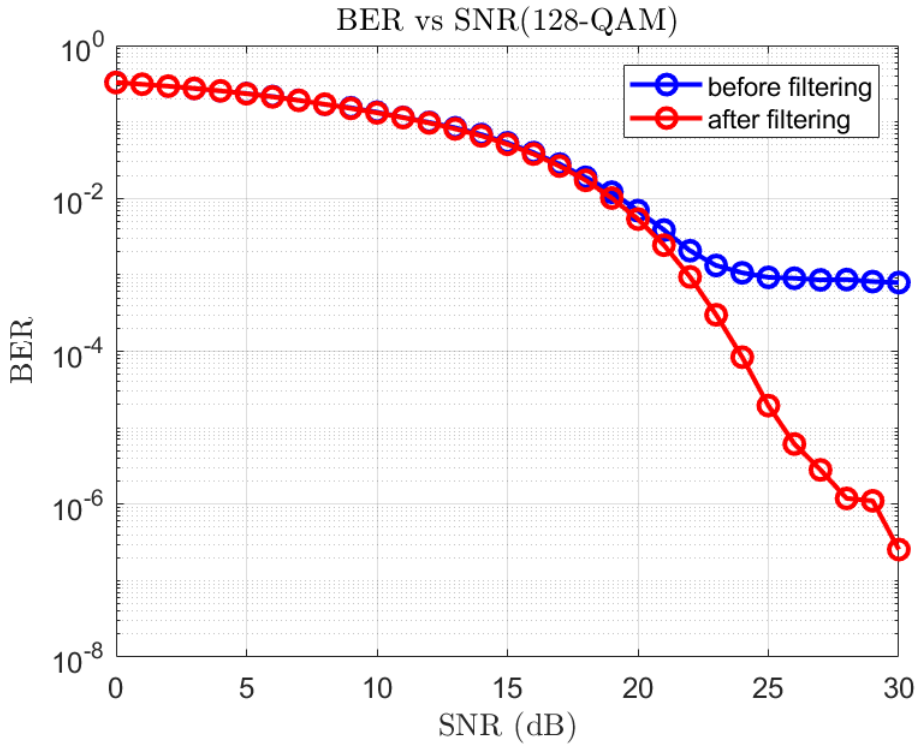

Figure 3.18: BER vs. SNR for 128-QAM with and without FIR filtering.

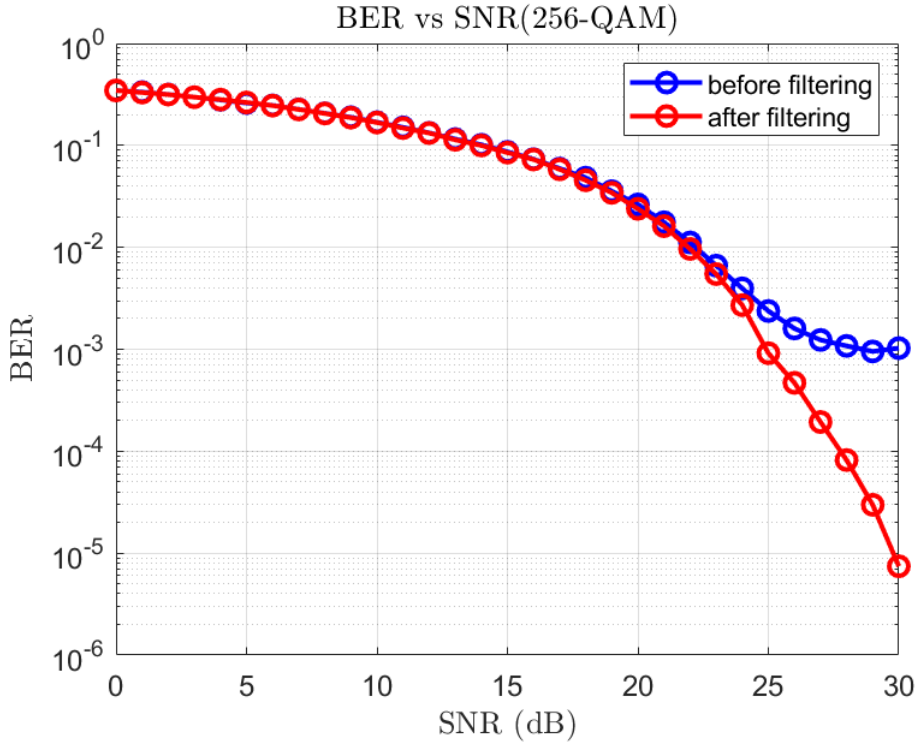

Figure 3.19: BER vs. SNR for 256-QAM with and without FIR filtering.

Discussion

The results across Figures 3.15–3.19 reveal a consistent pattern: when only time alignment is applied, a BER floor emerges at moderate to high SNR levels due to residual inter-numerology interference. This floor becomes more prominent with higher modulation orders, where symbols are more sensitive to interference.

The application of FIR filtering to the interfering numerology dramatically improves BER performance across all schemes. For lower-order modulations (e.g., QPSK and 16-QAM), near-error-free decoding is achieved at relatively low SNRs. For higher-order schemes (e.g., 128-QAM and 256-QAM), filtering enables the system to surpass the BER floor and follow a steeper slope consistent with ideal AWGN conditions.

These findings confirm that while time-domain alignment alleviates some INI, frequency-domain suppression is essential to achieve reliable performance, especially when higher spectral efficiency is desired.

3.3.3 EVM, SINR and Spectral Efficiency Analysis

In this subsection, we evaluate the impact of the proposed mitigation techniques on three key performance metrics: Error Vector Magnitude (EVM), Signal-to-Interference-plus-Noise Ratio (SINR), and Spectral Efficiency (SE). These metrics are computed only for the 16-QAM case, since they are modulation-agnostic in their relative trends.

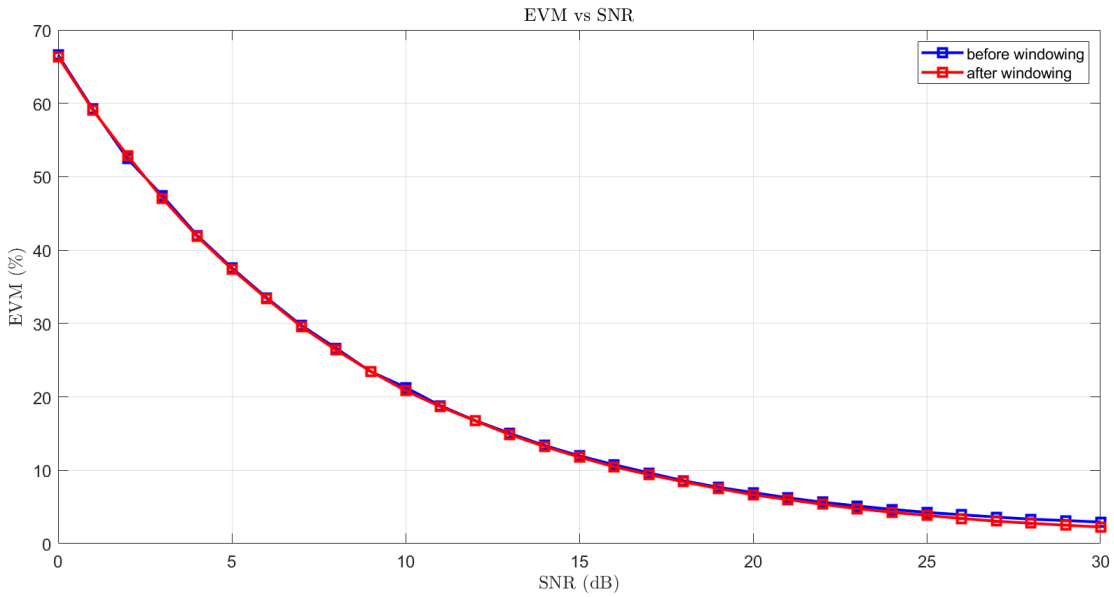

Figure 3.20: EVM performance before and after filtering.

Figure 3.20 shows the evolution of the EVM as a function of SNR. We observe that applying time alignment and high-pass filtering consistently reduces the EVM across the entire SNR range. This reduction confirms that the received symbols are more accurately clustered around their ideal constellation points, corroborating the qualitative improvement observed in the constellation diagrams.

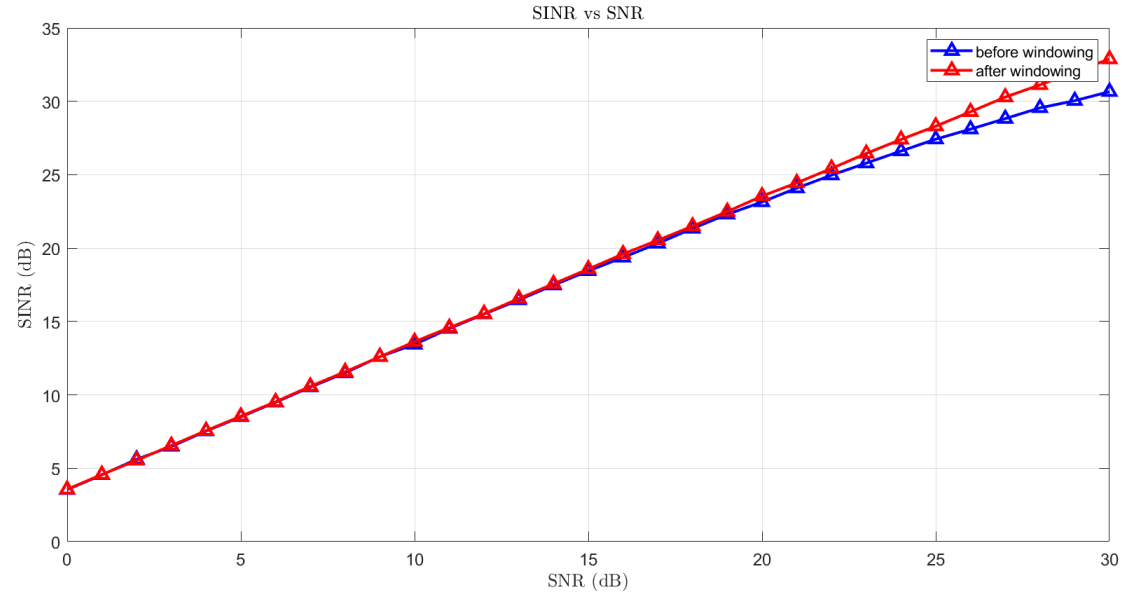

Figure 3.21: SINR performance before and after filtering.

Figure 3.21 illustrates the SINR improvement obtained after mitigation. The filtering effectively suppresses the interfering sidelobes from Numerology 2, thereby enhancing the signal clarity of Numerology 1. The SINR gain becomes more noticeable at higher SNR levels, where noise is less dominant and interference constitutes the primary limiting factor.

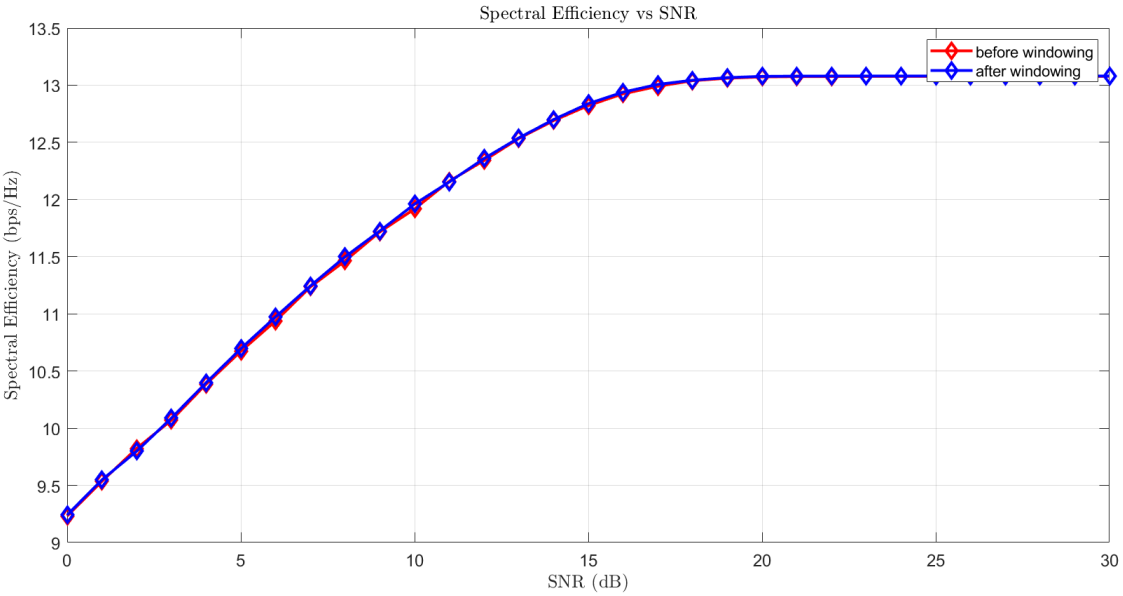

Figure 3.22: Spectral efficiency before and after filtering.

Finally, Figure 3.22 presents the spectral efficiency obtained before and after mitigation. Notably, since we avoided introducing guard bands in our design, the effective occupied bandwidth was not reduced. As a result, the system benefits from a slight increase in spectral efficiency, especially at high SNRs where bit recovery is highly

accurate. This demonstrates that careful filtering can improve signal quality without sacrificing bandwidth utilization, thereby preserving or even enhancing overall system capacity.

Conclusion

This chapter has presented a thorough evaluation of inter-numerology interference (INI) in a dual-numerology OFDM system and proposed a two-pronged mitigation approach combining time-domain symbol alignment and frequency-domain filtering.

In the absence of any mitigation, we observed severe degradation in all key performance metrics. High error floors, elevated EVM, and low SINR levels revealed the vulnerability of low-SCS users to spectral leakage from adjacent numerologies. Even at high SNRs, the demodulation performance remained capped due to persistent interference, confirming that INI is the dominant limiting factor.

To address this challenge, time alignment via resampling was introduced to synchronize the OFDM symbols of different numerologies. While this significantly improved signal quality, particularly in low-order modulation scenarios, it proved insufficient in isolation. High-order modulations such as 128-QAM and 256-QAM continued to suffer from residual interference.

The addition of a high-pass FIR filter applied to the interfering numerology demonstrated a clear benefit: constellation points became more tightly clustered, BER dropped by several orders of magnitude, and SINR values increased substantially. Importantly, by avoiding the use of guard bands and applying zero-phase filtering, we preserved spectral efficiency,achieving both robustness and bandwidth efficiency.

In summary, this chapter establishes that time alignment is a necessary but not always sufficient condition for INI mitigation. For high-throughput, interference-sensitive applications, spectral filtering becomes indispensable. The combined strategy ensures that 5G networks can support flexible multi-numerology deployments without compromising on reliability or spectral efficiency. Future work may explore adaptive filtering, interference-aware scheduling, or machine learning-based waveform design as next steps in this optimization landscape.

Conclusion and Future Work

1 Summary of Contributions

This thesis has addressed the challenge of **inter-numerology interference (INI)** in 5G New Radio (NR) systems through a detailed simulation-based evaluation and mitigation framework. INI arises when multiple numerologies, each with different subcarrier spacings (SCS), are deployed within a shared spectrum. While this flexibility enables heterogeneous service support (e.g., eMBB, URLLC, mMTC), it disrupts the orthogonality of OFDM subcarriers, leading to spectral leakage and performance degradation.

The main contributions of this work are as follows:

- Development of a **comprehensive MATLAB-based simulation platform** for dual-numerology downlink OFDM systems that realistically models time-domain signal generation, numerology misalignment, and INI under 3GPP-compliant parameters.
- **Design and integration of two lightweight mitigation techniques**: (i) a time-domain alignment strategy via rational resampling to synchronize OFDM symbol boundaries across numerologies, and (ii) a high-order FIR-based spectral filter applied to suppress out-of-band (OOB) emissions from higher-SCS numerologies.
- **Performance evaluation across a wide set of modulation orders** (QPSK to 256-QAM), highlighting the conditions under which time alignment alone is sufficient, and when filtering becomes essential, particularly in high-order modulation scenarios.
- **Quantitative comparison of system performance metrics** including BER, EVM, SINR, and spectral efficiency, both with and without filtering. Results demonstrate clear improvements when filtering is added, especially in mitigating the BER floor and constellation distortion caused by INI.
- **Spectral analysis and system modeling insights**, including a visual interpretation of filtering impact on power spectral density and time-domain waveform characteristics.

This study provides practical insight into the trade-offs involved in low-complexity INI mitigation strategies and shows that high performance can be achieved without guard bands or iterative cancellation methods.

2 Limitations of the Current Work

Despite promising results, the present study has a number of limitations:

- The simulation focuses on a **two-numerology scenario** and does not account for more complex interference dynamics in systems with three or more overlapping numerologies.

  rust Copier Modifier

- The high-order FIR filter used to suppress BWP2's OOB emissions introduces **slight in-band distortion** to the BWP2 signal, potentially impacting the quality of service for users operating under the higher-SCS configuration.
- The current filtering approach is **static and non-adaptive**; it does not dynamically adjust to varying channel conditions, traffic loads, or user mobility.
- **Only downlink performance was studied**, under perfect synchronization assumptions. Uplink scenarios and asynchronous interference patterns remain unaddressed.
- Practical considerations such as **implementation cost, computational complexity, and hardware feasibility** of real-time FIR filtering and up/downsampling operations were not examined.

These limitations identify key areas where the proposed system can be further extended and optimized.

3 Future Research Directions

Building upon the current findings, several future research paths can be pursued:

- **Distortion-aware filter design:** Investigate window or FIR designs that minimize interference leakage while explicitly preserving the in-band integrity of the filtered numerology (e.g., constrained optimization of filter ripple in passband).
- **Dynamic filtering and scheduling:** Combine the filtering strategy with adaptive resource allocation or numerology-aware scheduling to jointly minimize INI and maximize throughput.
- **Multi-user and uplink extensions:** Extend the current system model to include uplink transmissions and multiple users with different numerologies transmitting simultaneously toward a shared base station.
- **Real-time feasibility analysis:** Analyze implementation cost and delay of the proposed methods on DSP/FPGA platforms to evaluate their viability in hardware.

– **INI-aware learning algorithms:** Integrate reinforcement learning or data-driven approaches for adaptive mitigation in dynamic 5G/6G environments with mobility, CSI variability, or evolving traffic patterns.

– **Scalability to 6G use cases:** Explore the applicability of these techniques in future networks with flexible waveform candidates (e.g., FBMC, GFDM), reconfigurable intelligent surfaces (RIS), and ultra-dense deployments.

4 Final Remarks

This work has demonstrated that simple yet effective INI mitigation in 5G multi-numerology systems is possible through time-domain alignment and carefully designed FIR filtering. Using MATLAB simulations, we have shown that the proposed approach significantly improves signal fidelity and demodulation performance for the lower-SCS user without relying on complex interference cancellation or introducing spectral overhead through guard bands.

While filtering introduces slight in-band distortion to the interferer (BWP2), the overall system capacity is preserved, and the user of interest benefits from dramatically reduced interference. These results pave the way for more balanced and adaptive interference-aware designs in future radio access networks.

Appendix A

Signal Processing Through Filtering Techniques

Introduction

Filtering, a cornerstone of signal processing, involves the selective modification of frequency components within a signal to extract pertinent information, suppress unwanted noise, or reshape the signal for subsequent analysis or processing. This process is fundamental across various domains, including audio and image processing, communication systems, biomedical engineering, and control systems, where signals often contain noise, interference, or irrelevant information that obscures the underlying phenomena of interest [137]. Filters are designed to selectively pass or attenuate specific frequency ranges, enabling the isolation and enhancement of desired signal components [138]. The design and implementation of effective filters require a deep understanding of signal characteristics, filter types, and the trade-offs between different design parameters, such as filter order, cutoff frequency, and passband ripple [139]. The versatility of filtering techniques stems from their ability to manipulate signals in both the time and frequency domains, offering a flexible toolkit for signal conditioning and analysis. Full-spectrum signal processing algorithm design is facilitated by filtering [140].

The essence of filtering lies in its capacity to discriminate between different frequency components within a signal, which is achieved by attenuating or amplifying specific frequency ranges [141]. This selective modification of the frequency spectrum enables the extraction of desired information, the suppression of noise, and the enhancement of signal quality [142]. Different filtering techniques are suited for different signal characteristics and application requirements. [139]. The selection of an appropriate filtering technique requires careful consideration of the signal's spectral content, the nature of the noise, and the desired characteristics of the filtered signal. Moreover, the implementation of filters involves trade-offs between performance, complexity, and computational cost, which must be carefully balanced to achieve optimal results. The prevention of distortions is vitally important considering the nature of the signals [143].

1 Fundamentals of Filter Design

The design of filters involves a systematic process that begins with defining the desired filter characteristics and culminates in the implementation of a physical or computational filter that meets those specifications [144]. The first step in filter design is to specify the filter's desired frequency response, which defines how the filter should attenuate or amplify different frequency components. These specifications typically include parameters such as the passband edge, stopband edge, passband ripple, and stopband attenuation, which quantify the filter's performance in different frequency ranges. Based on the desired frequency response, a filter approximation is chosen, which is a mathematical function that approximates the desired frequency response.

1.1 Filter Types and Characteristics

Filters can be broadly categorized into analog and digital filters, each with its own set of advantages and limitations. Analog filters operate on continuous-time signals using electronic components such as resistors, capacitors, and inductors, while digital filters operate on discrete-time signals using digital signal processing techniques. The selection of the appropriate filter type depends on factors such as the signal characteristics, the application requirements, and the available hardware or software resources. Digital filters offer greater flexibility, programmability, and immunity to component variations, making them well-suited for a wide range of applications. Furthermore, filters are categorized based on their impulse response characteristics.

A. Analog Filters

Constructed using continuous-time electronic components, analog filters are crucial in signal conditioning and processing due to their real-time operation and simplicity [145]. Passive filters composed of resistors, capacitors, and inductors, do not require external power sources and are generally used for basic frequency selection. Active filters, which incorporate active components like operational amplifiers, provide gain and can realize more complex filter responses. Butterworth, Chebyshev, and Bessel filters are commonly used for their unique characteristics, such as flat passband response, sharp cutoff, or linear phase response. Analog filters are still important in high-frequency applications and situations where quick processing is needed despite the growing popularity of digital filters.

B. Digital Filters

Digital filters process discrete-time signals using digital signal processing techniques on sampled data and are implemented in software or specialized hardware. Finite Impulse Response filters and Infinite Impulse Response filters are two main types of digital filters, each with unique characteristics and applications [146].

C. Finite Impulse Response Filters

FIR filters are characterized by their finite-duration impulse response, meaning that their output settles to zero after a finite number of samples in response to an impulse input. This property ensures that FIR filters are always stable, as there is no feedback mechanism that can cause oscillations or instability. Furthermore, FIR filters can be designed to have linear phase response, which preserves the time-domain characteristics of the signal by ensuring that all frequency components are delayed by the same amount of time. FIR filters are widely used in applications where linear phase response is critical, such as audio processing, image processing, and data communication.

D. Infinite Impulse Response Filters

IIR filters, in contrast, are characterized by their infinite-duration impulse response, meaning that their output can theoretically continue indefinitely in response to an impulse input. This is due to the presence of feedback in the filter structure, which allows the output to depend on previous output values as well as current and past input values. IIR filters can achieve sharper cutoff responses and require fewer coefficients compared to FIR filters for the same filter order [139]. However, IIR filters can be more challenging to design and implement due to the risk of instability, which can occur if the feedback coefficients are not chosen carefully.

1.2 Filter Design Techniques

Numerous techniques are available for designing filters, each offering unique trade-offs between performance, complexity, and computational cost.

A. Windowing Method

The windowing method is a simple and intuitive technique for designing FIR filters. It involves truncating an ideal impulse response with a window function to obtain a finite-length filter coefficient sequence [147]. The window function shapes the frequency response of the filter and reduces the undesirable effects of truncation, such as ripples in the passband and stopband [148]. Common window functions include the rectangular window, Hamming window, Hanning window, and Blackman window, each with its own characteristics in terms of main lobe width and side lobe attenuation.

B. Frequency Sampling Method

The frequency sampling method designs FIR filters by specifying the desired frequency response at a set of discrete frequencies. The filter coefficients are then obtained by taking the inverse discrete Fourier transform of the sampled frequency response. This method allows for precise control over the frequency response of the filter, but it can be computationally intensive for high-order filters.

C.Optimal Filter Design

Optimal filter design techniques aim to minimize a cost function that quantifies the deviation between the actual filter response and the desired filter response.

1.3 Filter Implementation

The implementation of filters involves translating the filter design into a physical realization, whether in hardware or software.

A. Direct Form

The direct form implementation is a straightforward and intuitive realization of a digital filter.

B. Cascade Form

The cascade form implementation decomposes a high-order filter into a series of lower-order filter sections, typically second-order sections.

C. Frequency-Domain Implementation

Frequency-domain implementation techniques leverage the properties of the discrete Fourier transform to perform filtering operations efficiently.

1.4 Filter Applications

The application of digital filters extends across a wide spectrum of disciplines, each leveraging the unique capabilities of these filters to address specific signal processing challenges.

A. Image Processing

Digital filters play a crucial role in image processing applications, where they are used for tasks such as noise reduction, edge detection, and image enhancement [149].

B.Audio Processing

Digital filters are indispensable in audio processing applications, where they are employed for tasks such as equalization, noise reduction, and audio effects.

D. Control Systems

Digital filters are widely used in control systems to smooth sensor data, stabilize feedback loops, and implement advanced control algorithms. The design of an efficient, reliable, simple, and economical filter is important [150]. Digital filters offer flexibility, programmability, and precise control over filter characteristics, making them well-suited for implementation in digital signal processors, microcontrollers, and general-purpose computers [151]. The utilization of digital signal processing offers possibilities, such as crossover filtering in multi-way loudspeakers, that are not achievable with analog filters [152]. Many digital speaker processors and digital crossovers offer multiple choices in high-pass, low-pass, and crossover filter selections, allowing users to tailor the audio signal to their specific needs [153]. Digital filters are employed to enhance the signal-to-noise ratio of digital sensors, although it's important to note that this enhancement can sometimes adversely affect the modulation transfer function [154].

1.5 Adaptive Filtering

Adaptive filtering represents a sophisticated signal processing technique that allows filters to dynamically adjust their parameters in response to changes in the input signal or the surrounding environment. This adaptability makes adaptive filters particularly well-suited for applications where the signal characteristics are non-stationary or unknown [155].

A.LMS Algorithm

The least mean squares algorithm is a widely used adaptive filtering algorithm due to its simplicity and computational efficiency.

B.RLS Algorithm

The recursive least squares algorithm is another popular adaptive filtering algorithm that offers faster convergence and better performance than the LMS algorithm, but at the cost of increased computational complexity.

Adaptive filtering has found widespread application in diverse fields, including noise cancellation, echo cancellation, channel equalization, and beamforming [156]. Adaptive filters are employed to mitigate baseline wander noise, which typically falls within the range of 0.15Hz to 0.3Hz and arises from factors like perspiration, respiration, and body movements [157]. Independent component analysis has been explored as a noise reduction technique for biomedical signals, with applications such as reducing artifacts in electrocardiogram signals caused by pacemaker activity.

Active noise control systems, which leverage adaptive filters, have achieved commercial success in various applications, including aircraft cabins, automobile cabins, and headsets, demonstrating the public health and economic benefits of this technology [158]. Moreover, adaptive filters are essential for online health monitoring, as they can adjust to the changing quality of incoming data [159].

The design and implementation of filters constitute a cornerstone of signal processing, empowering engineers and scientists to manipulate signals in a myriad of ways to extract valuable information, enhance signal quality, and mitigate unwanted interference. From the fundamental concepts of filter types and specifications to the intricacies of filter design techniques and adaptive filtering algorithms, a thorough understanding of filters is essential for anyone working with signals. To better situate the wide range of filter types used across analog and digital domains, Table A.1 provides a comparative overview of major filter categories, highlighting their operating domains, design characteristics, trade-offs, and use cases.

Table A.1: Taxonomy of Common Filters in Signal Processing

Filter Type	**Domain**	**Advantages**	**Disadvantages**	**Common Applications**
Analog Filters	Continuous-time	Low latency; no sampling noise	Limited flexibility; sensitive to component drift	RF front ends, audio pre-processing
Digital Filters	Discrete-time	Flexible, programmable; stable design	Requires ADC/DSP; latency can be an issue	Audio processing, biomedical signals, communication systems
FIR (Finite Impulse Response)	Digital	Always stable; linear phase possible; simple implementation	Higher order needed for sharp cutoff	Audio EQ, data comms, phase-sensitive systems
IIR (Infinite Impulse Response)	Digital	Efficient (fewer taps); sharp cutoff	Potential instability; nonlinear phase	Control systems, low-pass filters, real-time DSP
Window-based FIR	Digital	Easy design; smooth sidelobe control	Wider mainlobe; trade-off needed	OFDM sidelobe suppression, pulse shaping
Adaptive Filters (e.g. LMS, RLS)	Digital	Self-adjusting; tracks time-varying environments	Computational complexity (esp. RLS); slower convergence (LMS)	Noise cancellation, echo suppression, beamforming

Conclusion

The field of filtering encompasses a wide range of techniques and applications, each tailored to specific signal processing challenges. The journey through filter design and implementation begins with a firm grasp of fundamental concepts, progresses through the intricacies of design methodologies, and culminates in the practical realization of filters for diverse applications.

As technology continues to evolve, the role of filtering in signal processing will only become more prominent, driving innovation and enabling new possibilities in various fields. Spatial filtering using adaptive or smart antennas has emerged as a promising technique to improve the performance of cellular mobile systems [160]. In tomographic images, the effective application of filters is crucial for suppressing statistical noise while preserving spatial resolution and contrast, directly impacting image quality and diagnostic accuracy [161].

Median filters are particularly effective at removing "salt and pepper" type noise while preserving edges, and mean filters are simple sliding window spatial filters that replace the center value in the window with the average of all the pixel values in the window [162]. Adaptive filters are used to changing the signal characteristics, it increases speed and complexity, and reducing power consumption. Linear filters and nonlinear filters are used for enhancing and restoring images with noise [163].

The ongoing research and development efforts in filter design and implementation promise to yield even more sophisticated and efficient filtering techniques, paving the way for advancements in signal processing and its myriad applications. The application of filters plays a critical role in areas such as enhancing sensitivity to particular brain sources to improve source localization and suppressing muscular or ocular artifacts [164]. Filters are not only fast and lightweight, but also flexible and extendable.

Appendix B

Simulation Algorithm Overview

This appendix outlines the main steps used in the MATLAB-based simulation of inter-numerology interference (INI) mitigation via time-domain alignment and high-pass FIR filtering in a downlink dual-numerology OFDM system.

Algorithm: Dual-Numerology OFDM with FIR-Based INI Mitigation

Algorithm 1 Simulation Algorithm for INI Mitigation

Input: BWP configurations (`bwp1`, `bwp2`), subcarrier spacing, FFT size, symbol count, modulation order
Generate random bits for both numerologies and modulate using QAM
Map QAM symbols to frequency-domain grids for each BWP
Perform OFDM modulation for each BWP using IFFT
Align time duration of `NUM1` and `NUM2` symbols
Design FIR Filter:
Specify:
- Sampling frequency f_s
- Stopband and passband edges $f_{\text{stop}}, f_{\text{cutoff}}$
- Filter order N

Use Chebyshev window to design a high-pass FIR filter
Apply zero-phase filtering to `NUM2` waveform (via `filtfilt`)
Upsample `NUM1` waveform to match the filtered `NUM2` sampling rate
Combine both waveforms in the time domain
For each SNR level:
Add AWGN to the combined signal
Downsample back to `NUM1` sampling rate
Perform OFDM demodulation on `NUM1`
Compute BER, EVM, SINR, and Spectral Efficiency
Plot PSD, constellation diagrams, and performance curves
Output: Performance metrics and visualizations

This algorithm accurately reflects the signal flow and INI mitigation strategy employed in the simulation. It emphasizes spectral domain isolation through FIR filtering and symbol alignment without introducing guard bands.

Bibliography

[1] A. Mämmelä and A. Anttonen, "Why will computing power need particular attention in future wireless devices?" *IEEE Circuits and Systems Magazine*, vol. 17, pp. 12–26, 01 2017. [Online]. Available: https://doi.org/10.1109/mcas.2016.2642679

[2] X. Cheng, R. Zayani, H. Shaïek, and D. Roviras, "Inter-numerology interference analysis and cancellation for massive mimo-ofdm downlink systems," *IEEE Access*, vol. 7, pp. 177 164–177 176, 01 2019. [Online]. Available: https://doi.org/10.1109/access.2019.2957194

[3] S. Bhat, "Leveraging 5g network capabilities for smart grid communication," *Deleted Journal*, vol. 20, pp. 2272–2283, 04 2024. [Online]. Available: https://doi.org/10.52783/jes.1994

[4] N. Trabelsi, L. C. Fourati, and C. S. Chen, "Interference management in 5g and beyond networks: A comprehensive survey," *Computer Networks*, vol. 239, pp. 110 159–110 159, 12 2023. [Online]. Available: https://doi.org/10.1016/j.comnet.2023.110159

[5] A. B. Kihero, M. S. J. Solaija, and H. Arslan, "Inter-numerology interference for beyond 5g," *IEEE Access*, vol. 7, pp. 146 512–146 523, 01 2019. [Online]. Available: https://doi.org/10.1109/access.2019.2946084

[6] J. Mao, L. Zhang, S. McWade, H. Chen, and P. Xiao, "Characterizing inter-numerology interference in mixed-numerology ofdm systems," *arXiv (Cornell University)*, 01 2020. [Online]. Available: https://arxiv.org/abs/2009.13348

[7] T. V. S. Sreedhar and N. B. Mehta, "Inter-numerology interference in mixed numerology ofdm systems in time-varying fading channels with phase noise," *IEEE Transactions on Wireless Communications*, vol. 22, pp. 5473–5485, 08 2023. [Online]. Available: https://doi.org/10.1109/twc.2023.3234363

[8] Y. Ouazziz, M. Azni, M. Tounsi, and H. E. Benmadani, "Tackling inter-numerology interference in 5g multi-numerology ofdm systems: A filtering approach," *Journal of Electrical Systems*, vol. 20, no. 3, pp. 325–336, 2024, online: journal/esrgroup.org/jes.

[9] A. Yazar and H. Arslan, "Reliability enhancement in multi-numerology-based 5g new radio using ini-aware scheduling," *EURASIP Journal on Wireless Communications and Networking*, vol. 2019, 05 2019. [Online]. Available: https://doi.org/10.1186/s13638-019-1435-z

[10] A. B. Kihero, M. S. J. Solaija, A. Yazar, and H. Arslan, "Inter-numerology interference analysis for 5g and beyond," 12 2018, pp. 1–6. [Online]. Available: https://doi.org/10.1109/glocomw.2018.8644394

[11] P. S. Kumar and K. U. Rani, "Inter numerology interference minimization using windowing and precoding techniques for 5g noma based ofdm numerologies," 12 2022, pp. 1–6. [Online]. Available: https://doi.org/10.1109/icmnwc56175.2022.10031998

[12] B. Cevikgibi, A. M. Demirtaş, T. Gırıcı, and H. Arslan, "Inter-numerology interference pre-equalization for 5g mixed-numerology communications," *arXiv (Cornell University)*, 01 2022. [Online]. Available: https://arxiv.org/abs/2201.09228

[13] T. V. S. Sreedhar and N. B. Mehta, "Inter-numerology interference in 5g new radio: Analysis and bounds for time-varying fading channels," 05 2022, pp. 4818–4823. [Online]. Available: https://doi.org/10.1109/icc45855.2022.9839119

[14] J. Mao, A. Farhang, L. Zhang, Z. Chu, P. Xiao, and S. Gu, "Interference analysis in multi-numerology ofdm systems: A continuous-time approach," 06 2021. [Online]. Available: https://doi.org/10.1109/iccworkshops50388.2021.9473482

[15] A. Yazar and H. Arslan, "Flexible multi-numerology systems for 5g new radio," *Journal of Mobile Multimedia*, vol. 14, pp. 367–394, 01 2018. [Online]. Available: https://doi.org/10.13052/jmm1550-4646.1442

[16] J. Mao, L. Zhang, P. Xiao, and K. Nikitopoulos, "Interference analysis and power allocation in the presence of mixed numerologies," *IEEE Transactions on Wireless Communications*, vol. 19, pp. 5188–5203, 05 2020. [Online]. Available: https://doi.org/10.1109/twc.2020.2990717

[17] S. McWade, M. F. Flanagan, L. Zhang, and A. Farhang, "Interference and rate analysis of multinumerology noma," *arXiv (Cornell University)*, 01 2020. [Online]. Available: https://arxiv.org/abs/2002.11588

[18] S. Edirisinghe, O. Galagedarage, I. Dias, and C. Ranaweera, "Recent development of emerging indoor wireless networks towards 6g," *Network*, vol. 3, pp. 269–297, 05 2023. [Online]. Available: https://doi.org/10.3390/network3020014

[19] A. Ly and Y. Yao, "A review of deep learning in 5g research: Channel coding, massive mimo, multiple access, resource allocation, and network security," pp. 396–408, 01 2021. [Online]. Available: https://doi.org/10.1109/ojcoms.2021.3058353

[20] A. Chagdali, S. E. Elayoubi, and A. M. Masucci, "Slice function placement impact on the performance of urllc with multi-connectivity," *Computers*, vol. 10, pp. 67–67, 05 2021. [Online]. Available: https://doi.org/10.3390/computers10050067

[21] M. A. Siddiqi, H. Yu, and J. Joung, "5g ultra-reliable low-latency communication implementation challenges and operational issues with iot devices," *Electronics*, vol. 8, pp. 981–981, 09 2019. [Online]. Available: https://doi.org/10.3390/electronics8090981

[22] D. Lynch, M. M. Tentzeris, V. Fusco, and S. D. Assimonis, "Super realized gain antenna array," *arXiv (Cornell University)*, 01 2023. [Online]. Available: https://arxiv.org/abs/2309.09889

[23] M. M. Ahamed and S. Faruque, *5G Backhaul: Requirements, Challenges, and Emerging Technologies*, 09 2018. [Online]. Available: https://doi.org/10.5772/intechopen.78615

[24] Y. Ullah, M. Roslee, S. M. Mitani, S. A. Khan, and M. H. Jusoh, "A survey on handover and mobility management in 5g hetnets: Current state, challenges, and future directions," pp. 5081–5081, 05 2023. [Online]. Available: https://doi.org/10.3390/s23115081

[25] N. Haghighi and J. A. Lott, "Electrically parallel three-element 980 nm vcsel arrays with ternary and binary bottom dbr mirror layers," *Materials*, vol. 14, pp. 397–397, 01 2021. [Online]. Available: https://doi.org/10.3390/ma14020397

[26] N. Marchetti, "Towards the 5th generation of wireless communication systems," *arXiv (Cornell University)*, 01 2017. [Online]. Available: https://arxiv.org/abs/1702.00370

[27] A. S. Mahomed and A. K. Saha, "Unleashing the potential of 5g for smart cities: A focus on real-time digital twin integration," *Smart Cities*, vol. 8, pp. 70–70, 04 2025. [Online]. Available: https://doi.org/10.3390/smartcities8020070

[28] A. Kaur and V. K. Joshi, "5g network of communication technology," 08 2022.

[29] X. Jiang, H. Shokri-Ghadikolaei, G. Fodor, E. Modiano, Z. Pang, M. Zorzi, and C. Fischione, "Low-latency networking: Where latency lurks and how to tame it," *arXiv (Cornell University)*, 01 2018. [Online]. Available: https://arxiv.org/abs/1808.02079

[30] M. Pons, E. Valenzuela, B. Rodríguez, J. A. Nolazco-Flores, and C. Del-Valle-Soto, "Utilization of 5g technologies in iot applications: Current limitations by interference and network optimization difficulties—a review," *Sensors*, vol. 23, pp. 3876–3876, 04 2023. [Online]. Available: https://doi.org/10.3390/s23083876

[31] R. M. Sohaib, O. Onireti, Y. Sambo, and M. A. Imran, "Network slicing for beyond 5g systems: An overview of the smart port use case," *Electronics*, vol. 10, pp. 1090–1090, 05 2021. [Online]. Available: https://doi.org/10.3390/electronics10091090

[32] N. F. Rabbi, "Introduction to 5g," 01 2020.

[33] J. Vihriälä, A. A. Zaidi, V. Venkatasubramanian, N. He, E. Tiirola, J. Medbo, E. Lähetkangas, K. Werner, K. Pajukoski, A. Cedergren, and R. Baldemair, "Numerology and frame structure for 5g radio access," pp. 1–5, 09 2016. [Online]. Available: https://doi.org/10.1109/pimrc.2016.7794610

[34] S. Zeb, A. Mahmood, S. A. Hassan, M. J. Piran, M. Gidlund, and M. Guizani, "Industrial digital twins at the nexus of nextg wireless networks and computational intelligence: A survey," *Journal of Network and Computer Applications*, vol. 200, pp. 103 309–103 309, 01 2022. [Online]. Available: https://doi.org/10.1016/j.jnca.2021.103309

[35] A. Yazar, B. Peköz, and H. Arslan, "Fundamentals of multi-numerology 5g new radio," *arXiv (Cornell University)*, 01 2018. [Online]. Available: https://arxiv.org/abs/1805.02842

[36] M. B. Shahab, R. Z. Abbas, M. Shirvanimoghaddam, and S. J. Johnson, "Grant-free non-orthogonal multiple access for iot: A survey," *arXiv (Cornell University)*, 01 2019. [Online]. Available: https://arxiv.org/abs/1910.06529

[37] Y. Xiao and M. Krunz, "Dynamic network slicing for scalable fog computing systems with energy harvesting," *IEEE Journal on Selected Areas in Communications*, vol. 36, pp. 2640–2654, 09 2018. [Online]. Available: https://doi.org/10.1109/jsac.2018.2871292

[38] D. Candal-Ventureira, J. M. Rúa-Estévez, P. Fondo-Ferreiro, F. Gil-Castiñeira, A. Fernández-Barciela, F. J. González-Castaño, E. Diéguez-Pazo, and L. Fernández-Ferreira, "5g network slicing as a service enabler for the automotive sector," *Engineering Reports*, vol. 7, 10 2024. [Online]. Available: https://doi.org/10.1002/eng2.13024

[39] D. Sharma, S. Singhal, A. Rai, and A. Singh, "Analysis of power consumption in standalone 5g network and enhancement in energy efficiency using a novel routing protocol," *Sustainable Energy Grids and Networks*, vol. 26, pp. 100 427–100 427, 01 2021. [Online]. Available: https://doi.org/10.1016/j.segan.2020.100427

[40] M. Höyhtyä, O. Apilo, and M. Lasanen, "Review of latest advances in 3gpp standardization: D2d communication in 5g systems and its energy consumption models," *Future Internet*, vol. 10, pp. 3–3, 01 2018. [Online]. Available: https://doi.org/10.3390/fi10010003

[41] A. Bishen, "Security considerations for the 5g era," 07 2020. [Online]. Available: https://www.5gamericas.org/security-considerations-for-the-5g-era/

[42] E. Dahlman, S. Parkvall, and J. Peisa, "5g wireless access," *IEICE Transactions on Communications*, pp. 1407–1414, 01 2015. [Online]. Available: https://doi.org/10.1587/transcom.e98.b.1407

[43] International Telecommunication Union Radiocommunication Sector (ITU-R), "IMT Vision – Framework and overall objectives of the future development of IMT for 2020 and beyond," https://www.itu.int/dms_pubrec/itu-r/

rec/m/R-REC-M.2083-0-201509-I!!PDF-E.pdf, 2015, recommendation ITU-R M.2083-0.

[44] H. Chen, R. Abbas, P. Cheng, M. Shirvanimoghaddam, W. Hardjawana, W. Bao, Y. Li, and B. Vucetic, "Ultra-reliable low latency cellular networks: Use cases, challenges and approaches," *arXiv (Cornell University)*, 01 2017. [Online]. Available: https://arxiv.org/abs/1709.00560

[45] C. Schellenberger, M. Zimmermann, and H. D. Schotten, "Wireless communication for modular production facilities," *arXiv (Cornell University)*, 01 2018. [Online]. Available: https://arxiv.org/abs/1804.08273

[46] O. Adamuz-Hinojosa, "Doctoral thesisslicing management for 5g radionetworks," 03 2022.

[47] M. A. Lema, A. Laya, T. Mahmoodi, M. Cuevas, J. Sachs, J. Markendahl, and M. Döhler, "Business case and technology analysis for 5g low latency applications," *IEEE Access*, pp. 1–1, 01 2017. [Online]. Available: https://doi.org/10.1109/access.2017.2685687

[48] Bachir and Dheya-Alhaq, "Etude des techniques de modulation pour les réseaux mobiles 5g et 6g de nouvelle génération," 01 2020.

[49] I. Afolabi, T. Taleb, P. A. Frangoudis, M. Bagaa, and A. Ksentini, "Network slicing-based customization of 5g mobile services," *arXiv (Cornell University)*, 01 2022. [Online]. Available: https://arxiv.org/abs/2201.07187

[50] T. Hu, Q. Liao, Q. Liu, and G. Carle, "Network slicing via transfer learning aided distributed deep reinforcement learning," *arXiv (Cornell University)*, 01 2023. [Online]. Available: https://arxiv.org/abs/2301.03262

[51] P. Varga, J. Pető, A. Frankó, D. Balla, D. Haja, F. N. Janky, G. Soós, D. Ficzere, M. Maliosz, and L. Toka, "5g support for industrial iot applications— challenges, solutions, and research gaps," *Sensors*, vol. 20, pp. 828–828, 02 2020. [Online]. Available: https://doi.org/10.3390/s20030828

[52] V. K. Quý, N. V. Hoai, L. D. Manh, L. A. Ngoc, and G. Jeon, "Wireless communication technologies for iot in 5g: Vision, applications, and challenges," *Wireless Communications and Mobile Computing*, vol. 2022, pp. 1–12, 02 2022. [Online]. Available: https://doi.org/10.1155/2022/3229294

[53] "Study on new radio access technology: Radio access architecture and interfaces," 3rd Generation Partnership Project (3GPP), Tech. Rep. TR 38.801 V14.0.0, 2017, available online: https://www.3gpp.org/ftp/Specs/archive/38_series/38.801/38801-140.zip.

[54] J. T. J. Penttinen, "Phase 2 system architecture and functionality," pp. 55–91, 03 2021. [Online]. Available: https://doi.org/10.1002/9781119645566.ch3

[55] N. Singh, "5g service-based architecture (sba)," 05 2023. [Online]. Available: https://techcommunity.microsoft.com/t5/azure-for-operators-blog/what-is-the-5g-service-based-architecture-sba/ba-p/3831367

[56] S. Kinney, "Four pillars of a service-based architecture," 04 2023. [Online]. Available: https://www.rcrwireless.com/20230410/telco-cloud/four-pillars-of-a-service-based-architecture

[57] "5g core network architecture," pp. 447–472, 04 2021. [Online]. Available: https://doi.org/10.1002/9781119778714.ch20

[58] M. S. Dahal, J. N. Shrestha, and S. R. Shakya, "Comparison of energy efficiency between macro and micro base stations using energy saving strategy," *Journal of the Institute of Engineering*, vol. 15, pp. 83–89, 10 2020. [Online]. Available: https://doi.org/10.3126/jie.v15i3.32021

[59] L. Korowajczuk, "Wireless communications network (wcn)," pp. 235–243, 06 2011. [Online]. Available: https://doi.org/10.1002/9781119970460.ch9

[60] S. Park, C. Chae, and S. Bahk, "Large-scale antenna operation in heterogeneous cloud radio access networks: a partial centralization approach," *IEEE Wireless Communications*, vol. 22, pp. 32–40, 06 2015. [Online]. Available: https://doi.org/10.1109/mwc.2015.7143324

[61] J. D. V. Sánchez, L. Urquiza-Aguiar, M. C. P. Paredes, and D. P. M. Osorio, "Survey on physical layer security for 5g wireless networks," *arXiv (Cornell University)*, 01 2020. [Online]. Available: https://arxiv.org/abs/2006.08044

[62] L.-H. Shen, C. Tsai, C.-Y. Wang, and K. Feng, "Hybrid controlled user association and resource management for energy-efficient green rans with limited fronthaul," *IEEE Access*, vol. 10, pp. 5264–5280, 01 2022. [Online]. Available: https://doi.org/10.1109/access.2022.3140814

[63] C. Wang, M. D. Renzo, S. Stańczak, S. Wang, and E. G. Larsson, "Artificial intelligence enabled wireless networking for 5g and beyond: Recent advances and future challenges," *arXiv (Cornell University)*, 01 2020. [Online]. Available: https://arxiv.org/abs/2001.08159

[64] W. Azariah, F. A. Bimo, C.-W. Lin, R. Cheng, N. Nikaein, and R. Jana, "A survey on open radio access networks: Challenges, research directions, and open source approaches," *Sensors*, vol. 24, pp. 1038–1038, 02 2024. [Online]. Available: https://doi.org/10.3390/s24031038

[65] G. Choudhary, J. Kim, and V. Sharma, "Security of 5g-mobile backhaul networks: A survey," *arXiv (Cornell University)*, 01 2019. [Online]. Available: https://arxiv.org/abs/1906.11427

[66] X. Ge, H. Cheng, M. Guizani, and T. Han, "5g wireless backhaul networks: challenges and research advances," *IEEE Network*, vol. 28, pp. 6–11, 11 2014. [Online]. Available: https://doi.org/10.1109/mnet.2014.6963798

[67] T. Pfeiffer, "Next generation mobile fronthaul and midhaul architectures [invited]," *Journal of Optical Communications and Networking*, vol. 7, 09 2015. [Online]. Available: https://doi.org/10.1364/jocn.7.000b38

[68] M. H. Adnan and Z. A. Zukarnain, "Device-to-device communication in 5g environment: Issues, solutions, and challenges," *Symmetry*, vol. 12, pp. 1762–1762, 10 2020. [Online]. Available: https://doi.org/10.3390/sym12111762

[69] L. Song, D. Niyato, Z. Han, and E. Hossain, *Basics of D2D communications*. Cambridge University Press, 03 2015, pp. 3–16. [Online]. Available: https://doi.org/10.1017/cbo9781107478732.002

[70] U. N. Kar and D. K. Sanyal, "An overview of device-to-device communication in cellular networks," *ICT Express*, vol. 4, pp. 203–208, 10 2017. [Online]. Available: https://doi.org/10.1016/j.icte.2017.08.002

[71] J. Choi, J. Ding, N. P. Le, and Z. Ding, "Grant-free random access in machine-type communication: Approaches and challenges," *arXiv (Cornell University)*, 01 2020. [Online]. Available: https://arxiv.org/abs/2012.10550

[72] A. Elnashar and M. El-saidny, "5g framework concepts for the next generation networks," *arXiv (Cornell University)*, 01 2019. [Online]. Available: https://arxiv.org/abs/1911.08879

[73] J. Lin, Z. Chang, L. Zong, S. K. Bose, T. Chang, and G. Shen, "From small to large: Clos network for scaling all-optical switching," *IEEE Communications Magazine*, vol. 61, pp. 136–141, 08 2023. [Online]. Available: https://doi.org/10.1109/mcom.002.2300008

[74] S. Yue, J. Ren, N. Qiao, Y. Zhang, H. Jiang, Y. Zhang, and Y. Yang, "Todg: Distributed task offloading with delay guarantees for edge computing," *IEEE Transactions on Parallel and Distributed Systems*, vol. 33, pp. 1650–1665, 10 2021. [Online]. Available: https://doi.org/10.1109/tpds.2021.3123535

[75] V. Sharma, "Functional security and trust in ultra-connected 6g ecosystem," *EAI Endorsed Transactions on Industrial Networks and Intelligent Systems*, vol. 9, 12 2022. [Online]. Available: https://doi.org/10.4108/eetinis.v9i4.2846

[76] "NR; physical channels and modulation (release 15)," 3rd Generation Partnership Project (3GPP), Tech. Rep. TS 38.211 V15.2.0, 2018, available: https://www.3gpp.org/ftp/Specs/archive/38_series/38.211/38211-152.zip.

[77] L. Marijanović, Štefan Schwarz, and M. Rupp, "Multiplexing services in 5g and beyond: Optimal resource allocation based on mixed numerology and mini-slots," *IEEE Access*, vol. 8, pp. 209 537–209 555, 01 2020. [Online]. Available: https://doi.org/10.1109/access.2020.3039352

[78] Q. Hu, M. Zhang, and R. Gao, "Key technologies in massive mimo," *ITM Web of Conferences*, vol. 17, pp. 1017–1017, 01 2018. [Online]. Available: https://doi.org/10.1051/itmconf/20181701017

[79] L. Rao, M. Pant, L. Malviya, A. Parmar, and S. Charhate, "5g beamforming techniques for the coverage of intended directions in modern wireless communication: in-depth review," *International Journal of Microwave and Wireless Technologies*, vol. 13, pp. 1039–1062, 12 2020. [Online]. Available: https://doi.org/10.1017/s1759078720001622

[80] M. M. Ahamed and S. Faruque, "5g network coverage planning and analysis of the deployment challenges," *Sensors*, vol. 21, pp. 6608–6608, 10 2021. [Online]. Available: https://doi.org/10.3390/s21196608

[81] A. Bindle, T. Gulati, and N. Kumar, "A detailed introduction of different beamforming techniques used in 5g," *International Journal of Communication Systems*, vol. 34, 01 2021. [Online]. Available: https://doi.org/10.1002/dac.4718

[82] J. G. Andrews, S. Buzzi, W. Choi, S. V. Hanly, A. Lozano, A. C. K. Soong, and J. C. Zhang, "What will 5g be?" *IEEE Journal on Selected Areas in Communications*, vol. 32, no. 6, pp. 1065–1082, 2014.

[83] "NR; nr and ng-ran overall description (release 15)," 3rd Generation Partnership Project (3GPP), Tech. Rep. TS 38.300 V15.2.0, 2018, available: https://www.3gpp.org/ftp/Specs/archive/38_series/38.300/38300-152.zip.

[84] I. Sahni and A. Kaur, "A systematic literature review on 5g security," *arXiv (Cornell University)*, 01 2022. [Online]. Available: https://arxiv.org/abs/2212.03299

[85] "NR; physical layer procedures for control (release 15)," 3rd Generation Partnership Project (3GPP), Tech. Rep. TS 38.213 V15.3.0, 2018, available: https://www.3gpp.org/ftp/Specs/archive/38_series/38.213/38213-153.zip.

[86] E. S. Lima, R. M. Borges, N. Andriolli, E. Conforti, G. Contestabile, and A. C. S., "Integrated optical frequency comb for 5g nr xhauls," *Scientific Reports*, vol. 12, 09 2022. [Online]. Available: https://doi.org/10.1038/s41598-022-20553-5

[87] A. O. Mufutau, F. P. Guiomar, M. A. Fernandes, A. Lorences-Riesgo, A. S. R. Oliveira, and P. P. Monteiro, "Demonstration of a hybrid optical fiber–wireless 5g fronthaul coexisting with end-to-end 4g networks," *Journal of Optical Communications and Networking*, vol. 12, pp. 72–72, 01 2020. [Online]. Available: https://doi.org/10.1364/jocn.382654

[88] Q. He, D. W. Huo, J. H. He, Y. J. Xiao, and B. Yu, "Carrier aggregation and its application in 230mhz power industry spectrum," *Applied Mechanics and Materials*, pp. 1003–1008, 09 2013. [Online]. Available: https://doi.org/10.4028/www.scientific.net/amm.427-429.1003

[89] J. Ling, S. Kanugovi, S. Vasudevan, and A. Pramod, "Enhanced capacity and coverage by wi-fi lte integration," *IEEE Communications Magazine*, vol. 53, pp. 165–171, 03 2015. [Online]. Available: https://doi.org/10.1109/mcom.2015.7060499

[90] "Study on new radio access technology; enhancements for lte-nr interworking and spectrum aggregation (release 15)," 3rd Generation Partnership Project (3GPP), Tech. Rep. TR 38.806 V15.0.0, 2018, available: https://www.3gpp.org/ftp/Specs/archive/38_series/38.806/38806-150.zip.

[91] "System architecture for the 5g system (5gs); stage 2 (release 15)," 3rd Generation Partnership Project (3GPP), Tech. Rep. TS 23.501 V15.2.0, 2018, available: https://www.3gpp.org/ftp/Specs/archive/23_series/23.501/23501-152.zip.

[92] N. Doty and M. Knodel, "Slicing the network: Maintaining neutrality, protecting privacy, and promoting competition," *arXiv (Cornell University)*, 01 2023. [Online]. Available: https://arxiv.org/abs/2308.05829

[93] V. Q. Rodriguez, F. Guillemin, and A. Boubendir, "Automating the deployment of 5g network slices with onap," *arXiv (Cornell University)*, 01 2019. [Online]. Available: https://arxiv.org/abs/1907.02278

[94] N. Nidhi, A. Mihovska, and R. Prasad, "Overview of 5g new radio and carrier aggregation: 5g and beyond networks," pp. 1–6, 10 2020. [Online]. Available: https://doi.org/10.1109/wpmc50192.2020.9309496

[95] S. Faruque, *Radio Frequency Multiple Access Techniques Made Easy*. Springer International Publishing, 08 2018. [Online]. Available: https://doi.org/10.1007/978-3-319-91651-4

[96] M. Aldababsa, M. Toka, S. Gökçeli, G. K. Kurt, and O. Kucur, "A tutorial on nonorthogonal multiple access for 5g and beyond," *Wireless Communications and Mobile Computing*, vol. 2018, 01 2018. [Online]. Available: https://doi.org/10.1155/2018/9713450

[97] "Channel sharing explained: Fdma, tdma and cdma," 10 2012. [Online]. Available: https://www.taitcommunications.com/en/about-us/news/2012/10/09/channel-sharing-explained-fdma-tdma-and-cdma

[98] S. Ilcev, "Analyses of space division multiple access (sdma) schemes for global mobile satellite communications (gmsc)," *TransNav, the International Journal on Marine Navigation and Safety of Sea Transportation*, vol. 14, pp. 821–830, 12 2020. [Online]. Available: https://doi.org/10.12716/1001.14.04.05

[99] S. Sesia, I. Toufik, and M. Baker, *LTE–The UMTS Long Term Evolution: From Theory to Practice*, 2nd ed. John Wiley & Sons, 2011.

[100] V. Šeba, B. Modlic, and G. Šišul, "Resource allocation with dynamic carrier assignment in wireless networks," *Frequenz*, vol. 68, 01 2014. [Online]. Available: https://doi.org/10.1515/freq-2013-0086

[101] E. F. Louis, "An introduction to lte-advanced: The real 4g," *Electronic design*, vol. 61, pp. 32–38, 01 2013. [Online]. Available: https://jglobal.jst.go.jp/en/detail?JGLOBAL_ID=201302279578641660

[102] R. Bhatia, "Multiple access techniques for 5g networks," 02 2018.

[103] Z. Ding, Y. Liu, J. Choi, M. Elkashlan, C. Y. I, and H. V. Poor, "Application of non-orthogonal multiple access in lte and 5g networks," *IEEE Communications Magazine*, vol. 55, no. 2, pp. 185–191, 2017.

[104] M. Hussain and H. Rasheed, "Nonorthogonal multiple access for next-generation mobile networks: A technical aspect for research direction," *Wireless Communications and Mobile Computing*, vol. 2020, pp. 1–17, 11 2020. [Online]. Available: https://doi.org/10.1155/2020/8845371

[105] H. Nikopour and H. Baligh, "Sparse code multiple access," in *2013 IEEE 24th International Symposium on Personal Indoor and Mobile Radio Communications (PIMRC)*. IEEE, 2013, pp. 332–336.

[106] M. Guri, D. Bykhovsky, and Y. Elovici, "air-jumper: Covert air-gap exfiltration/infiltration via security cameras & infrared (ir)," *arXiv (Cornell University)*, 01 2017. [Online]. Available: https://arxiv.org/abs/1709.05742

[107] C. E. Shannon, "A mathematical theory of communication," *Bell System Technical Journal*, vol. 27, pp. 379–423, 07 1948. [Online]. Available: https://doi.org/10.1002/j.1538-7305.1948.tb01338.x

[108] S. Ahmadi, *Downlink Physical Layer Functions*. Elsevier BV, 10 2013, pp. 399–720. [Online]. Available: https://doi.org/10.1016/b978-0-12-405162-1.00009-5

[109] L. Miuccio, D. Panno, P. Pisacane, and S. Riolo, "A qos-aware and channel-aware radio resource management framework for multi-numerology systems," *Computer Communications*, vol. 191, pp. 299–314, 05 2022. [Online]. Available: https://doi.org/10.1016/j.comcom.2022.05.009

[110] A. R. Aitken, R. Brueck, and D. R. Ziemer, "Recent advances in speech-compression techniques," *The Journal of the Acoustical Society of America*, vol. 35, pp. 789–789, 05 1963. [Online]. Available: https://doi.org/10.1121/1.2142444

[111] I. G. Pereira, L. F. Q. Silveira, and L. M. G. Gonçalves, "Video synchronization with bit-rate signals and correntropy function," *Sensors*, vol. 17, pp. 2021–2021, 09 2017. [Online]. Available: https://doi.org/10.3390/s17092021

[112] M. S. Hassan, M. E. Taruni, and R. A. Zrae, "A joint adaptive modulation and channel coding scheme for multimedia communications over wireless channels," *International Journal of Wireless and Mobile Computing*, vol. 9, pp. 99–99, 01 2015. [Online]. Available: https://doi.org/10.1504/ijwmc.2015.071679

[113] M. J. Baker, "Introduction to downlink physical layer design," pp. 135–140, 02 2009. [Online]. Available: https://doi.org/10.1002/9780470742891.ch6

[114] E. Dahlman, S. Parkvall, and J. Sköld, "Ofdm transmission," 01 2011.

[115] A. C. Andrews, S. Dolinar, D. Divsalar, and J. Thorpe, "Design of low-density parity-check (ldpc) codes for deep-space applications," *Interplanetary Network Progress Report*, pp. 1–14, 11 2004. [Online]. Available: https://ipnpr.jpl.nasa.gov/progress_report/42-159/159K.pdf

[116] C. Xiong, J. Lin, and Z. Yan, "Symbol-decision successive cancellation list decoder for polar codes," *IEEE Transactions on Signal Processing*, vol. 64, pp. 675–687, 10 2015. [Online]. Available: https://doi.org/10.1109/tsp.2015.2486750

[117] I. Tal and A. Vardy, "List decoding of polar codes," *arXiv (Cornell University)*, 01 2012. [Online]. Available: https://arxiv.org/abs/1206.0050

[118] S. S. Hadi and T. Tiong, "Adaptive modulation and coding for lte wireless communication," vol. 78. IOP Publishing, 04 2015, pp. 12 016–12 016. [Online]. Available: https://doi.org/10.1088/1757-899x/78/1/012016

[119] L. Boppana, C. N. Amanchi, and R. K. Kodali, "Coding rates and mcs using adaptive modulation for wimax in ofdm systems using gnu radio," pp. 53–58, 12 2013. [Online]. Available: https://doi.org/10.1109/raics.2013.6745446

[120] "5g physical layer specifications," 04 2022. [Online]. Available: https://medium.com/5g-nr/5g-physical-layer-specifications-e025f8654981

[121] J. J. Escudero-Garzás and M. Morales-Céspedes, "Orthogonal multiple access," pp. 1–24, 01 2021. [Online]. Available: https://doi.org/10.1002/9781119471509.w5gref028

[122] F. Launay, "5g-nr radio interface – the physical layer," pp. 89–140, 08 2021. [Online]. Available: https://doi.org/10.1002/9781119851288.ch4

[123] A. Ancora and S. Sesia, "Reference signals and channel estimation," pp. 159–180, 02 2009. [Online]. Available: https://doi.org/10.1002/9780470742891.ch8

[124] A. K. M. Baki, "Comparison of different new radio (nr) waveforms for wireless communications," *PLoS ONE*, vol. 18, 04 2023. [Online]. Available: https://doi.org/10.1371/journal.pone.0283886

[125] "NR; base station (bs) radio transmission and reception (release 15)," 3rd Generation Partnership Project (3GPP), Tech. Rep. TS 38.104 V15.2.0, 2018, available: https://www.3gpp.org/ftp/Specs/archive/38_series/38.104/38104-152.zip.

[126] Y. Zhou, H. Yin, J. Xiong, S. Song, J. Zhu, J. Du, H. Chen, and Y. Tang, "Overview and performance analysis of various waveforms in high mobility scenarios," pp. 35–40, 02 2024. [Online]. Available: https://doi.org/10.1109/iccet62255.2024.00013

[127] X. Zhang, L. Zhang, P. Xiao, D. Ma, J. Wei, and Y. Xin, "Mixed numerologies interference analysis and inter-numerology interference cancellation for windowed ofdm systems," *IEEE Transactions on Vehicular Technology*, vol. 67, pp. 7047–7061, 04 2018. [Online]. Available: https://doi.org/10.1109/tvt.2018.2826047

[128] S. Gökçeli, T. Levanen, J. Yli-Kaakinen, T. Riihonen, M. Renfors, and M. Valkama, "Papr reduction with mixed-numerology ofdm," *IEEE Wireless Communications Letters*, vol. 9, pp. 21–25, 09 2019. [Online]. Available: https://doi.org/10.1109/lwc.2019.2939521

[129] J. Zhang, W. Xie, and F. Yang, "An architecture for 5g mobile network based on sdn and nfv," 01 2015. [Online]. Available: https://doi.org/10.1049/cp.2015.0918

[130] D. Wang, O. Saraci, R. Sattiraju, Q. Zhou, and H. D. Schotten, "Effect of variable physical numerologies on link-level performance of 5g nr v2x," *arXiv (Cornell University)*, 01 2023. [Online]. Available: https://arxiv.org/abs/2303.12086

[131] N. Correia, F. Al-Tam, and J. Rodríguez, "Optimization of mixed numerology profiles for 5g wireless communication scenarios," *Sensors*, vol. 21, pp. 1494–1494, 02 2021. [Online]. Available: https://doi.org/10.3390/s21041494

[132] A. B. Kihero, M. S. J. Solaija, and H. Arslan, "Multi-numerology multiplexing and inter-numerology interference analysis for 5g," *arXiv (Cornell University)*, 01 2019. [Online]. Available: https://arxiv.org/abs/1905.12748

[133] E. Memişoğlu, A. B. Kihero, E. Başar, and H. Arslan, "Guard band reduction for 5g and beyond multiple numerologies," *IEEE Communications Letters*, vol. 24, pp. 644–647, 12 2019. [Online]. Available: https://doi.org/10.1109/lcomm.2019.2963311

[134] A. F. Demir and H. Arslan, "Inter-numerology interference management with adaptive guards: A cross-layer approach," *IEEE Access*, vol. 8, pp. 30 378–30 386, 01 2020. [Online]. Available: https://doi.org/10.1109/access.2020.2972287

[135] J. Mao, L. Zhang, and X. Pei, "Filteredofdm: An insight into intrinsic in-band interference," pp. 25–41, 11 2020. [Online]. Available: https://doi.org/10.1002/9781119652434.ch2

[136] M. Zambianco and G. Verticale, "Intelligent multi-branch allocation of spectrum slices for inter-numerology interference minimization," *Computer Networks*, vol. 196, pp. 108 254–108 254, 06 2021. [Online]. Available: https://doi.org/10.1016/j.comnet.2021.108254

[137] A. Latrach, "Application of deep learning for predictive maintenance of oilfield equipment," *arXiv (Cornell University)*, 01 2023. [Online]. Available: https://arxiv.org/abs/2306.11040

[138] I. A. Sulaiman, H. M. Hassan, M. Danish, M. Singh, P. Singh, and M. Rajoriya, "Design, comparison and analysis of low pass fir filter using window techniques method," *Materials Today Proceedings*, vol. 49, pp. 3117–3121, 12 2020. [Online]. Available: https://doi.org/10.1016/j.matpr.2020.10.952

[139] A. Antoniou, *Digital Filters: Analysis, Design and Applications*, 01 1979. [Online]. Available: https://openlibrary.org/books/OL1731288M/Digital_filters

[140] F. Shin and D. Kil, "Full-spectrum signal processing using a classify-before-detect paradigm," *The Journal of the Acoustical Society of America*, vol. 99, pp. 2188–2197, 04 1996. [Online]. Available: https://doi.org/10.1121/1.415407

[141] H. L. Kennedy, "Lecture notes on the design of low-pass digital filters with wireless-communication applications," *arXiv (Cornell University)*, 01 2022. [Online]. Available: https://arxiv.org/abs/2211.07123

[142] R. W. Hamming and S. Stearns, *Digital Filters*, 01 1977. [Online]. Available: https://ieeexplore.ieee.org/iel5/21/4310064/04310079.pdf

[143] J. P. do Vale Madeiro, P. C. Cortez, J. M. da Silva Monteiro Filho, and P. R. F. Rodrigues, *Techniques for Noise Suppression for ECG Signal Processing*. Elsevier BV, 12 2018, pp. 53–87. [Online]. Available: https://doi.org/10.1016/b978-0-12-814035-2.00009-8

[144] D. M. Miljanovic, M. Potrebić, and D. V. Tošić, "Design of microwave multibandpass filters with quasilumped resonators," *Mathematical Problems in Engineering*, vol. 2015, pp. 1–14, 01 2015. [Online]. Available: https://doi.org/10.1155/2015/647302

[145] H. G. Dimopoulos, *Analog Electronic Filters*. Springer Nature (Netherlands), 09 2011. [Online]. Available: https://doi.org/10.1007/978-94-007-2190-6

[146] A. Hannah and G. K. Agordzo, "A design of a low-pass fir filter using hamming window functions in matlab," *Computer Engineering and Intelligent Systems*, 02 2020. [Online]. Available: https://doi.org/10.7176/ceis/11-2-04

[147] V. Jamuna, P. Gomathi, and A. Arun, "Design and implementation of fir filter architecture using high level transformation techniques," *Indian Journal of Science and Technology*, vol. 11, pp. 1–5, 05 2018. [Online]. Available: https://doi.org/10.17485/ijst/2018/v11i17/122769

[148] J. Christopher, N. H. Shabrina, C. Cornelia, and Y. Zakhary, "Comparison of fir window filter variation results on pink noise audio," *Ultima Computing Jurnal Sistem Komputer*, pp. 1–7, 07 2022. [Online]. Available: https://doi.org/10.31937/sk.v14i1.2120

[149] R. Pugmire, "The properties and training of a neural network based universal window filter (uwf)," vol. 1995, pp. 642–646, 01 1995. [Online]. Available: https://doi.org/10.1049/cp:19950738

[150] S. Kawamura, "Design and operation of high-rate filters-part 1," *American Water Works Association*, vol. 67, pp. 535–544, 10 1975. [Online]. Available: https://doi.org/10.1002/j.1551-8833.1975.tb02291.x

[151] N. Kehtarnavaz and N. Kim, *FIR/IIR Filtering System Design.* Elsevier BV, 01 2005, pp. 79–94. [Online]. Available: https://doi.org/10.1016/b978-075067914-5/50009-x

[152] H. Korhola, "Perceptual study of loudspeaker crossover filters," 01 2008. [Online]. Available: http://lib.tkk.fi/Dipl/2008/urn011933.pdf

[153] W. Rakowski, C. A. Dube, and M. G. Goldstein, "Considerations for extending the transtheoretical model of behavior change to screening mammography," *Health Education Research*, vol. 11, pp. 77–96, 01 1996. [Online]. Available: https://doi.org/10.1093/her/11.1.77

[154] D. Brüllmann and B. d Hoedt, "The modulation transfer function and signal-to-noise ratio of different digital filters: a technical approach," *Dentomaxillofacial Radiology*, vol. 40, pp. 222–229, 04 2011. [Online]. Available: https://doi.org/10.1259/dmfr/33029984

[155] R. Yarlagadda, "Digital signal processing," *IEEE Transactions on Acoustics Speech and Signal Processing*, vol. 24, pp. 586–586, 12 1976. [Online]. Available: https://doi.org/10.1109/tassp.1976.1162867

[156] R. C. de Lamare, "Adaptive space-time beamforming in radar systems," *arXiv (Cornell University)*, 01 2013. [Online]. Available: https://arxiv.org/abs/1302.2343

[157] "Noise reduction techniques in ecg using different methods," *International Journal of Modern Trends in Engineering Research*, vol. 4, pp. 209–216, 09 2017. [Online]. Available: https://doi.org/10.21884/ijmter.2017.4273.rjypn

[158] D. Shi, B. Lam, W. Gan, J. Cheer, and S. J. Elliott, "Active noise control in the new century: The role and prospect of signal processing," *NOISE-CON proceedings*, vol. 268, pp. 5141–5151, 11 2023. [Online]. Available: https://doi.org/10.3397/in_2023_0730

[159] V. P. Surender and R. Ganguli, "Adaptive myriad filter for improved gas turbine condition monitoring using transient data," *Journal of Engineering for Gas Turbines and Power*, vol. 127, pp. 329–339, 04 2005. [Online]. Available: https://doi.org/10.1115/1.1850491

[160] G. Tsoulos, "Smart antennas for mobile communication systems: benefits and challenges," *Electronics Communications Engineering Journal*, vol. 11, pp. 84–94, 04 1999. [Online]. Available: https://doi.org/10.1049/ecej:19990204

[161] M. Lyra and A. Ploussi, "Filtering in spect image reconstruction," *International Journal of Biomedical Imaging*, vol. 2011, pp. 1–14, 01 2011. [Online]. Available: https://doi.org/10.1155/2011/693795

[162] A. Ch, "A survey on different filters for noise reduction in digital images," *International Journal for Research in Applied Science and Engineering Technology*, vol. 7, pp. 63–70, 09 2019. [Online]. Available: https://doi.org/10.22214/ijraset.2019.9010

[163] S. K. Satti, D. Suganya, P. Dhar, and P. Srinivasan, "An efficient noise separation technique for removal of gaussian and mixed noises in monochrome and color images," *International Journal of Innovative Technology and Exploring Engineering*, vol. 8, pp. 588–601, 08 2019. [Online]. Available: https://doi.org/10.35940/ijitee.i1122.0789s219

[164] A. Apicella, P. Arpaïa, G. Mastrati, and N. Moccaldi, "Eeg-based detection of emotional valence towards a reproducible measurement of emotions," *Scientific Reports*, vol. 11, 11 2021. [Online]. Available: https://doi.org/10.1038/s41598-021-00812-7

Abstract

The fifth generation (5G) of wireless networks supports multi-numerology operation, enabling different subcarrier spacings (SCS) to coexist for diverse services like eMBB, URLLC, and mMTC. However, this flexibility breaks OFDM orthogonality, causing inter-numerology interference (INI) that degrades performance—especially without guard bands or under high-order modulations.

This thesis examines INI in downlink dual-numerology OFDM systems and proposes a two-stage mitigation method: (1) time-domain resampling to align OFDM symbols, and (2) a high-order FIR high-pass filter to suppress out-of-band (OOB) emissions from the higher-SCS numerology.

The approach is implemented in MATLAB using a 3GPP-compliant framework. Performance is evaluated from QPSK to 256-QAM using BER, EVM, SINR, and SE. Results show time alignment suffices for lower-order modulations, while FIR filtering is crucial at higher orders. Operating without guard bands improves spectral efficiency, with minor distortion to the filtered signal.

Overall, the proposed method achieves effective INI mitigation without complex cancellation or channel knowledge, offering a practical solution for real-time 5G applications.

Keywords:5G NR, Multi-Numerology, INI, OFDM, FIR Filtering, Time Alignment, Spectral Leakage, BER, EVM, SINR, Spectral Efficiency, MATLAB.**:** Facial kinship verification, NDM, MSRCP+GRF, CNN, Hist-2DDWT, Hist-DTCWT, TXQDA+WCCN, LR fusion.

Résumé

La cinquième génération (5G) des réseaux sans fil prend en charge le fonctionnement multi-numérologie, permettant la coexistence de différents espacements de sous-porteuses (SCS) pour répondre à divers services comme l'eMBB, l'URLLC et le mMTC. Cependant, cette flexibilité compromet l'orthogonalité de l'OFDM, entraînant des interférences inter-numérologies (INI) qui dégradent les performances, notamment sans bandes de garde ou avec des modulations d'ordre élevé.

Cette thèse étudie l'INI dans les systèmes OFDM à double numérologie en liaison descendante et propose une méthode de réduction en deux étapes : (1) un rééchantillonnage temporel pour aligner les symboles OFDM, et (2) un filtre passe-haut FIR d'ordre élevé pour atténuer les émissions hors bande (OOB) de la numérologie à SCS plus élevé.

La méthodologie est implémentée sous MATLAB selon une simulation conforme au 3GPP. Les performances sont évaluées de la QPSK à la 256-QAM à l'aide des indicateurs BER, EVM, SINR et efficacité spectrale. Les résultats montrent que l'alignement temporel suffit pour les modulations faibles, tandis que le filtrage FIR est crucial pour préserver l'exactitude à haut ordre. L'absence de bandes de garde améliore l'efficacité spectrale, au prix d'une légère distorsion sur la numérologie filtrée.

Dans l'ensemble, la méthode proposée permet une atténuation efficace de l'INI sans annulation itérative ni connaissance du canal, offrant une solution pratique pour les applications 5G en temps réel.

Mots clés : 5G NR, Multi-numérologie, INI, OFDM, Filtrage FIR, Alignement temporel, Fuite spectrale, TEB, EVM, SINR, Efficacité spectrale, Simulation MATLAB.

ملخص

لتلبية متطلبات خدمات متنوعة (SCS) مما يسمح بتعايش فواصل مختلفة بين النواقل الفرعية ،(Multi-Numerology) التشغيل متعدد التعدادات (5G) تدعم شبكات الجيل الخامس إلا أن هذه المرونة تؤدي إلى .(mMTC) والاتصال الكثيف بين الآلات ،(URLLC) والاتصال فائق الاعتمادية منخفض الكمون ،(eMBB) مثل النطاق العريض المتنقل المحسن INI يُضعف الأداء، خصوصًا في غياب نطاقات الحماية أو عند استخدام تعديلات مرتفعة.تتناول هذه الرسالة مشكلة (INI) مما يسبب تداخلًا بين التعدادات ،OFDM فقدان التعامدية في بين التعدادات، و(2) OFDM ثنائية التعداد في الربط النزولي، وتقترح طريقة تخفيف مكونة من مرحلتين: (1) إعادة التوسيم في النطاق الزمني لمحاذاة رموز OFDM في أنظمة ضمن إطار محاكاة متوافق MATLAB الأعلى. تم تنفيذ المنهجية في بيئة SCS من التعداد ذو (OOB) تمرير عالي من رتبة عالية لتقليل الانبعاثات خارج النطاق FIR تطبيق مرشح والكفاءة الطيفية ،(SINR) نسبة الإشارة إلى التداخل والضجيج ،(EVM) مقدار خطأ المتجه ،(BER) وقد تم تقييم الأداء باستخدام مقاييس مثل معدل الخطأ في البتات .GPPمع 3 أظهرت النتائج أن المحاذاة الزمنية كافية للتعديلات المنخفضة، بينما يصبح الفلترة ضرورية للحفاظ على دقة فك التعديل .QAM-وتصل إلى 256 QPSK عبر تعديلات تبدأ من ،(SE) في الحالات الأعلى. كما أن غياب نطاقات الحماية يعزز الكفاءة الطيفية رغم التسبب في تشوه بسيط داخل النطاق في التعداد المُرشّح.بشكل عام، تُظهر الطريقة المقترحة قدرة على تقليل .متعددة الخدمات Gبكفاءة دون الحاجة إلى إلغاء تكراري أو معرفة القناة، ما يجعلها حلاً عمليًا للتطبيقات الفورية في شبكات 5 INI بيانات كبيرة وصغيرة. تشير التقييمات المقارنة إلى أن طرقنا تتفوق على الأساليب الحديثة، مما يؤكد فعاليتها وقابليتها للتعميم.

الكلمات المفتاحية :

نسبة ،(EVM) مقدار خطأ المتجه ،(BER) المحاذاة الزمنية، تسرب طيفي، معدل الخطأ في البت ،FIR ترشيح ،OFDM ،(INI) تعددية التعداد، تداخل بين التعدادات ،5G NR .MATLAB الكفاءة الطيفية، محاكاة ،(SINR) الإشارة إلى التداخل والضجيج